Aalto University
School of Engineering

Geometallurgical characterization of the Kittilä gold ore deposit

Konstantinos Bis

School of Engineering

Master thesis
Espoo 24/10/2018

Supervisors

Prof. Jussi Leveinen
Prof. Dominique Ngan-Tillard
Prof. Bernd Lottermoser

Advisor

M.Sc. Lasse Kangas

Copyright © Konstantinos Bis

Author Konstantinos Bis

Title Geometallurgical characterization of the Kittilä gold ore deposit

Degree programme Geoengineering

Major European Mining Course **Code of major** ENG3077

Supervisors Prof. Jussi Leveinen. Prof. Brendt Lottermosser, Prof. Dominique Ngan-Tillard

Advisor MS.c Lasse Kangas

Date 24.10.2018 **Number of pages** 81+10 **Language** English

Abstract

Comminution testing is a key component to geometallurgical characterization of different ore types. Through comminution tests, valuable information is extracted regarding the breakage mechanisms of the rock, which can be used to enhance the processing operations, including ore blending, circuit design and mill optimization. Most geotechnical tests require large amounts of sample, expensive equipment and are very time consuming. Standard test methods like uniaxial compressive strength and fracture toughness are not considered appropriate in comminution characterization. Alternatively, simple and rapid methods have been used in this study to determine comminution indexes. The results from the comminution tests were used to characterize the grindability and crushability properties of six different ore types from the Kittilä Au deposit in Northern Finland. In summary, the tests which were conducted for this study include the Bond Ball mill grindability test, the Los Angeles abrasion test, the Point Load Strength test and the JK Drop Weight impact test. Additionally, the mineral composition, content and microstructures of the ore types have been determined through optical microscopy and the Scanning Electron Microscope (SEM). Statistical interpretation and correlations were carried out between the comminution tests and the mineral composition of the six sample groups, using the statistical software IBM SPSS and Matlab programming software. From the results, the six ore groups were classified in the range of moderate hard crush to hard crush, while the grindability ranged from moderate hard grinding to very hard grinding. It is concluded that the mineral composition, textures and microstructures have an effect on the ore's resistance to breakage mechanisms. Due to the simplicity and empirical nature of the comminution tests used in this study, the data cannot be used directly for mill circuit optimization. However, the data from this study can be implemented in future research for determining geometallurgical properties by using rapid-remote techniques that will utilize real time mine to mill information.

Keywords Geometallurgical testing, Comminution , Grindability, Crushability, Kittilä

Preface

This thesis is fundamentally initiated from my passion to further develop optimum methods for ore characterization and innovation in the field of mining engineering and mineral processing.

I wish to thank my supervisors Jussi Leveinen, Dominique Ngan-Tillard and Bernd Lottermoser, as well as my instructor Lasse Kangas for their exceptional guidance and support throughout my thesis project and for demonstrating geometallurgical concepts. Additionally, I wish to thank my entire research group for complementing my work and assisting me in conducting my experiments.

I would like to express my gratitude to the Aalto laboratory technicians from the civil engineering department, for providing me with important knowledge about operating equipment critical for this thesis and assisting me to construct and maintain the required devices for comminution testing.

Additionally I would like to thank Laboratory Manager Otto Hedström for his thorough assistance with the equipment setup and transportation of the ore to the test tunnel.

Furthermore, I would like to express my gratitude towards Agnico Eagle for providing me with samples from the Kittilä gold ore deposit and enabling this thesis work to be composed.

The financial support from the organization Business Finland (Tekes), a Finnish funding agency for technology and innovation, is greatly acknowledged.

Finally, I wish to thank my family for supporting me during my entire studies and understanding the reasons for my absence.

Otaniemi, 10/09/2018 Konstantinos Bis

Table of contents

List of Figures

List of Tables

Symbols and Abbreviations

F80: 80% passing size of feed
P80: 80% passing size of product
g: Gravitational constant, 981gm/cm2
G: Grindability of the mill g/rev
Gbp: Bond's standard ball mill grindability g/rev
n: Speed of ball mill, rpm
N: Number of balls
P: Power draw kW
Pi: screen size for performing the test μm
Is_{50}: Point load strength index
BMWi: Bond Ball Mill work index
DWi: Drop Weight index
Ecs: Specific comminution energy
Ei: impact breakage energy
md: mass of drop weight head
mp: mean particle mass
SCSE: Specific energy for the standard circuit
kWh/t: Kilowatt Hours per Ton
kV: Kilovolt
nA: nanoampere

JKRMC: Julius Kruttschnitt Mineral Research Centre
UCS: Uniaxial Compressive Strength
SEM: Scanning Electron Microscope
GTK: Geological Survey of Finland
MML: Mafic massive lavas
MPL: Mafic pillow lavas
MVX: Mafic volcanogenic explosive
GFZ: Graphitic failure zone
SAG: Semi-Autogenous
ROM: Run of mine
L.A: Los Angeles
ISRM: International Society for Rock Mechanics
ASTM: American Society for Testing and Material
EDS: Energy Dispersive X-Ray Spectroscopy
PCA: Principal component analysis

1 Introduction

This master's thesis is part of the Kaivos project, a joint research project funded by the organization Business Finland (Tekes). The results from this study provide a basis for comprehending the geometallurgical properties of the Kittilä gold ore deposit. The findings will be incorporated in further development of remote techniques to acquire real time mine-to-mill information for processing optimization.

Geometallurgical characterization is enabled from the integration of geological variables to comminution indices. Comminution is the most fundamental and standard unit operation in most metallurgical processes (Lamberg 2011). It is the process in which solid materials are reduced in crushing and grinding circuits (Lynch 2005). Comminution indexes are commonly incorporated into the early stages of developing an improved circuit design, a key driver to value realization (Deutch 2013).

The research objectives resolved in this thesis include the identification and classification of the geometallurgical properties of six ore groups from the Kittilä gold deposit in Northern Finland. The aim of this geometallurgical study is to understand and map inherent comminution variability across the Kittilä deposit providing information critical for mine/mill design and optimization.The structure of this study is the following. Chapter 2 provides information regarding the geological background of the project and the processing plant in Kittilä. Chapter 3 explains the fundamentals of geometallurgy with a focus on the comminution unit, while the existing comminution methods applied in the industry are briefly discussed. Chapter 4 involves the characterization of the samples received for this study, including the mineral content, microstructures and density measurements of the ore specimens. Furthermore, Chapter 5 provides a detailed description of the methods used in this study for ore comminution testing, while the results from all the tests are illustrated in Chapter 6. Finally, Chapter 7 contains the interpretation and discussion of the results, with an emphasis on the various correlations between the comminution tests and the corresponding mineral content. Overall conclusions are given in Chapter 8 followed by recommendations for future work in Chapter 9.

Most comminution test methods are time consuming, expensive and with large sample requirements (Wills & Napier-Munn 2006). The modern industry trend involves simple and rapid comminution testing methods which are more efficient in terms of requirements (Mwanga et al. 2015). Therefore, this study comprises empirical test methods which are proven to be effective predictors of comminution behavior and are easy to conduct.

The three fundamental categories of comminution methods applied in this study, include rock mechanical testing, particle breakage tests and bench scale grindability tests**.** The comminution indices which describe the crushability of the ore include the (A*b) and (t10) parameters which are determined from the Drop Weight Impact test. Additionally, rock strength is determined through the Point Load Strength Index, an estimate of the uniaxial compressive strength of the rock. Grindability of the ore is determined from the Bond Work Index (BMWi), an index defined from the Bond Ball Mill grindability test. Furthermore, resistance of the ore to abrasion is derived from the Los Angeles abrasion test.

1.1 Hypothesis

The thesis is based on the determination of the geometallurgical properties of the Kittilä gold deposit aimed at testing the following hypothesis:

Comminution testing of complex heterogeneous ore provides a practical means of optimizing size reduction processes including crushing and grinding. Additionally, comminution tests allow key ore properties to be identified and implemented into the circuit design.

The properties of multi-component ores can thereby be exploited to enable the assessment of interactions between separation processes and mineral composition, leading to an innovative processing circuit configuration.

1.2 Thesis structure

The following structure was followed for this study:

- Chapter 2 includes the literature review and explains the fundamentals of geometallurgy with a focus on the comminution unit and the existing comminution methods applied in the industry.
- Chapter 3 provides information regarding the geological background of the project and the processing plant in Kittilä.
- Chapter 4 involves the characterization of the samples received for this study, including the mineral composition, microstructures and density measurements of the ore specimens.
- Chapter 5 provides a detailed description of the methods used in this study for ore comminution testing.
- Chapter 6 includes the detailed results from all the comminution tests and the summary of the results.
- Chapter 7 contains the statistical interpretation and discussion of the results, with an emphasis on the various correlations between the comminution tests and the corresponding mineral composition.
- Chapter 8 contains the conclusions from the study and the answers to the research questions.
- Chapter 9 provides recommendations for future work and the path forward to be followed in the next phase of the research.

1.3 Research questions

Based on the hypotheses, the following research questions were established as the primary goals of this thesis:

- How do the sample groups from Kittilä differ in terms of grindability and crushability?
- What empirical tests are commonly used to measure the comminution properties of ores simply and rapidly?
- How does the mineral composition of the Kittilä ore correlate with comminution?
- How can the determination of the geometallurgical properties be implemented in circuit design and optimization?

- How could the variance in the comminution behavior be implemented in future work to improve processing efficiency?

1.4 Objectives

To answer the research questions, the following objectives are addressed in the case studies of this thesis:

- Define the breakage mechanisms that are responsible for grinding and crushing of the ore.
- Describe empirical test methods used for comminution testing.
- Evaluate the limitations of the comminution tests used for this study.
- Obtain numerical data from the various tests and classify the sample groups based on their grindability and crushability.
- Review the relationship between the comminution indices derived from the test.
- Determine the correlations between the mineral composition and the corresponding comminution indices.
- Conduct principle component analysis to reduce noise and dimensionalities in the data set.
- Classify the sample groups and define clusters of covariance between the sample groups.
- Recommend path forward and explain the potential of implementing the results to circuit design and optimization.

2 Literature review

This chapter reviews the literature and explains why comminution testing is essential in order to obtain a substantial improvement in crushing and grinding efficiency. It is argued that the key to the design of the future generation of processing plants is to understand and respond to the ore properties (Powell & Morrison 2007).Therefore, it is necessary to ensure that the properties of ore components can be adequately determined. While typical configurations adopted by the minerals industry are generally efficient for cases where the entire stream is treated as having a uniform set of properties, multi-component ores present the possibility of their properties being exploited.

2.1 Geometallurgy

Geometallurgy is the dynamic integration of geological data with small-scale physical measurements to define the spatial variability of a deposit and aid prediction of metallurgical performance (Powell & Morrison 2007). Geometallurgy provides the basis for an informed selection of metallurgical tests to determine metallurgical behavior of an orebody. However, the quantitative data regarding the modal mineralogical composition of the ore are not being used to their fully potential in metallurgical circuit design (Walters & Kojovic 2006).

This study focuses on the comminution unit of the processing plant. The aim is to determine the optimum size reduction method based on the grindability and the crushability of the ore. Feed properties such as input energy particle size distribution, mineral composition, micro texture and grain size compose the criteria to select the adequate test method. Equipment settings and input parameters are decided in correlation with the desired product properties to

be determined. More specifically, parameters such as power, machine capacity, charge fillings and mill rounds per minute (rpm) are designed to reduce particle size to a specific size according to the corresponding standards of the test. These parameters can be modelled using conventional geostatistical techniques to support a metallurgical process model. An illustrative schematic of the geometallurgical modeling and simulation system is provided in (Figure 2-1).

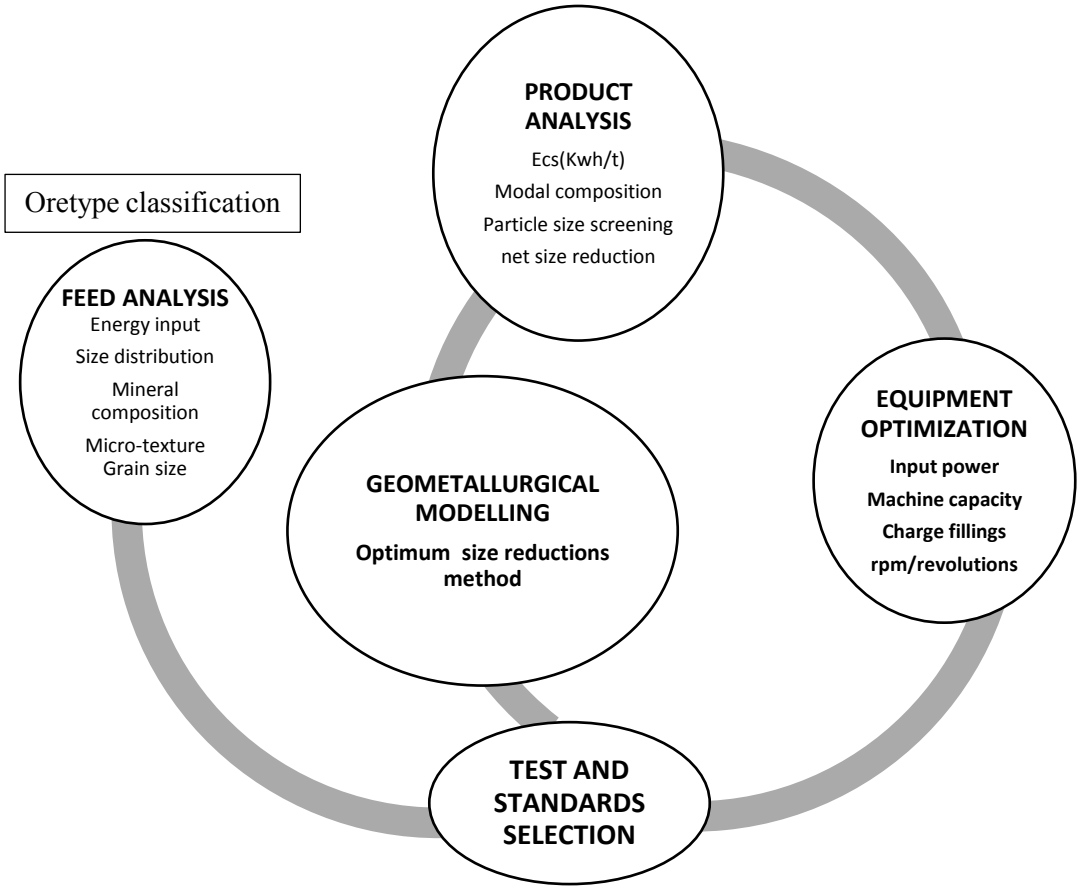

Figure 2-1 Flowchart illustrating the correlation between the feed and product analysis with selecting the appropriate comminution testing and geometallurgical modeling

2.2 Comminution

Comminution is the process in which solid materials are reduced in crushing and grinding circuits (Lynch 2005). The main process in comminution are breakage and classification. Breakage is a size reduction process and it occurs by impact, compression, shear or attrition (Figure 2-2). Classification is a size separation process that occurs by screening or by the differential movement of particles in liquids or gases. Closed circuits, which involve recycling the coarse fraction from the classifier back to the mill, are commonly used for comminution processes. It is important to optimize both the sizes of machines in the circuits at the design stage and the operating conditions of the circuits at the production stage. Measures of impact hardness and grindability are suitable for comminution modelling and mill design.

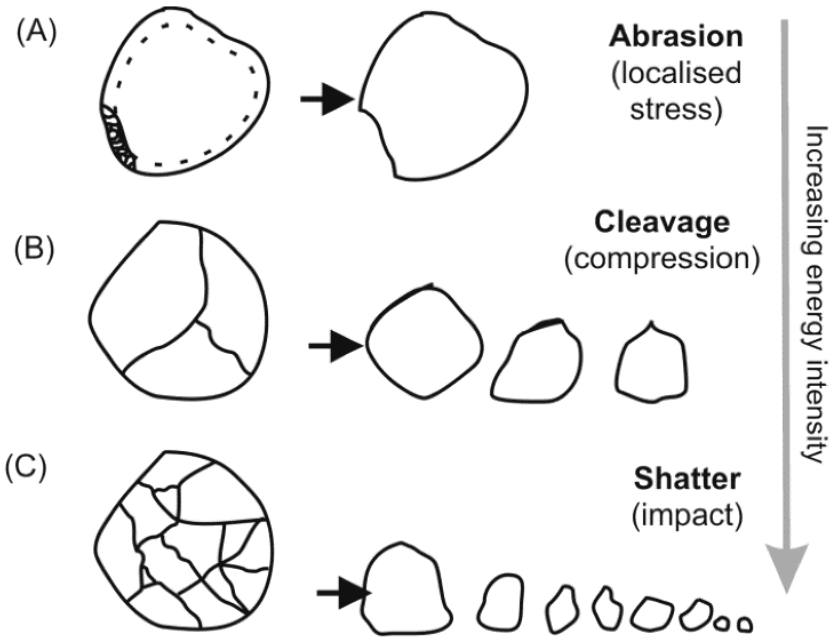

Figure 2-2 Particle breakage mechanisms (Antikoi et al. 2018)

In most cases, more than one breakage mechanisms occur during milling or crushing, while one mechanism is usually the dominant one. In principal, impact and compression are more effective for coarse size fractions, while abrasion is more effective for finer particles.

Abrasion occurs when particles rub against each other and the shear forces create finer particles. Additionally, abrasion can be promoted from rubbing with the grinding media.

Compression breakage occurs by applying compression to a set of particles or a single particle, leading to size reduction. This method is the most efficient method from an aspect of energy utilized. Energy transferred to particles by means of surrounding particles, hence inter-particle breakage occurs.

Impact breakage refers to the size reduction of a particle achieved by forces acting on the particle, resulting from the kinetic energy of the grinding media.

In mineral processing, comminution can be considered to consist of blasting, crushing, and grinding processes (Wills & Napier-Munn 2006). The crushing and grinding units from the processing flowchart are of interest for this study. (Figure 2-3). The geometallurgical properties derived from the comminution tests can be implemented in a process simulation software and provide real time information about equipment performance, circuit energy consumption and feed/product analysis.

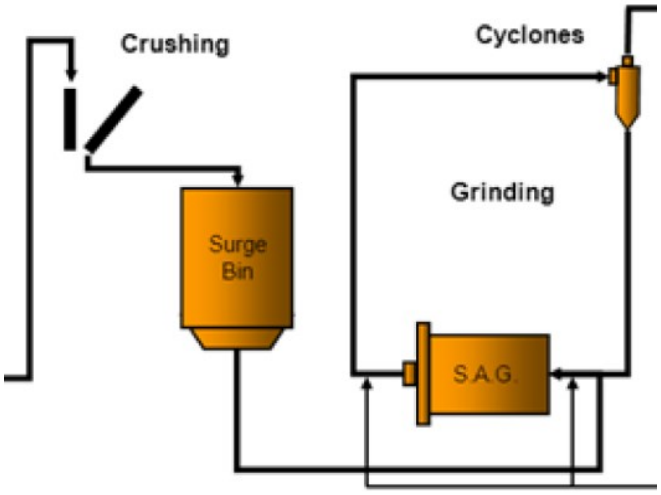

Figure 2-3 Comminution unit of Agnico Eagle processing flowchart (Agnico Eagle 2009)

In order to successfully incorporate comminution indices to geometallurgical characterization, the tests have to fulfill the following criteria:

- The tests have to be simple, rapid and easy to conduct. It should use instruments that are readily available in conventional analytical and mineral processing laboratories.
- It should be possible to repeat the test based on standard guidelines
- Minimum sample requirements and preparation.
- The costs of the test should be relatively low in order to allow for repeatability and simplicity
- Comminution tests should provide indices that can be implemented in circuit design, process modelling and simulation.

Another criterion is the precision and the statistical quality of the test results. With respect to accuracy, a proper quantification is not an easy task, since the entire chain of sampling and sample preparation, in conjunction with the test and analysis method, needs to be considered. Statistical quality is a parameter that, from the perspective of geometallurgy, not only has to be judged with respect to the repetition of single tests but also in relation to generating a comprehensive data set for the entire geometallurgical program, *i.e.*, a compromise between the quality of single measurements and the overall quantity of measured points must be reached.

2.3 Crushing and Grinding

Grinding and crushing are the most fundamental and standard unit operations in most metallurgical processes. (Kojovic et al. 2010) Particle size reduction as a function of energy input is a key factor to an optimum processing cycles and one of the most important factors in a grinding process. Comminution in the processing plant is accomplished in a sequence of crushing and grinding cycles. Crushing results to particle size reduction until it is small enough

to be grinded in the mill. Grinding is carried out until mineral liberation occurs so that the gangue and minerals are separate particles.

Crushing takes place when the ore is compressed against rigid surfaces or impacted against surfaces in a constrained motion path (Kojovic et al. 2010). It is usually a dry process which is performed in multiple stages. There are different types of crushers, such as gyratory, jaw crushers, high pressure role, cone and impact crushers.

Grinding is possibly the most energy intensive unit process in the mechanical process industry. (Krogh 1980). There are various types of mills that are used in processing plants. Milling also refers to particle size reduction as a result of impact, compression and abrasion. These are the basic breakage mechanisms that occur during milling (Figure 2-4).

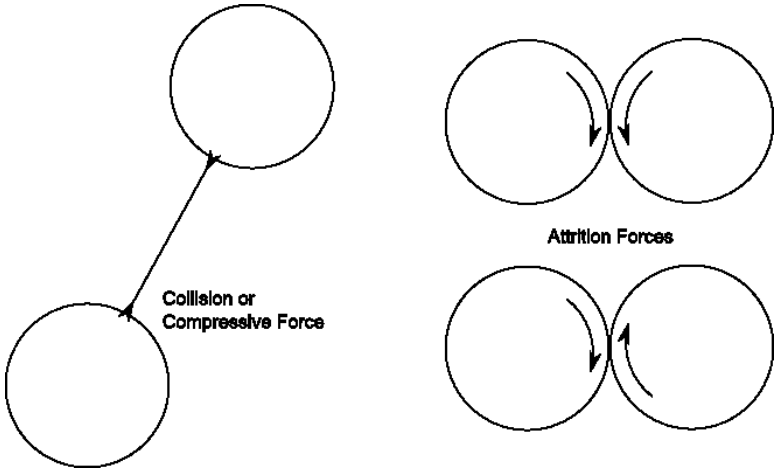

Figure 2-4 Breakage mechanisms that occur during grinding (Thomas et al. 1999).

Dimensioning of the grinding mill, specific comminution energy and specifications regarding number of revolutions and mill speed, are all based on determining the grindability of the material that will be processed. There are various factors that affect the grinding efficiency. The most important ones are listed below (Austin 1984).

- Mill speed
- Feed rate
- Grinding media
- Mill liner
- Ore properties
- Mill type
- Sludge viscosity (for wet grinding)

The tests conducted in this research emphasize on determination of comminution indices that characterize the breakage mechanisms of the ore and therefore its geometallurgical behavior. Grindability was determined from the Bond Ball Mill Work Index (BMWi), a widely used comminution index that provides information about the grindability of the ore.

Crushability of the ore was determined from the Drop Weight impact test and the point load test. Specifically, the Drop Weight index (DWi) was determined, a parameter which describes the resistance of an ore to crushing. The DWi in combination with the Point Load strength index (Is50) can be used to determine the resistance of the ore to crushing. Further information about the ore's resistance to abrasion and attrition mechanisms was obtained through the Los Angeles abrasion test.

2.4 Existing comminution methods

This chapter includes the methods which are usually applied for ore comminution testing. Most of these methods fulfill the requirements mentioned in Chapter 2.1 for accurate, simple and rapid determination of the comminution indices. The methods illustrated in Figure 2-5 have the potential to be incorporated in geometallurgical characterization and modelling.

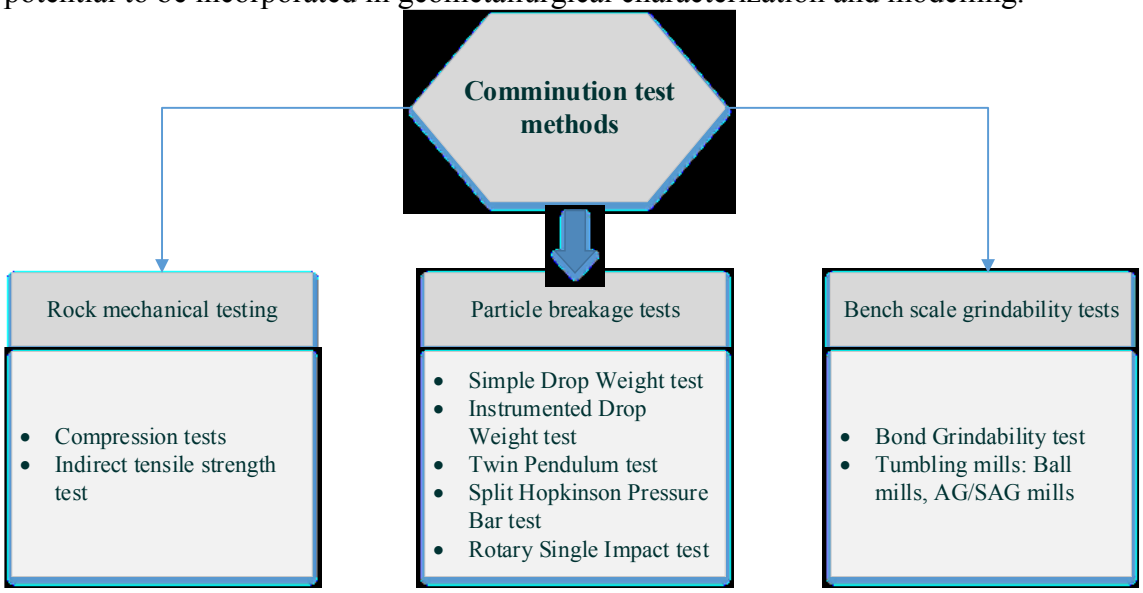

Figure 2-5 Review of the existing comminution test methods (Mwanga et al. 2015)

The three fundamental categories of comminution methods include Rock mechanical testing, Particle breakage tests and Bench scale grindability tests.

Rock mechanical tests to determine rock strength are commonly carried out with compressive loading instruments. The loading force is increased slowly and steadily in comparison with other comminution methods. Various standard test methods are used that have different loading conditions. The common tests are the uniaxial compressive test, the triaxial test, the point load test and the hardness test.

Particle breakage test can be distinguished in single particle breakage or multiple particle breakage. In principal, these types of tests provide information about the resistance of the specimens to impact breakage. There are multiple tests () which result to the acquisition of various comminution indices, leading to a versatile understanding of particle size reduction.

Bench scale grindability tests are the basis for comminution circuit design. Commonly, grindability tests rely on a known size distribution of feed, specific comminution energy requirements and a measured product size distribution. (Source). The Bond grindability test is the most typical method to determine resistance to grinding mechanisms, while tumbling mills are used to determine ball mill and AG/SAG mill characteristics.

The purpose of use for each test method relevant to crushing and grinding is facilitated in (Table 2-1), based on the crushing and screening handbook from Metso (Metso 2011). Metso laboratories have tested thousands of rock samples in order to obtain representative statistics. (Table 3-1) provides a baseline for the evaluation of rock geometallurgical properties.

Table 2-1 Common comminution tests and their purpose of use according to Metso Mining laboratories. (Metso 2011)

	Laboratory/Test Plant					Purpose of Use										
Test Methods	Tampere(Finland)	Macon(France)	Sorocaba(Brazil)	Ahmedabad(India)	Danville(U.S)	Crushing Process Plant	Milling Process Plant	Crusher Selection	Mill Selection	Screen Selection	Screen Media Selection	Capacity	Product Gradation	Product Shape	Power Consumption	Customer acceptance for end product
Solid Density	X	X	X	X	X	X	X	X	X	X		X				
Bond Ball Mill Work Index			X		X		X		X						X	
Bond Rod Mill Work Index			X		X		X		X			X			X	
Crushability	X	X	X	X	X	X		X				X	X	X	X	X
Abrasiveness	X	X	X	X	X	X		X			X				X	X
Bond Abrasion index	X		X		X	X		X			X				X	X
Los Angeles	X					X		X				X	X	X	X	X
Uniaxial Compressive Strength				X				X				X	X	X	X	X
Particle size	X	X	X	X	X					X	X					X
Particle shape	X	X	X							X	X					X
Point Load Index	X		X			X	X									
Drop Weight Test			X			X	X			X						
Sag Mill Comminution			X			X	X	X								

2.5 Existing correlations between comminution and geometallurgical properties

Significant correlations have been found from various studies between the Bond Work Index and the mechanical properties of rocks, including hardness, abrasion, compressive strength and modulus of elasticity. However, it should be noted that the population of the samples used in most studies is not statistically representative (Haffez 2012).

Haffez (2012) compared different mechanical properties of some ore and rock samples from Saudi Arabia (bauxite, kaolinite, granodiorite, magnetite, granite, feldspar and quartz) to the bond work index. Haffez concluded that the bond work index is positively correlated with the modulus of elasticity (R 2 = 0.90) (Figure 2-6).

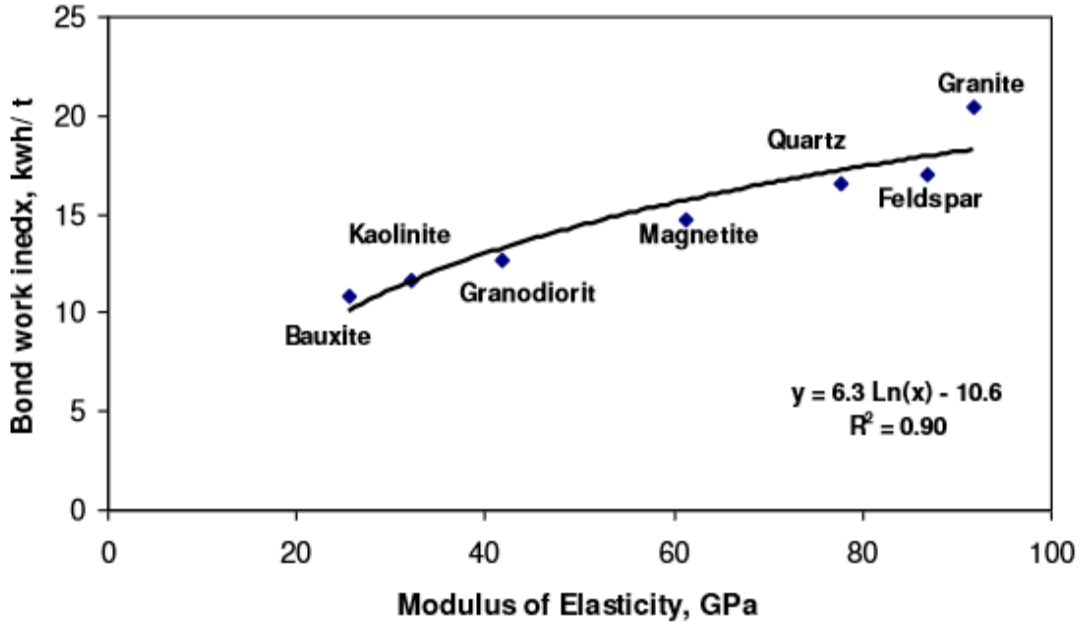

Figure 2-6 Effect of the modulus of elasticity of the different studied materials on BMWi

The relationship between the compressive strength of the tested rocks and the Bond work index is illustrated in (Figure 2-7). It appears that the compressive strength (UCS) is positively correlated with Bond work index (R 2 = 0.81), this meaning that an increase in the c9ompressive strength corresponds to an increased bond work index (BMWi).

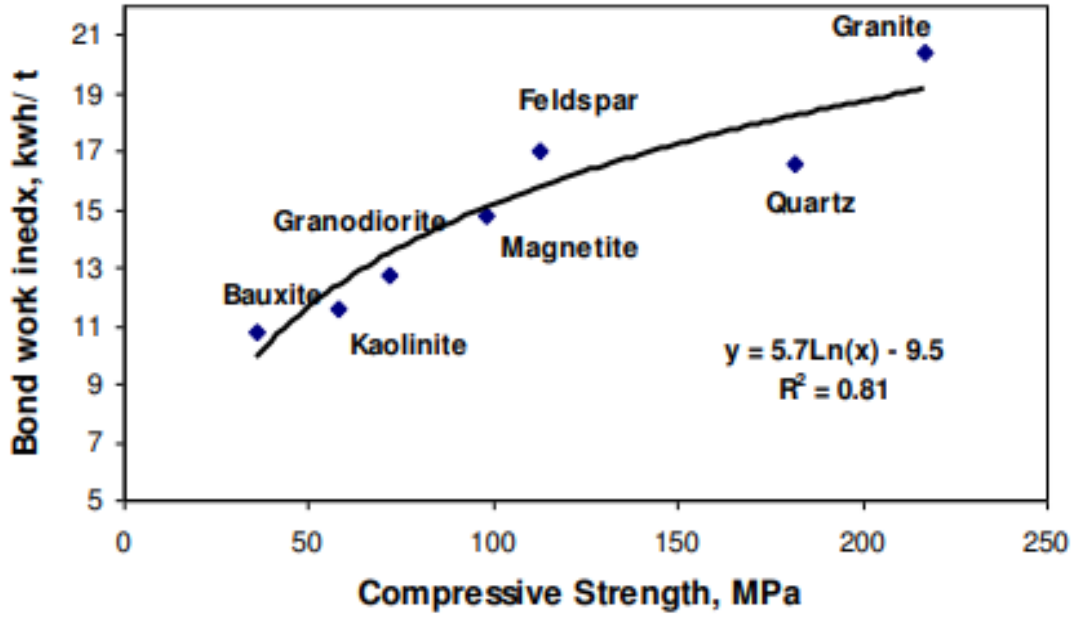

Figure 2-7 The Effect of Compressive Strength of different materials on the BMWi

Abrasion is negatively correlated to the Bond work index (R 2 = 0.80) (Figure 2-8)

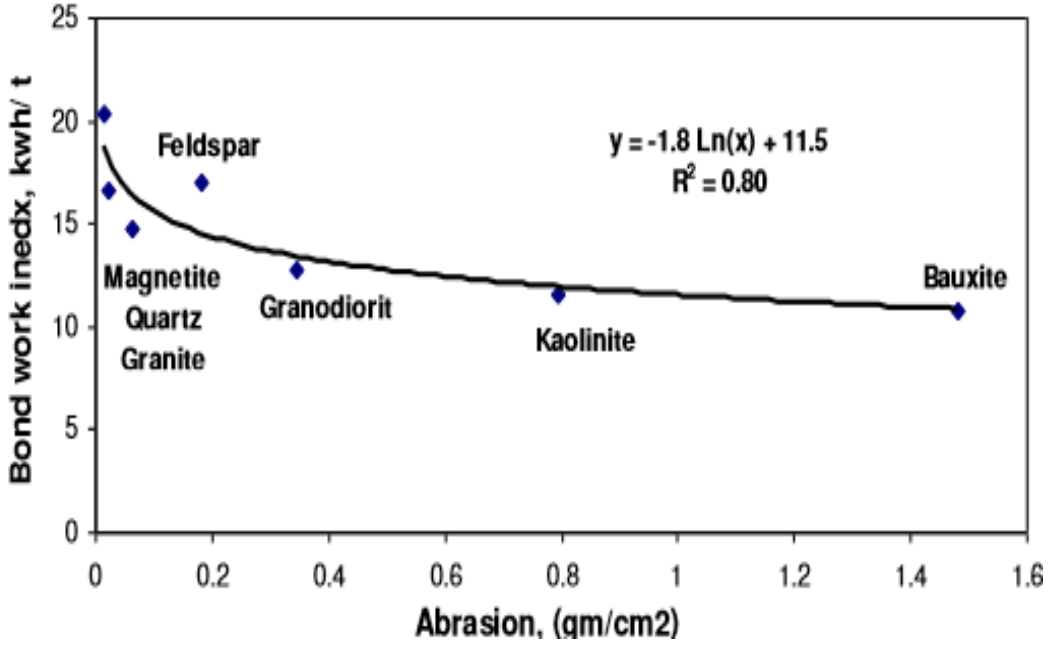

Figure 2-8 Effect of abrasion of different materials on the BMWi

Swain and Rao (2009) correlated the BMWi with the friability value for different ore types. Friability was determined from the brittleness test, an impact crushing test with the same principals as the drop weight impact test. Friability is defined as the tendency of a material to break by attrition (Swain and Rao 2009). A good correlation was found between BWi and friability, shown in (Figure 2-9). The R square value was 0.93. Thus, it may be possible to predict the value of bond work index with a small error using this correlation for a similar ore type.

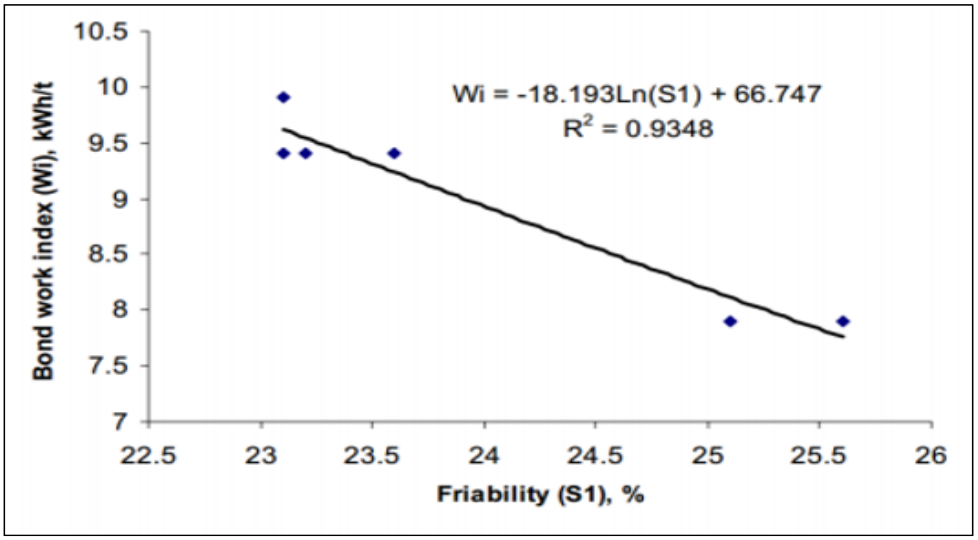

Figure 2-9 The correlation between BMWi and Friability (Swain & Rao 2009)

3 Geological background and ore processing at Kittilä

The orogenic Kittilä gold deposit occurs within the Paleoproterozoic Central Lapland Greenstone Belt (Figure 3-1), approximately 50km northeast of the town of Kittilä in Finnish Lapland. The surrounding region is composed of mafic volcanic and sedimentary rocks from the Greenstone Belt (Hölttä et al. 2007). The combination of the metamorphic grade with the host rock lithology and alteration assemblages, make it to one of the best-known deposits in green-stone belts throughout the world. It is assumed that the nature of the deposit is structurally controlled by the regional deformation. (Härkönen & Keinänen 1989).

3.1 Regional Geology

The Kittilä group comprises three main ore deposits, the Suurikuusikko, Rouravaara and Rimpi. Additionally, there are two minor deposits, the Ketola and Etelä. Based on the geochemical heterogeneity among the Kittilä group rocks, it can be assumed that the group is a composite of arc terranes and oceanic plateau which was amalgamated during oceanic convergence (Hanski & Huhma 2005). Subsequent ground geophysical surveys and geochemical sampling lead to the identification of the Kiistala Shear Zone (KiSZ), the deposit's host structure, which strikes N to NE and dips steeply to subvertical to the west (Patison 2007).

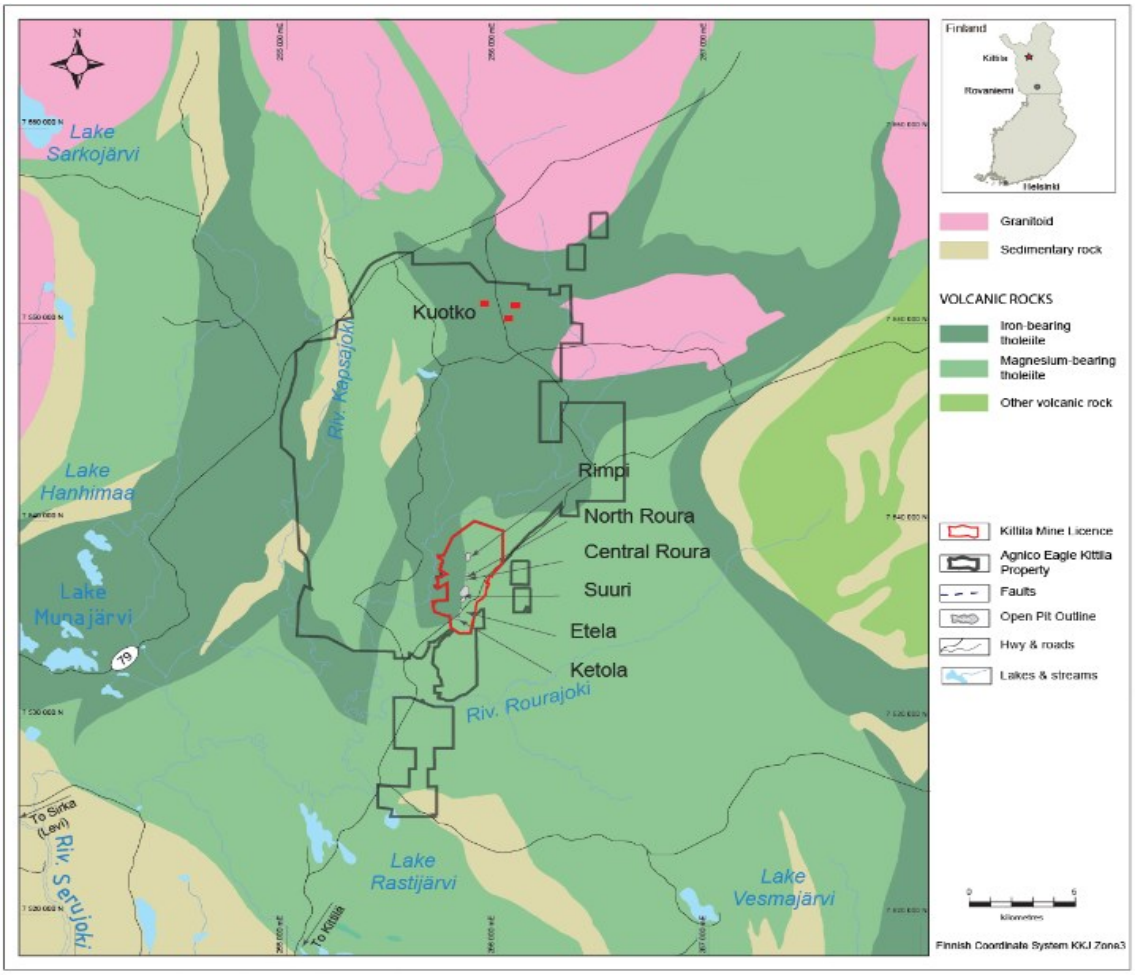

Figure 3-1 Geological map of Kittilä based on the 1:600000 scale (Agnico Eagle 2018)

The KiSZ approximately extends for 30km and appears to be consistently anomalous in gold occurrence for about 15km (Eilu et al. 2007). All the deposits are allocated and subdivided into two major formations, the Kautoselkä Formation with Fe-tholeiite igneous rocks, and the Vesmajärvi Formation with Mg-tholeiite igneous rocks. Metamorphosis has taken place up to the greenschist-faces, while there in intense alteration present, mostly albitization, sericitisation and carbonization. (Eilu et al. 2007; Patison 2007).

3.2 Host rock lithology

The mineralized host rocks of the Kittilä deposit are composed by a large interbed between Fe and Mg-tholeiitic mafic volcanic rocks. More specifically, the mineralization occurs within mafic to intermediate rocks characterized by abundant pumaceous material, Mafic lava breccias and pyroclastic textures (Figure 3-2). Besides the mafic volcanic rocks, there are also some units of ultramafic rocks which appear to have almost no deformation. These units are not mineralized at all. (Patison 2007).

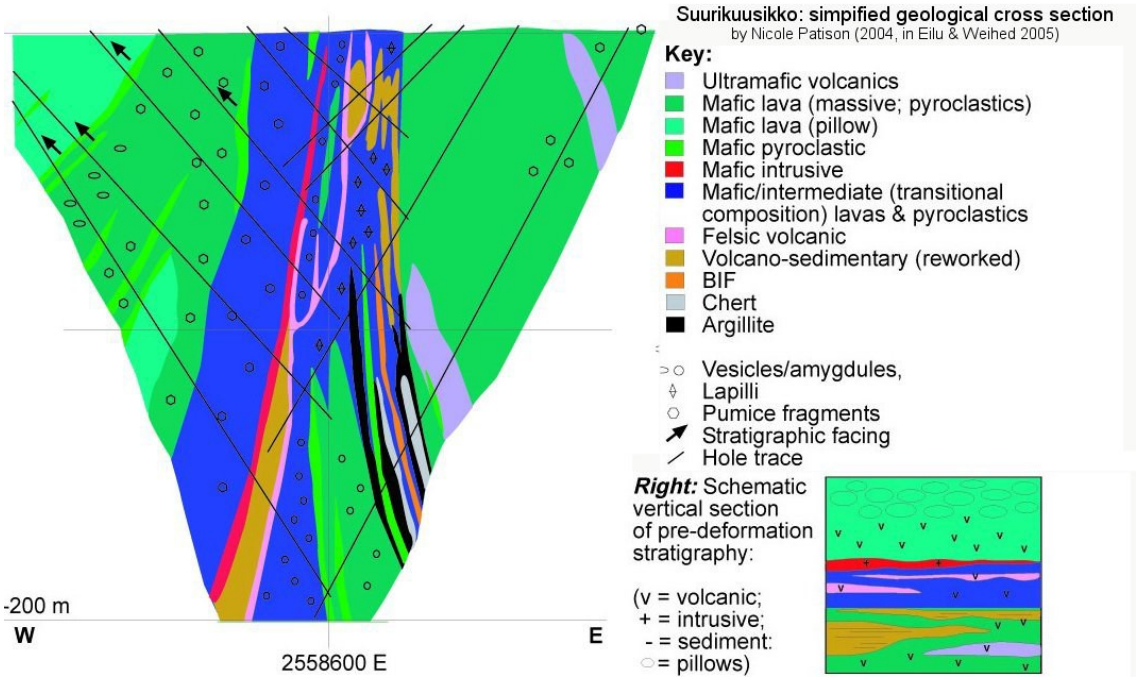

Figure 3-2 Simplified geological cross section of Suurikuusiko (GTK 2018)

Intense shearing and mineralization are accompanied by graphite, albite and carbonate alterations (Patison 2007). This could imply that the Na-rich fluids that were responsible for the albitization were also the hydrothermal epigenetic fluids that caused the mineralization after the major stage of deformation.

The host rocks are divided into three major lithologies: mafic massive lavas (MML), mafic pillow lavas (MPL), and mafic volcanogenic explosive (MVX) rocks, the last one being the predominant lithology (Härkönen & Keinänen 1989). Shearing is abundant within the deposit and is defined as graphitic failure zones (GFZ). Graphitic failure zones should not be considered as a lithology but correspond to strongly sheared zones within MML and MVX.

The major lithologies, which characterize the host rock, are illustrated in (Figure 3-3) according to their location, expanding from the westernmost part in the footwall to the easternmost part in the hanging wall. Additionally, the intercepting graphite bearing shear zone and graphite occurrences are shown in the cross section marked with blue and dotted blue respectively. The yellow, orange and red dotted lines represent the various iron sulphides mineralogy (Figure 3-3).

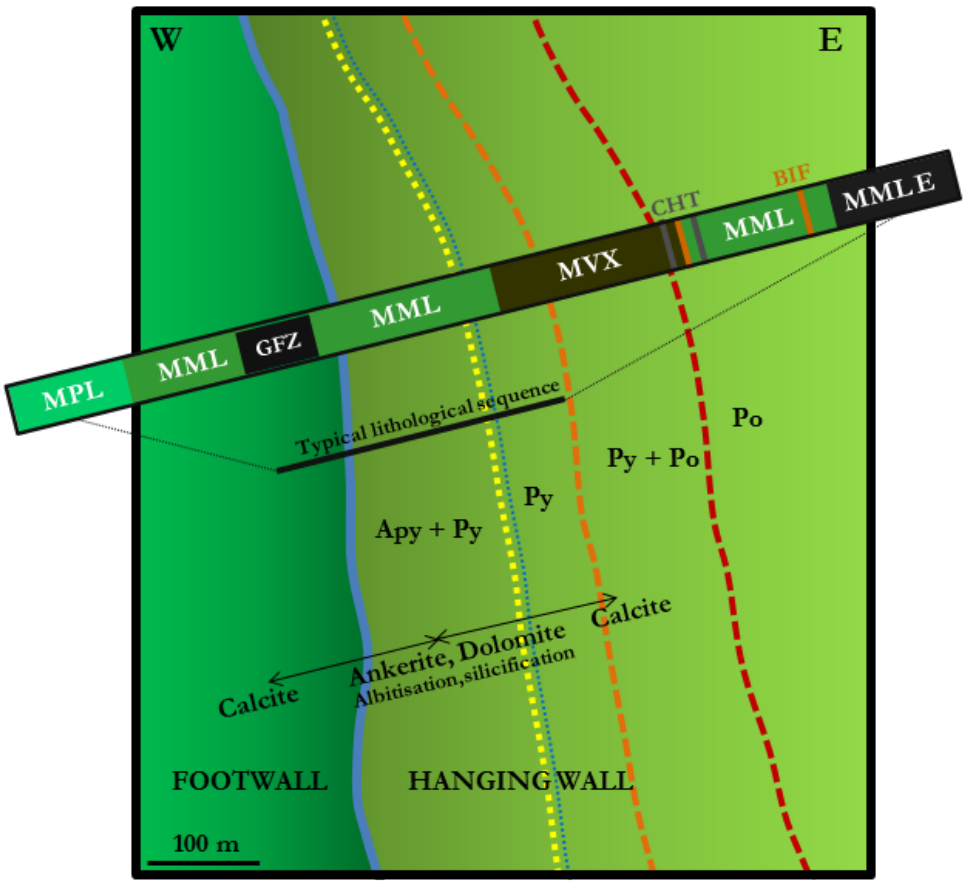

Figure 3-3 Schematic cross section perpendicular to the gold mineralization showing the lithological sequence, alteration and main sulphides mineralogy at actual mining depths (Doucet et al. 2010)

The lithologies present different grades of shearing and brecciation. These features are related to the occurrence of the gold bearing mineralization. Clearly epigenetic, orogenic gold mineralization with a distinct structural control, as derived from data in references. (Patison 2007).

All of the main lodes consist of a set of parallel sublodes, and most of them are indicated to be interconnected, but generally there are three subparallel mineralized subzones in each area. Very thin graphite veins and up to 1-2 cm wide albite-carbonate and sulphides veins brecciate the host rock. Mostly thick units of MPL and MML lavas exist in the footwall and are defined by less brecciation and reworking. A graphite-bearing shear zone, in places up to 2 m wide, delimits the footwall and the mineralization. MML also occurs in the hanging wall and as the grade of reworking of volcano-sedimentary material increase, transition to MVX occurs; the

transition from MML and MVX may be diffuse. The mineralized zone is composed of several semi parallel ore lenses of variable width, from decimeters up to a few meters, and typically occurring within MVX and MML lithologies. Intersections within the ore lenses are not rare. In addition, graphite-rich areas occurring within these lithologies can be enriched in gold. The mineralization in the hanging wall is delimited by semi-continuous graphitic zones and mafic massive lavas (Hanski & Huhma 2005).

3.3 Major and Minor minerals

As a result of the intense shearing and metamorphism that characterizes the Kittilä deposit, it is a complex task to distinguish between mineralogical paragenesis related to mineralization from alteration or metamorphosis. Such a classification has not been attempted in this thesis due to the lack of adequate data. The mineralogy was examined by using optical microscopy, scanning electron microscope (SEM) and macroscopic observations.

The mineral composition of the described mineralized host rocks is characterized by an intergrowth of pyrite and arsenopyrite as major minerals, which are bound in a matrix of graphite, albite and carbonate alterations. (Figure 3-4) .

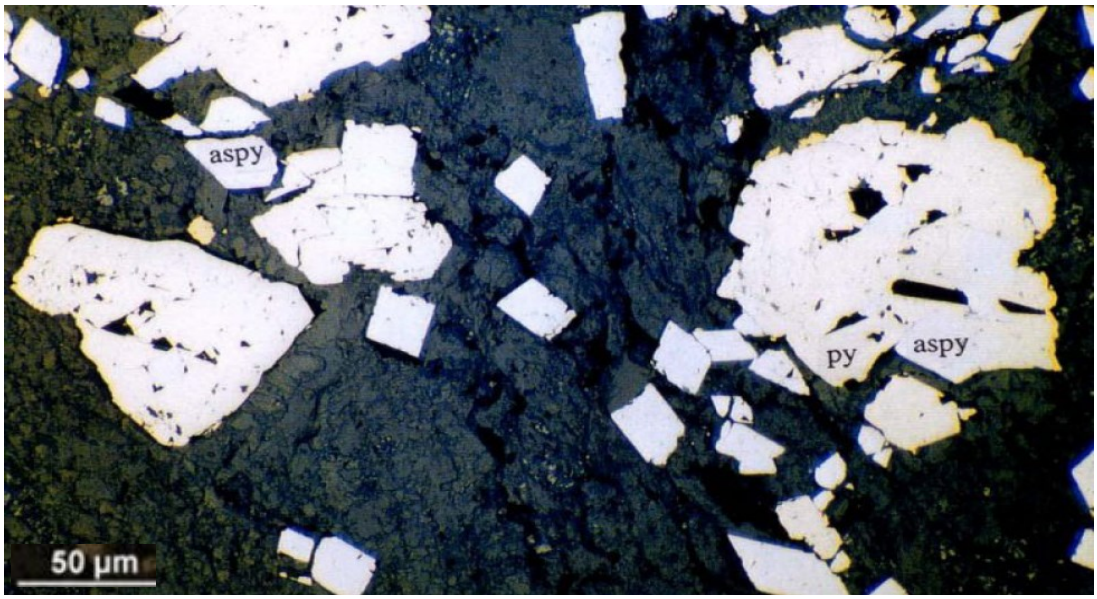

Figure 3-4 Intergrowth of arsenopyrite and disseminated pyrite. Visible graphite alteration.

These are the most economically valuable minerals since they may contain Au. Visible gold was discovered SW of Suurikuusikko by the Geological Survey of Finland (GTK) in 1986. Gold occurs mostly as refractory gold associated with arsenopyrite (49 –2700 ppm Au content in arsenopyrite), pyrite (1 –585 ppm Au content in pyrite) and occasionally gersdorffite. The main part of the gold 73.2 %) is bound in the lattice of arsenopyrite or exists as tiny inclusions, 22.7 % in pyrite and 4.1 % as free gold, both native and electrum (Kojonen & Johanson 1999).

Gold occurrence is rather easy to predict with the naked eye, mainly due to the arsenopyrite content and the visible alteration zones. This criterion is used for characterization of the boundaries and auriferous zones, since the host rock is challenging to define from the high

graphite content which covers a large percentage of the rock surface. Besides the major minerals which contain gold, there are various minor minerals which are also of economic value. These are bismuth, bornite and bournonite which commonly occur as inclusions or intergrowths with the major ore minerals.

3.4 Kittilä Mineral Processing Plant

Approximately 4.500 tons of ore are fed to the Kittilä processing plant per day. The ore is treated through grinding, flotation, pressure oxidation, and carbon-in-leach circuits (Figure 3-5). Kittilä has Agnico Eagle's only pressure oxidation circuit (autoclave), which is required because of the ore's refractory nature. Gold from the leach circuit is stripped from the carbon and recovered from solution using electrowinning, and then smelted in a furnace and poured into doré bars. Gold recovery of 86% is expected over the life of the mine.

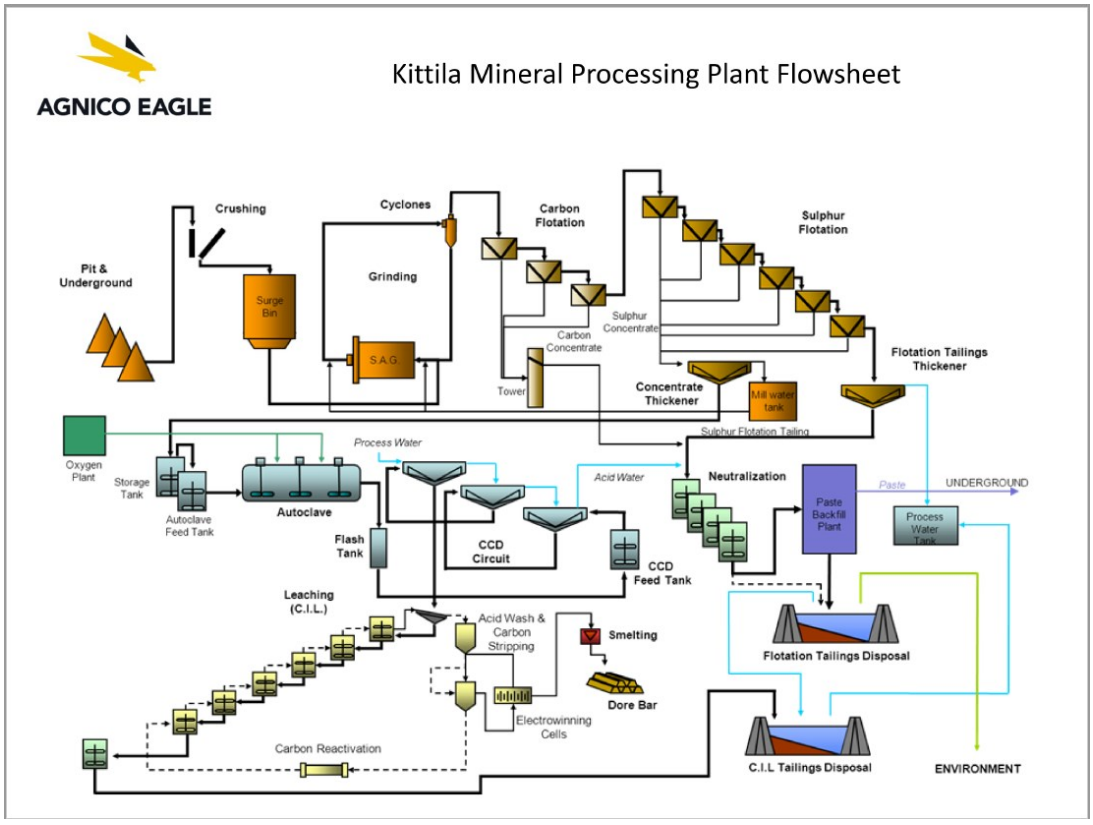

Figure 3-5 Kittilä Mineral Processing Plant flowsheet (image courtesy Agnico Eagle 2009).

A four-phase mill expansion is expected to increase throughput from the current level of 1.6 million tons per year to 2.0 million tons per year by 2021. The mill expansion will involve installation of a secondary crushing circuit, new thickener and reactor capacity, and minor modifications to the existing grinding circuit and autoclave. (Agnico Eagle 2009).

4 Sample characterization

The samples used for this thesis correspond to three different locations from the Kittilä deposit. For each location, duplicate samples are tested in order to examine the heterogeneity among the ore groups. All samples are classified as mafic volcanic rocks based on macroscopic descriptions and mineral composition. The Suurikuusikko primary ore and the Rouravaara ore intersection are both characterized by mafic volcanogenic explosive rocks (MVX). The selection of the samples was carried out by the Senior Geologist of Kittilä mine Jukka Välimaa.

The samples tested in this study are lavas of green-brown to black colours with intense shearing and present alterations. According to the SEM results provided in Chapter 4.2.3 the main mineral composition includes ankerite, quartz, pyrite, arsenopyrite, micas and graphite.

Information about the labeling and the corresponding weight of each sample category is provided in (Table 4-1). Each sample code begins with the letter S or R. S stands for Suuri and R stands for Roura. Suuri and Roura are two different parts of the deposit as explained in Chapter 2.1. The three digit number following the letter represents the depth at which these samples have been extracted from, while the following letter and numbers correspond to the location coordinates of the stope of extraction. In terms of simplicity, the original sample codes were modified according to (Table 4-1).

Table 4-1 Sample labeling and the total weight per sample group

Original Sample Label	Simplified label	Total sample weight(kg)
S425L178-1-1	S4-1-1	39.045
S425L178-1-2	S4-1-2	26.590
S350L170-1-1	S3-1-1	26.955
S350L170-1-2	S3-1-2	28.740
R190PL227-226-1-1	R-1-1	28.065
R190PL227-226-1-2	R-1-2	27.665

The sample groups differ in mineral composition, texture and microstructures. The mineral compositions are derived from the scanning electron microscope (SEM) while the textural characteristics are investigated from the stereoscopic microscope.

4.1 Mineralogical and textural characterization

The specimens that were used in this study are mafic volcanic host rocks with sulphides mineralization composed mainly of pyrite and arsenopyrite. Most samples are highly brecciated and are characterized by sulphides, quartz and carbonate veins. (Figure 4-1). Graphite and albite alterations are present in all samples but have not been considered in the geometallurgical characterization of the ore in this study due to limitations in the resources and the equipment available for this study.

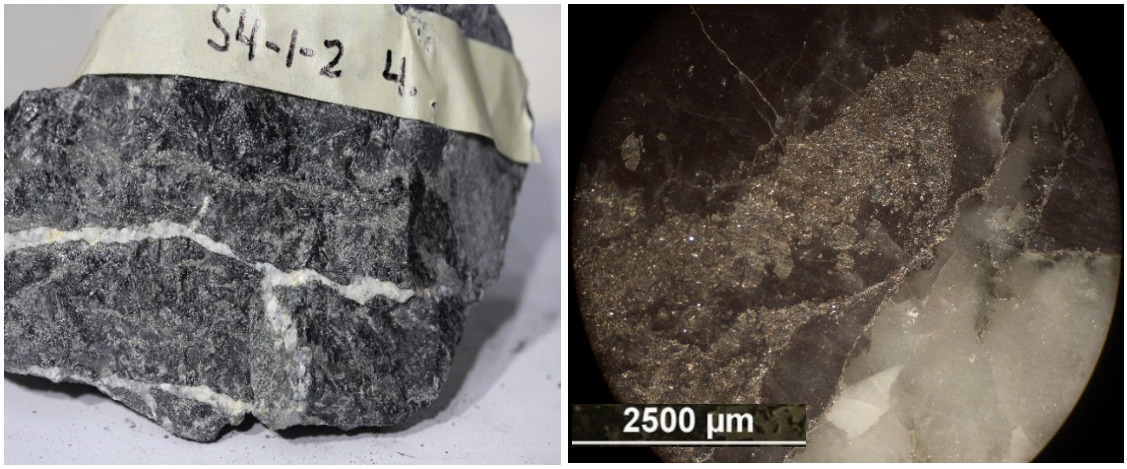

Figure 4-1 Macroscopic and microscopic view of the volcanic mafic host rock. Brecciation is visible as well as the mineralization of the sulphides, quartz and carbonates. The right photo was taken from a stereoscopic microscope.

Mineral textures can be of significant importance for a wide range of metallurgical aspects, such as comminution, liberation and recovery. However, textural classification models are usually subjective and not calibrated against metallurgical performance. (Walters & Kojovic 2008). The mineral textures of the samples tested in this study can be classified in three major categories: Massive - granoblastic, banded - foliated and granoblastic - banded texture. Each sample group is mainly characterized by one texture (Table 4-2). However, due to the heterogeneity of the deposit, both textures can be identified in most sample groups.

Table 4-2Mineral texture classification of all the ore groups

Sample Code	Mineral texture
S425L178-1-2	massive - granoblastic
S425L178-1-1	massive - granoblastic
R190PL227-226-1-2	banded - foliated
R190PL227-226-1-1	banded - foliated
S350L170-1-1	granoblastic - banded
S350L170-1-2	granoblastic - banded

The banded-foliated textures are related to slow lava rework and increased content of fine grained minerals like muscovite and other micas. Muscovite is a soft mineral that has a perfect cleavage yielding remarkably thin laminae (sheets) which are often highly elastic. The massive granoblastic texture is a result of high-pressure metamorphic events. Folded and boudinaged Qz-Cb veins brecciate all the specimens. (Figure 4-2).

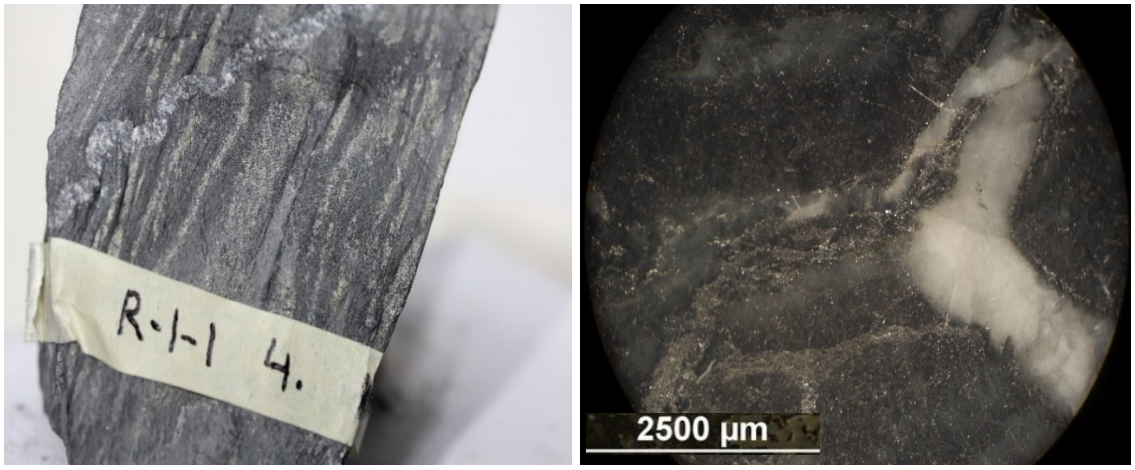

Figure 4-2 Folded and boudinaged Qz-Cb vein. Foliated and layered texture. The image on the right is obtained from the stereoscopic microscope. Sample group R-1-1(4).

The gold-bearing arsenopyrite and pyrite occur disseminated in micro fractures and shear fabrics as a result of the intense micro tectonics which were applied on the deposit during the greenschist-phase metamorphic events which are related to the deposit's origin. (Figure 4-3).

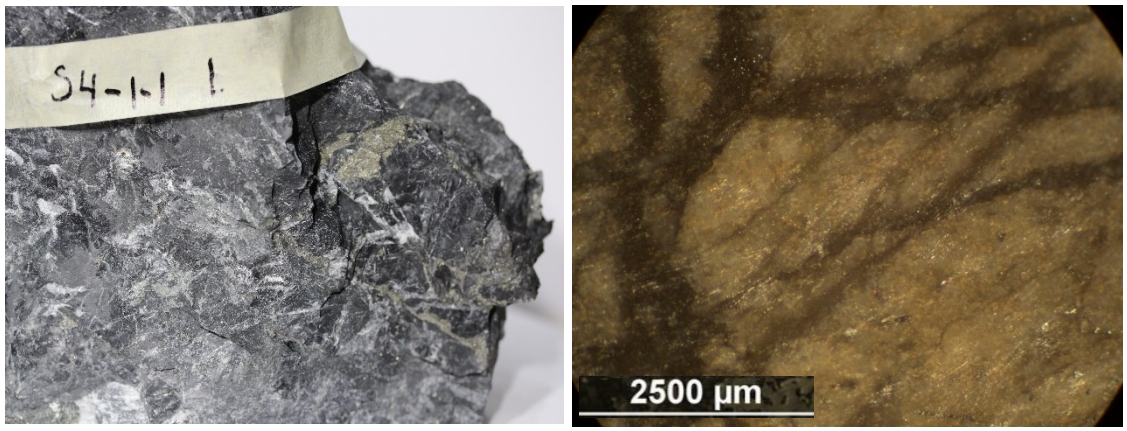

Figure 4-3 Stereoscopic microscope image of pyrite occurring disseminated in micro fractures and shear fabrics. The image on the right is obtained from the stereoscopic microscope Sample group S4-1-1(1).

The

All sample groups used in this study contain graphite in the form of graphitic failure zones ore flakes. Graphite rich zones are characterized by strong shearing and an abundant presence of graphite. Graphite is visible in thin flakes and graphitic alteration. (Figure 4-4). Graphite is fine grained and accounts to an average of (10-15%) of the mineral composition within the sample groups. The comminution of the ore is affected by the failure zones related to graphite, leading to differences in the crushing and grinding indices derived from the comminution tests.

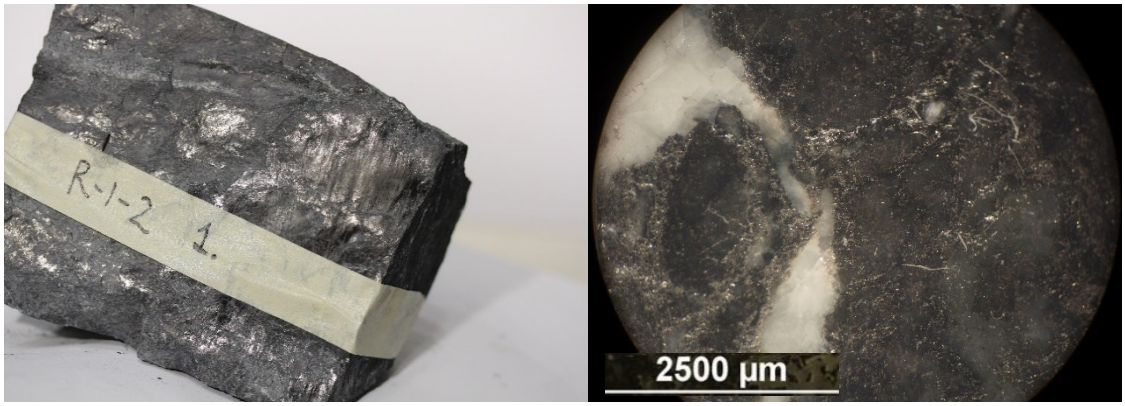

Figure 4-4 Graphite occurrence in flakes and as graphitic alteration. Graphite is visible both in a macroscopic and microscopic scale. The image on the right is obtained from the stereoscopic microscope. Sample group R-1-2(1).

4.2 Scanning Electron Microscope (SEM)

The mineralogy of the samples from the Kittilä deposit in this thesis is mainly determined by the Scanning Electron Microscope (SEM). With SEM, it was possible to estimate the average mineral content of the six sample groups and investigate the connection to breakage mechanisms responsible for the different test results between the sample groups. The modal mineralogy derived from the SEM was used as one of the key proxies to conduct correlations between certain minerals and their influence on geometallurgical behavior.

4.2.1 Equipment description

The electron optical work has been carried out at the FE-SEM Laboratory of the Geological survey of Finland (GTK). Mineral concentrations were analyzed using a Field Emission Scanning Electron Microscope (FE-SEM), model JEOL JSM-7100F Schottky equipped by an Oxford Instruments energy dispersive spectroscopy (Figure 4-5). DS-spectrometer X-Max 80 mm^2 (Silicon Drift Detector). The run conditions were: 20 kV acceleration voltages and 0.5 nA probe current.

INCA Feature phase detection and classification software has been used to characterize the mineralogical composition of the samples. The INCA Feature software performs automatic scans over the sample area and detects the grains using the backscattered electron image by recording size, shape and grey level. Subsequently, the software analyses and classifies the phases by Energy Dispersive X-Ray Spectroscopy (EDS).

From each sample 10.000 individual particles were analyzed. The quality of the EDS analyses is semi quantitative and the results are normalized to 100%. The phase identification is based on the numerical elemental composition. Exact identification of phases is not always possible based on the EDS data. Especially phases/minerals which contain C, OH- or H2O-groups, Be or lighter elements are difficult to positively identify.

Figure 4-5 Scanning Electron Microscope (SEM) basic setup.

4.2.2 Sample preparation

Sample specifications for the Scanning Electron Microscope include core samples with a diameter of 25.44mm and a height of approximately 9.5mm (Figure 4-6). All specimens were made in the ‘’Kivipaja’’ technical laboratory of the civil engineering department in Aalto university. The drill cores were extracted from the bulk specimens received from Kittilä. Once the drill cores were extracted, they were then sawed to the required size. Four samples from each of the six sample groups were used, accounting to a total of 24 samples. The sample surfaces were grinded in three consecutive stages. The primary and secondary grinding were carried out on rotating steel plates with specified roughness, while the third grinding stage was conducted by using sandpapers in an order of descending roughness from P 250 to P 2000. Once the grinding process was completed, the samples were polished in three consecutive steps (3µm, 1µm and 0.25µm). To achieve the highest efficiency in polishing, high performance diamond product was used which contained exclusively polycrystalline diamonds.

Figure 4-6 Polished core samples according to the Scanning Electron Microscope (SEM) sample specifications.

4.2.3 SEM Results

This chapter focuses on the minerals which are related to the comminution behavior of the ore samples. A summary of the average mineral content per sample group is provided in (Table 4-3). Approximately four samples were analyzed per each sample group, corresponding to a total of 24 samples.

Table 4-3 Major minerals identified from SEM for all sample groups

MINERAL (Average %)	R-1-1	R-1-2	S3-1-1	S3-1-2	S4-1-1	S4-1-2
Quartz	20.00	27.80	19.20	19.90	8.10	6.90
Ankerite	24.90	12.50	24.50	28.00	26.20	29.50
Pyrite	8.80	5.80	7.40	7.20	11.80	10.80
Muscovite	13.20	4.20	5.30	6.60	31.80	28.30
Graphite	7.20	11.00	13.90	10.20	19.10	24.00
Arsenopyrite	0.90	1.02	2.87	2.99	4.10	3.88

From the results, it can be concluded that all the sample groups are characterized by a significant amount of quartz, and ankerite. Due to the hardness of these minerals, the ore is harder to crush and grind. Thus, all the samples appear to be relatively hard rocks. The fluctuations in the Qz-Cb content is a key factor to explain the difference in the geometallurgical properties of the six ore types.

In addition to quartz and ankerite, muscovite is a soft mineral with a perfect cleavage, yielding significantly thin, elastic sheets (Vaughan & Guggenheim 1986). Thus, the breakage mechanisms of the ore change, since the micas may form failure zones within the microstructure of the ore. Additionally, an important factor is the orientation of the cleavage. A force which is applied perpendicular to the structural planes will not force the layers to separate, while a force parallel to the cleavage would be more likely to result to tensile failure.

Among the sulphides which are present in the samples, pyrite is the dominant mineral accounting to an average of (7.5-10%) of the mineral content in all sample groups. Furthermore, arsenopyrite comprises approximately (1-4%) of the mineral content. Pyrite veins brecciate all the samples along with the Qz-Cb veins. An illustrative example of the Scanning Electron Microscope from sample group R-1-1 is provided in (Table 4-4). The number of features representing the adequate mineral is provided in respect to the total area of the sample.

Table 4-4 Scanning Electron Microscope results for sample R-1-1 [4]

R114		
Class	Features	% total features
Quartz	2336	43.2
Pyrite	1034	19.1
Muscovite	785	14.5
Ankerite	417	7.7
Feldspar. mixed	252	4.7
Albite	176	3.3
Biotite	133	2.5
Olivine	80	1.5
K-fsp	57	1.1
Wollastonite	37	0.7
Plagioclase	20	0.4
Rutile_Ti-Ox	17	0.3
Apatite	17	0.3
Mg-biotite	13	0.2
Gypsum	11	0.2
Arsenopyrite	10	0.2
Chlorite	5	0.1
Pyrrhotite	5	0.1
Ilmenite	3	0.1
SUM	5412	100

4.3 . Density Measurements

Density measurements for rocks are based on Archimedes' principle that the weight of a displaced fluid has a direct analogy to the volume of the displaced fluid. In simple terms, the principle states that the buoyant force on an object is proportional to the weight of the fluid displacement. Commonly the density of rocks is expressed as specific gravity relative to the density of water. Usually the density of water is 1g/cm3 but if the temperature changes then the density also fluctuates.

For this study, density measurements were conducted for 30 samples, corresponding to five samples per sample group. The average density from each sample group is provided in (Table 4-5) while the detailed report of the measurements is provided in Appendix D. To determine the density, the samples are first weighed on air, when they are still dry, and then they are weighed in water. Based on its temperature of 19°C, the density of the waters density is 0.9984 $kg/m^{3.}$ Equation (1) is used to determine the solid density of the samples. The density range for all sample groups is illustrated in (Figure 4-7).

$$\rho_{solid} = \rho_{water} * \frac{Dry\ weight}{(Dry\ weight - Wet\ weight)} \quad (1)$$

Where,
ρsolid: Solid density (kg/m^3)
ρwater: Water density (kg/m$^{3)}$

Table 4-5 Average solid density values for all sample groups

Sample Code	ρsolid AVERAGE
S4-1-2	2.89
S4-1-1	2.77
R-1-1	3.02
S3-1-1	2.85
S3-1-2	2.75
R-1-2	2.94

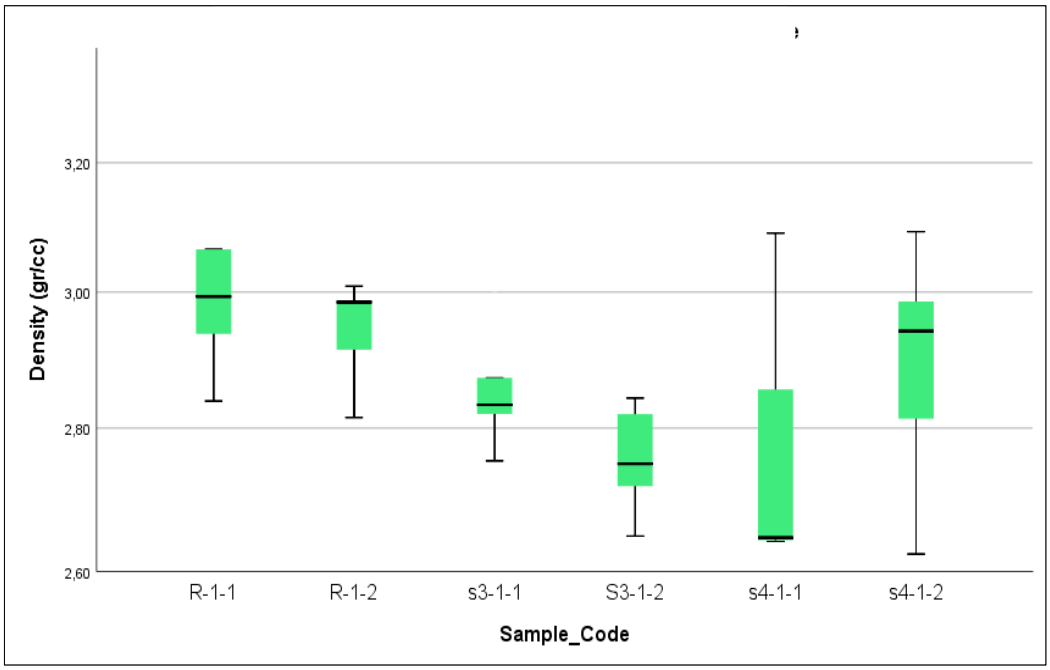

Figure 4-7 Density range for all the sample groups. The horizontal line represents the mean of the values while the green boxplot represents the range.

5 Methods for ore comminution testing

The direct measurements for this study involve the traditional comminution tests that are illustrated in Chart 5-1. The purpose of these methods is to provide information regarding the four pillars of comminution: rock mechanical tests, particle breakage tests, abrasion tests and bench scale grindability tests.

The criteria for the comminution tests to be advantageous and acceptable for this study include simplicity, repeatability, sample requirements and the potential to be linked to comminution modelling.

Rock mechanical tests for rock strength are conducted by means of universal test machines or simplified instruments. Several standard test methods are used, which vary in the loading conditions applied (Russell et al. 2009). For this study, the Point Load test is used since it is a standard method for simple and rapid determination of rock strength with minimum sample requirements.

Particle breakage tests, also known as fracture tests, involve the tests where specimens are broken with certain energy and the particle size distribution of the progeny particles is measured for defining the energy required for size reduction. The simple Drop-Weight test is used in this study due to the simplicity of the test and the minimum sample requirements. (Morrell 2004)

The Bench scale grindability test used in this study is the Bond Ball Mill test, an industry standard used to analyze the grindability of material. Furthermore, attrition and abrasion of the ore are determined through the Los Angeles abrasion test for rocks.

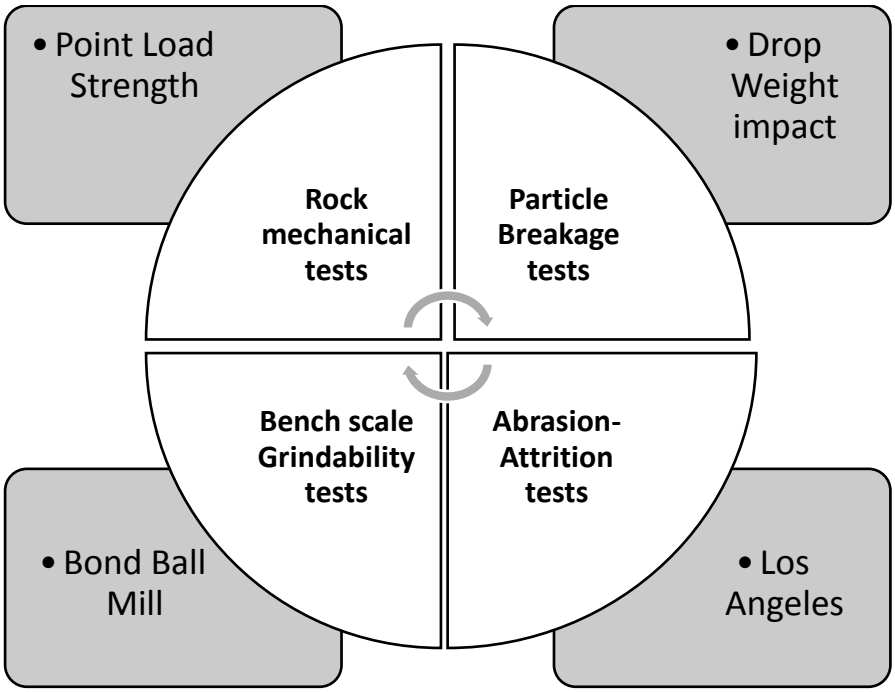

Chart 5-1 Types of comminution tests and the methods applied in this study

5.1 Drop Weight Test

The Drop Weight test was first developed at the Julius Kruttschnitt Mineral Research Centre and was designed to generate rock hardness data for process optimization and circuit design. The Drop Weight test has been commercialized by JKTech and is applied widely through most

metallurgical test laboratories. From the Drop Weight test, it is possible to develop models that give an indication of the likelihood of fracture when an event or events occur where a particle is impacted with some specified amount of energy (Morrell 2004). In other words, drop tests are usually applied for determining the breakage characteristics of ores and other materials, while the data derived from the test can be used for simulating the degradation of ore in handling. The data derived from this specific test is useful for rock mass characterization in mining applications and determination of geometallurgical properties related to comminution. The test is considered a simple and rapid empirical method with minimum sample requirements and is therefore ideal for this study.

5.1.1 Test description

The drop weight device is suitable for determination of the various breakage mechanisms, which characterize different ore types. It is based on the energy generated from the impact of a weight, which performs a free fall on a specified number of particles of the same size fraction. The device comprises a steel drop head, which is raised by a pneumatic winch, then dropped onto the target rock particle and subsequently crushed. (Figure 5-1).

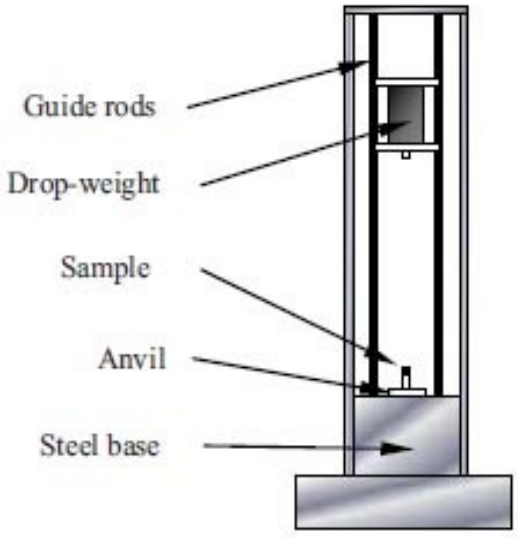

Figure 5-1 Drop Weight Testing device components illustration.

The Drop head used for this test weighed 13.671 kg. In addition to the typical guide rods, the steel head was attached to a single steel rod, which was locked in the required positions and released by an adjustable wrench. The innovative setup is a novelty of the laboratory technicians from the rock engineering laboratory of the civil engineering department in Aalto university. It is considered a prototype due to the single steel rod which comprises the setup. The test material was positioned under the drop weight on a steel anvil. (Figure 5-2). Additionally, support structures were installed to keep the steel base as stable as possible.

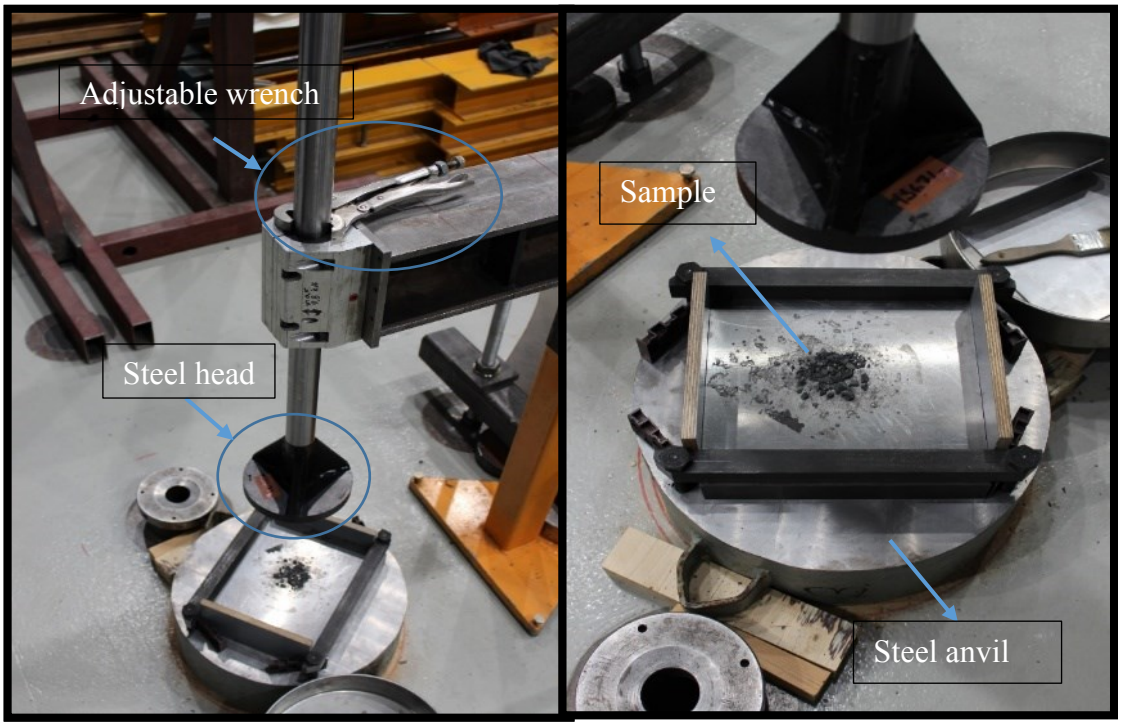

Figure 5-2 Drop Weight Equipment setup.

5.1.2 Test procedure

The test involves breaking particles of various sizes with specific energies in the range of 0.1-4 KWh/t. The particle sizes used and the energies with which they were broken are given in (Table 5-1). The range of specific energies are achieved by adjusting the drop height and drop head mass. The impact energy level is calculated from equation (2), while the specific comminution energy is determined from equation (3). (Wills & Napier-Munn 2005).

$$E_i = m_d * g * (h_i - h_f) \quad (2)$$

Where,

E_i: the impact breakage energy ($m^2 * kg/sec^2$)

m_d: the mass of the drop weight head (kg)

h_i: is the initial height of the drop weight. (m)

h_f: is the final height from the steel anvil, after the impact. (m)

g: gravitational acceleration (9.81 m/s^2)

$$Ecs = \frac{E_i}{m_p} \quad (3)$$

Where,

Ecs: Specific comminution energy (kWh/t)

m_p: Mean particle mass (gr)

The test was carried out for three energy levels per particle size, for four size fractions. In total 72 drops were conducted, corresponding to 12 drops per sample group.

An example of the drop weight specifications regarding the energy levels, particle sizes and number of particles is provided in (Table 5-1), concerning sample R-1-2.

Table 5-1 Drop-weight specifications for sample R-1-2.

Test size fraction(mm)	Nominal test size(mm)	Ecs (KWh/t)	No. of particles broken
-17.0+16.0	16.3	0.25	80
		0.40	80
		0.55	80
-9.5+8.0	8.2	0.54	100
		0.71	100
		1.17	100
-5.5+4.0	4.4	1.03	120
		1.58	120
		1.84	120
-3.5+2.0	2.4	2.47	200
		4.96	200
		7.21	200

After each impact, the breakage product was screened in order to obtain the t10 parameter. The t10 is defined as the per cent passing one tenth of the original particle size and can be considered an index of fineness and is related to the product size distribution. In other words, if the t10 parameter is known the entire product size distribution can be generated.
For a known rock, the t_{10} parameter is related to the specific comminution energy based on equation (4). (Nappier-Munn et al, 2005).

$$t_{10} = A * \left(1 - e^{-b*Ecs}\right) \quad (4)$$

Where:
Ecs: Specific comminution energy (kWh/t)
t_{10}: Percentage of material passing one tenth of the initial particle size sieve
A, b: Drop Weight test parameters that vary according to ore hardness

5.2 Point Load Test

Point load testing is a common geotechnical practice which is widely used to predict rock strength indexes. It is a remote and simple method that can be used in a field setup to determine the uniaxial compressive strength of the rocks (Bieniawski 1975). The test has been around for approximately 46 years and is still being widely applied. It was first introduced in 1972 by Broch and Franklin and incorporated in the ISRM standard practices. There have been multiple researches that improved the specifications of the test as well as the precision of the strength estimations. In the United States, Hassani et al. used the point load tests on core samples to study the relationship of weakness planes in rock core to microstructural defects in the rock

material (Hassani et al. 1980). Their starting point was a simple formulation for strength, which was progressively modified in order to estimate the uniaxial compressive strength of rocks. The point load method enables economical testing of either regular or irregular samples in field and laboratory settings. For this study, only axial core samples are used according to ASTM standards, due to limitations in the amount of samples received from Kittilä.

5.2.1 Test description

This test method can be performed either in the field or in a simple laboratory setting. The test is typically used in the field because the testing machine is portable, little or minimal specimen preparation is required, while specimens can be tested within a short time frame of being collected. Thus, the samples can be tested shortly after being obtained and any influence of moisture condition on the test data is minimized (Broch & Franklin 1972). However, the results can be highly influenced by how the specimen is treated from the time it is obtained until the time it is tested. Thus, it may be required to treat specimens in accordance with ASTM Practice D5079 (Bieniawski 1975) and to consider moisture conditions during the data interpretation. The test does not take into consideration anisotropic factors, which may influence the resulting values.

The procedure involves compressing a sample (regular or irregular) between two conical steel platens until failure occurs (Franklin et al 1985). Usually failure occurs within 10 to 60 seconds and is often sudden; therefore, a peak load indicator is necessary to record the failure load. The test is rejected in the cases where failure occurred in one loading point only. A rigid frame, two-point load platens, a hydraulically activated ram with pressure gauge and a scale that determines the distance between the metal cones comprise the equipment setup (Figure 5-3).

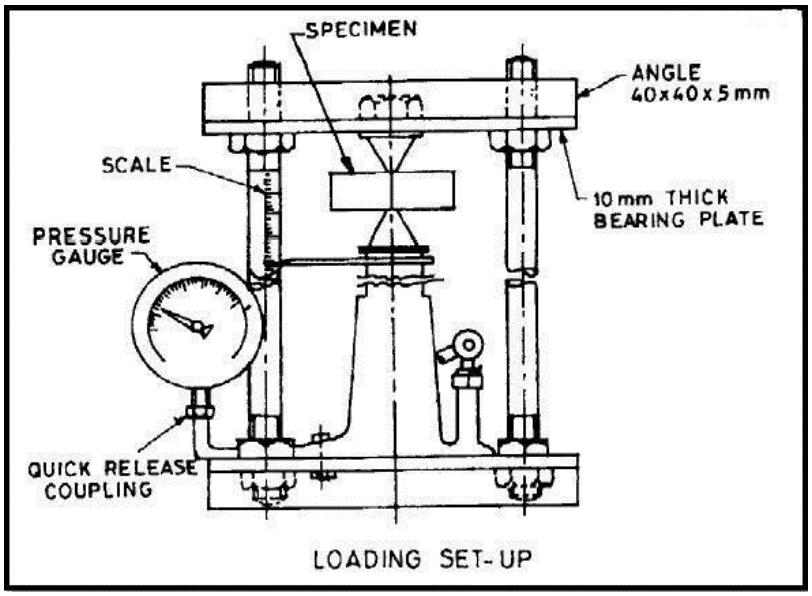

Figure 5-3 Point Load testing machine set up

For the setup used in this study the point load device is connected to a hydraulic pump, which allows for adjusting the pressure flow by adjusting the volume flow valve. The hydraulic pump was installed by the laboratory technicians of Aalto University. By using the hydraulic pump,

it is possible to control the speed at which the test is conducted. The pressure is increased gradually and linearly, not exponentially, which is the case when mechanical pumps are used for the point load test. A sophisticated scheme of the point load setup used in this study is provided in (Figure 5-4).

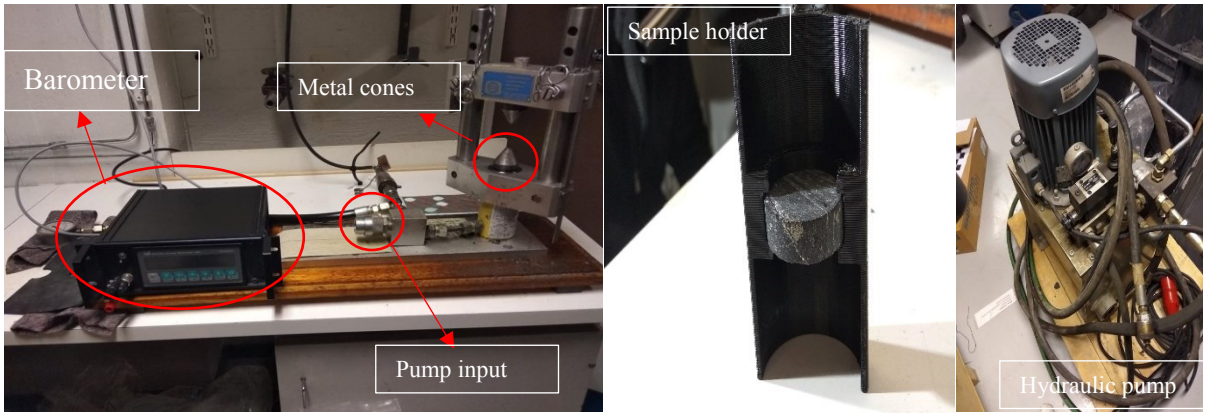

Figure 5-4 Point Load test equipment setup

A digital barometer is connected to the system to measure the applied pressure. It was set so that it would capture the maximum pressure at which failure occurred. Once all $I_s$values are obtained, they are then multiplied with a correction factor of approximately 0.85 to estimate the Is_{50} index. A sample holder was designed with OpenScad 3D-modelling software and printed with LULZBOT mini 3D-printer in order to ensure centralization of the sample during the test. The sample holder was created according to the sample specifications and always placed the sample in such a way that the metallic cones of the point load device would always apply force in the center of the surface.

Sample preparation**:**

The rock samples are divided in six different groups. From each sample group 10 axial cores were extracted, accounting to 60 cores in total. The samples were prepared according to ASTM standards. The size and shape requirements for axial testing shall conform with the recommendations shown in (Figure 5-5). A 25mm reference diameter is used for point load testing in this study (Brook 1980), this being the optimum core size when testing brittle ore. The length of the core sample depends on the type of test (Figure 5-5).

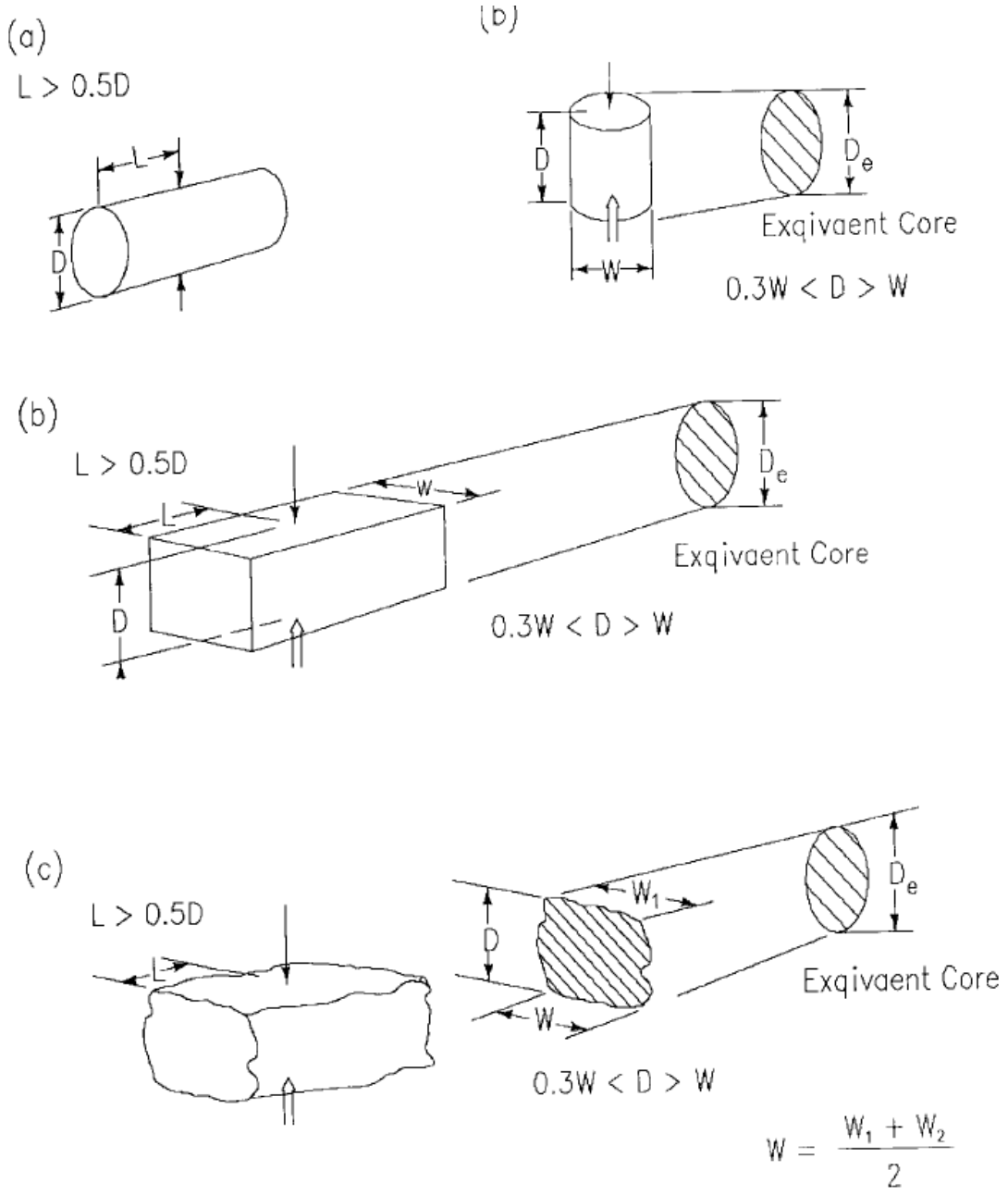

NOTE 1—Legend: L = length, W = width, D = depth or diameter, and D_e = equivalent core diameter

Figure 5-5 Load configurations and specimen shape requirements for (a) the Diametral test, (b) the axial test, (c) the Block test and (d) the irregular lump test (ASTM standards 5731-95)

For this study, only axial tests were conducted due to limitations in the amount of samples and the heterogeneity that characterizes the Kittilä ore. The axial test is conducted on rock core sample of small length. Ten specimens are required to find out the average value of the point load strength index. The test is conducted on the core specimens, which are completely dry. Specimens with a diameter to length ratio of approximately 3/1 is considered suitable for this test (Figure 5-6). The samples were prepared at the ‘’Kivipaja’’ laboratory in the civil engineering department of Aalto University.

$$\frac{\text{Diameter}}{\text{Length}} \cong \frac{3}{1}$$

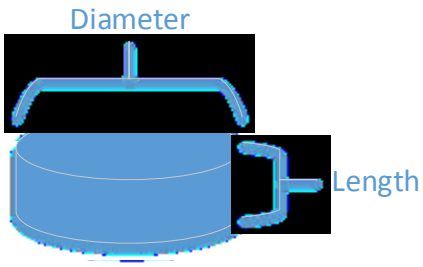

Figure 5-6. Demonstration of the sample specifications for the axial point load test

In order to avoid abrupt irregularities on the sides of the specimens additional grinding was performed on the edges after saw cutting the core samples. The majority of the tests were performed perpendicular to the structural planes of the specimens since that way appropriate test results are obtained. (Ghosh & Sirivastava 1991) The angle between the axis of the core and the structural planes did not exceed 30 degrees according to ISRM standards. 10 tests were performed for each of the six ore-types examined in this thesis, corresponding to 60-point load tests in total.

5.2.2 Test procedure

For the first step of the computations, the uncorrected Point Load Strength Index was calculated for each sample according to equation (5).

$$\mathrm{I_s} = \frac{\mathrm{P}}{{D_e}^2}, (\mathrm{MPa}) \qquad (5)$$

Where,
P: Failure load measured in Newton
D_{e^2}: Equivalent core diameter measured in mm^2, $4A/\pi$ for axial
I_s: Point Load Strength Index

Once the Strength Index (I_s) was determined, a shape correction factor F was implemented in the calculations in order to obtain a representative value, which was used for rock strength classification. With the correction factor a new Is index was determined, the $\mathrm{Is_{50}}$ which is defined as the value of Is which would have been measured by a diametric test with De=50mm. The size correction factor can be obtained from (Figure 5-7).

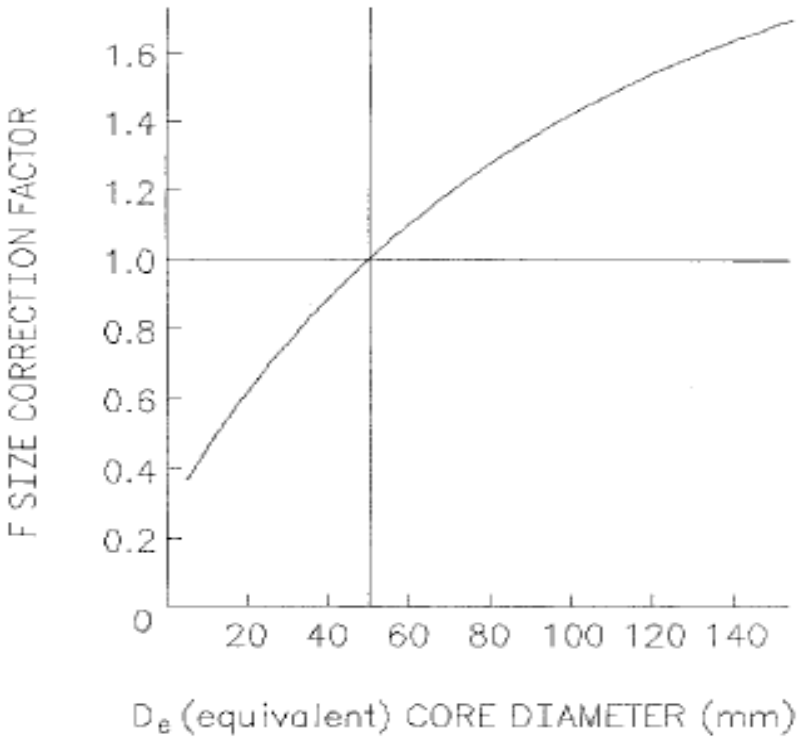

Figure 5-7 Size correction factor for a given equivalent core diameter (Brook 1980)

Once the size correction F is determined, it is possible to acquire the new Point Load Index Is_{50} according to equation (6).

$$I_{s_{50}} = \mathrm{F} * I_s \,, (\mathrm{Mpa}) \tag{6}$$

The data from the Point Load test can be used as a reference to estimate the Uniaxial Compressive Strength (UCS). The UCS is the most common geotechnical property used in rock strength characterization. It is usually the first estimate of the possible issues that are likely to occur during ore excavation and processing. (Rusnak & Mark 2000). The relationship between UCS and the point load strength is described in equation (7) (Bieniawski 1975).

$$UCS = 24 * I_{s_{50}}, (Mpa) \tag{7}$$

In order to achieve more accurate results, a confidence interval has been implemented to the relationship between the Point Load Index and the Uniaxial Compressive strength.
The confidence interval is calculated based on equation (8).

$$CI_{95\%} = 1.96 * \frac{SD}{\sqrt{n}} \tag{8}$$

Where,
SD: The standard deviation of the UCS values estimated from equation (7),
$\sqrt{n}$: The square root of the number of tests conducted.

5.3 Los Angeles Abrasion Test

The Los Angeles abrasion test is a widely used method to measure degradation of mineral aggregates and rock samples of standard grinding procedure. Additionally, the test provides information about rock hardness and resistance to breakage mechanisms. Commonly this is an empirical method used for aggregate classification. However, various studies have indicated that the Los Angeles value correlates positively with ore crushability (Metso 2011) as shown in (Figure 5-8).

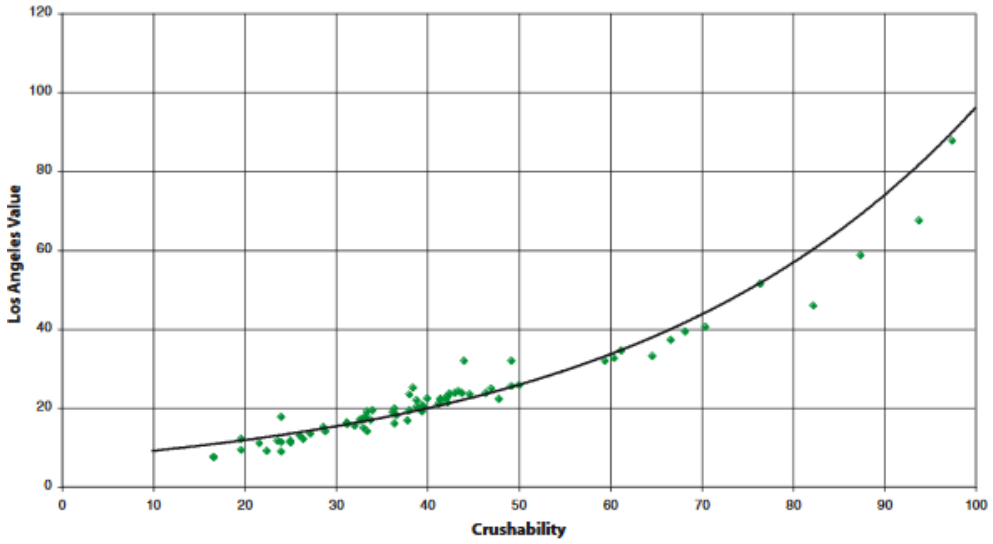

Figure 5-8 Correlation between Los Angeles values and crushability (Metso 2011).

Metso Mining laboratories have conducted hundreds of comminution tests and have been able to identify multiple purposes of use for the Los Angeles test in geometallurgical modelling as explained in Chapter 4.2.

5.3.1 Test Description

The Los Angeles (L.A) test is used in this thesis to determine the crushability of ore specimens from the Kittilä deposit based on size reduction caused by abrasion, when subjected to a rotating drum containing a specified number of steel spheres. Sample preparation includes crushing approximately 5000g of ore to a particle size range between 11.2 and 12.5mm (Cargill & Shakoor 1990). According to ASTM standards, the feed must contain 70% of 12.5mm or 30% of 11.2mm particles. Additionally, a combination of 11 steel balls weighing 445g each were placed in the rotating drum along with the feed. The total weight of the steel balls was approximately 4700g. However, the number of steel balls can be regulated according to the starting weight of the sample. If less material is used to begin with, then the number of steel balls must be less.

The L.A device is comprised by a cylindrical rotating drum, a revolution counter to determine the rounds per minute of the drum, an access cover to seal the drum, and a metallic tray to capture the material after the test is conducted (Figure 5-9).

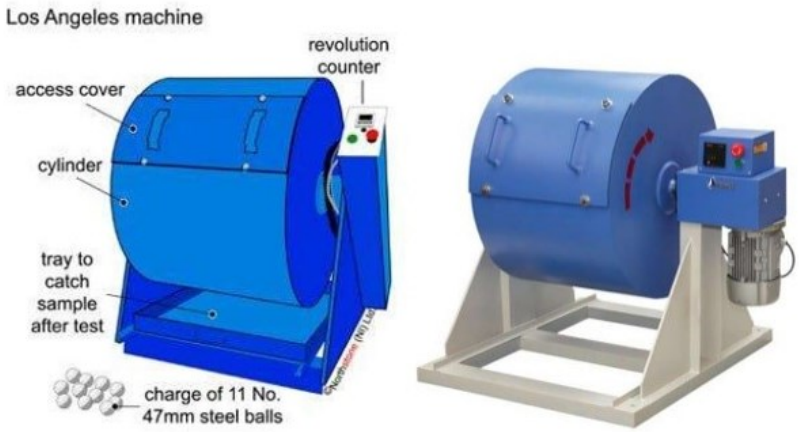

Figure 5-9 Los Angeles abrasion test device configuration

As the drum rotates, the feed particle size reduces due to abrasion and impact with other ore particles and the steel spheres. The breakage mechanisms are illustrated in (Figure 5-7). Once the test is complete, the total mass of ore that has been broken to smaller sizes is expressed as a percentage of the total mass of aggregate. Therefore, lower L.A. abrasion loss values indicate aggregate that is harder and more resistant to abrasion.

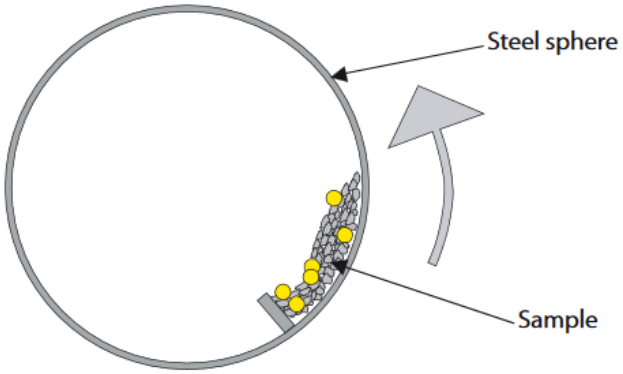

Figure 5-7 Breakage mechanisms during the Los Angeles abrasion test.

5.3.2 Test procedure

After being subjected to the rotating drum, the material is sieved on a No. 12 sieve (1.70 mm) to determine the amount of material passing from the 1.70mm sieve, which is then subtracted from the original weight to obtain a percentage regarding the loss of material. Therefore, an L.A. abrasion loss value of 30 indicates that 30% of the original sample passed through the No. 12 (1.70 mm) sieve.

The loss of material as a percentage of the starting sample mass is determined according to equation (9).

$$Loss = \left(\frac{m_{original} - m_{final}}{m_{original}}\right) \times 100 \quad (9)$$

Where,

$m_{original}$: original sample mass(g)

m_{final}: product sample mass(g)

5.4 Bond Ball Mill Grindability Test

The test has existed for more than 60 years. It was developed by Fred Bond in 1952 and modified in 1961 (JKMRC 2006). Despite the long history of this test, there is little information which explains why the test is done the way it is done. Based on previous research, it is concluded that the test is done this way because of three main reasons. First, to make the test simple and rapid. Secondly, due to sample requirements of approximately 15kg. Finally, the test can give results that are suitable for ball mill scale-up, plant power estimation and for comparing different materials' resistance to ball milling.

5.4.1 Test description

The Bond Ball Mill Grindability Test is a locked-cycle laboratory-grinding test (Lynch 2015). The method was developed to predict the energy required in grinding a ton of ore from a known feed to a specific product size. From the test, the Bond Ball Mill Work Index (BMWi) is calculated, an index used to express the resistance of a material to ball milling. Additionally, this industry standard is used in characterizing the power used in crushing and grinding. More specifically, the plant energy consumption is expressed in kWh per ton of ore in correlation to its grindability.

For this research work a laboratory mill (Figure 5-8) was used with the following special features; the size of the mill is Ø 305 x 305 mm corresponding to 1/100 of a base mill. The frequency of the revolutions (mill speed) can be regulated within wide limits from the control system, while a magnetic sensor is installed on the mill to record the number of revolutions. Additionally, the mill is equipped with all the necessary aids for loading and unloading the sample and separating it from the grinding media.

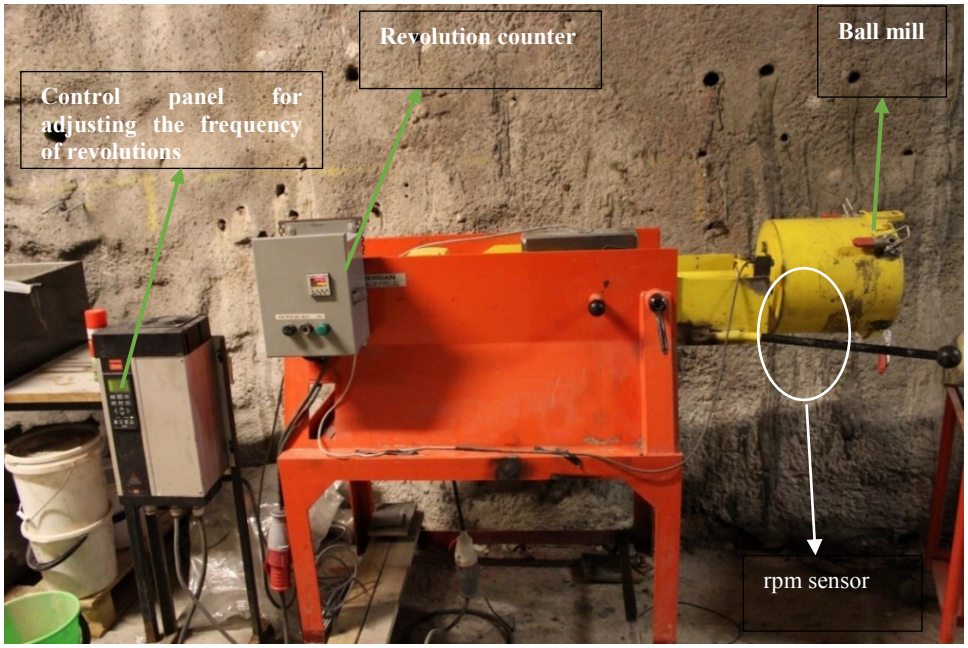

Figure 5-8 Basic ball mill setup including the control system, revolution counter and rpm sensor

5.4.2 Test procedure:

For the first step of the test the ball mill had to be cleaned to avoid contamination with other material, followed by counting and weighing the exact number of steel balls to be used for the grinding test. The charge was composed of 285 steel balls weighing approximately 20.18 kg in total. (Figure 5-9). This particular amount of balls half fills the mill, and it's also the amount where the energy consumption per kg of grinding media is at maximum (Levin 1989). With a smaller ball charge the energy consumption significantly increases while with a heavier ball charge the fore mentioned increase is very slow. The dimension-based blending of the steel ball charge was made according to the industry standards:

- *25 balls of 1-1/2"*
- *39 balls of 1-1/4"*
- *60 balls of 1"*
- *68 balls of 7/8"*
- *93 balls of 3/4"*

Figure 5-9 Steel ball charge for the bond ball mill

Feed

Besides the grinding media, the feed particles have to be analyzed and sized down according to standards. The optimum feed is composed by 10 kg of material which has been crushed down to pass a 3.35mm sieve, (McKen & Williams 2005). Finer feed was used where necessary. The 10kg of material were rifled into 500gr charges. Each charge was sieve analyzed to obtain the F80 value (the sieve size at which 80% of the material goes through). Once the feed was screened, it was placed in a graduated cylinder until it reached 700ml.

Once it was weighed, the material was placed into the mill along with the steel balls and grinded for the first grinding period of 100 revolutions, at a speed of 70rpm. Once grinded, the mill was dumped, the ball charge was screened out and the product was sieved to determine the amount of undersize and oversize material. The closing sieve which defined the under and oversized material was 75 microns according to the industry standards. The aim is to reach a 250% recirculating load, which means that the oversized material will be 2.5 times more than the undersize for 3 consecutive grinding cycles. In other words, the undersize must remain as 1/3.5 of the total material for three grinding rounds in a row. (Rowland 1982).

The 1/3.5 ratio is calculated based on the number of revolutions from the previous cycle and the amount of under size material produced per 1 revolution, also known as Gbp. If Gbp is the ball mill grindability in net g/rev., its value is determined according to equation (10).

$$\text{Gbp} = \frac{\text{mass of 75 microns undersize in grams}}{\text{number of revs of mill}} \qquad (10)$$

Product:

Once the 250% recirculation load was achieved, the undersize from the last grinding cycle was screen analyzed to determine the P80 value, which corresponds to the sieve size at which 80% of the material passes, or else 20% of it is retained.

The Ball Mill Work index (BMWi) is determined from the equation (11) (Magdalinović 1989).

$$W_i = \frac{49.1}{P_1 \times \mathrm{Gbp}^{0.82\times\left(\frac{10}{\sqrt{P80}}-\frac{10}{\sqrt{\mathrm{F80}}}\right)}} \quad (11)$$

Where,
W_i: Work Index, kWh/t
P_1: Closing sieve
Gbp: ball mill grindability in net grams/revolution
P80: Sieve size that 80% of the product passes
F80: Sieve size that 80% of the feed passes

Furthermore, the Plant data W represents the energy consumption in kWh/ton for the calculated bond work index. The formula for the Plant data W is described in equation (12)

$$\mathrm{W} = W_i \times \left(\frac{10}{\sqrt{\mathrm{P}}} - \frac{10}{\sqrt{\mathrm{F}}}\right) \quad (12)$$

In order to adjust the energy requirements for dry grinding to a specific commercial circuit installation, efficiency factors such as open circuit ball milling, oversized feed, diameter efficiency and the ratio of reduction ball milling have to be considered. Based on these factors, the bond model can be used to determine the energy requirement for a specific grinding duty.

Limitations of the Bond Method

There are numerous limitations of the Bond method which have to be considered for this thesis. Older studies (Austin & Brame 1983) have reviewed several of the limitations from this specific test. Possibly the most important in a fundamental sense is Bond's claim that equation (11) can be applied as a universal law. This cannot be possible since the method ignores the fact that the shape of the product size distribution and the corresponding energy consumption are not the same in the case of a locked-cycle test, a steady-state continuous mill and a batch test.

Further limitations include the tendency of the test to be a poor predictor of what happens in a real closed circuit when throughput is constantly fluctuating. As already mentioned, the test does not represent a system where size distribution slopes change. Another limitation is that the test is not a good predictor of the grinding of particles with irregular shapes, although this is a general problem which concerns any method relying on sieving for the determination of particle size. Net energy consumption has to be determined and measured precisely. The number of revolutions required to reduce the ore to a specific size fraction is not enough to accurately calculate the energy consumption. The real input power is dependent on the properties of the material, flow properties and frictional characteristics, not only on the particle size. Due to the fact that heterogeneous materials have been proven to fluctuate strongly at different stages of fineness, it is important that the grinding test is conducted according to the industrial process standards.
Application of the BMWi to AG/SAG mills is limited since it cannot be used directly for process circuit optimization. It is necessary to calculate a work index from operating data, from

a pilot plant, so that the power draw and milling size can be defined. The Bond theory is a physical model which estimates a closed-circuit ball mill, and so product sizing and flowrates of each stream can be extracted. Ongoing research at the JKMRC involves testing the use of this data to define the related parameters for a ball mill model.

6 Results from ore comminution testing

This chapter includes all the results from the comminution tests described in chapter 5. Illustrative graphs are provided in correlation with the test values for each method used.
The results from each method will be described individually, while a summary of the overall values will be provided in the end of the chapter.

6.1 Drop Weight Test

For each sample group, the t10 parameter was calculated. An example of the particle sizes, energy levels and t10% distribution derived from a complete test is given in (Table 6-1). The data corresponds to sample group R-1-2 while the detailed report including the data from all the sample groups is provided in Appendix C-1.

Table 6-1 Drop weight test specifications for sample R-1-2 and its resulting t10 values

Particle size(mm)	Energy levels (Ecs, KWh/t)	Starting weight(g)	Weight(g)passing 10% sieve	t10%
16	0.25	57.2	1.98	3.46
	0.40	78.6	4.48	5.70
	0.55	114.9	8.77	7.63
8	0.54	26.5	1.07	4.04
	0.71	44.8	3.38	7.54
	1.17	53.6	5.24	9.78
4	1.03	13.9	0.527	3.79
	1.58	20.05	0.976	4.87
	1.84	34.1	1.983	5.82
2	2.47	5.8	0.125	2.16
	4.96	6.4	0.29	4.53
	7.21	8.7	0.538	6.18

Once the Ecs (KWh/t) and t10% distribution was determined for all sample groups, breakage functions were established to analyze the data from the test. Specifically, the parameters A and b were derived from equation (4). Non-linear regression was applied on the Ecs and t10% values, with the use of the statistical software SPSS.

An example of the nonlinear regression for sample group R-1-2 is provided in (Table 6-2). A summary of the A*b breakage parameters is given in (Table 6-3).

Table 6-2 Nonlinear Regression Analysis, sample R-1-2

Iteration Number	Residual Sum of Squares	Parameter A	b
1.0	148.983	10.000	1.000
1.1	126.061	3.611	2.167
2.0	126.061	3.611	2.167
2.1	54.151	5.914	2.917
3.0	54.151	5.914	2.917
3.1…	48.140	5.422	4.962
…17.0	46.643	5.655	6.066
17.1	46.643	5.655	6.062
18.0	46.643	5.655	6.062
18.1	46.643	5.655	6.063

		95% Confidence Interval	
Parameter	Estimate	Lower Bound	Upper Bound
A	5.655	3.972	7.338
b	6.063	-7.827	19.954

Table 6-3 The A and b parameters summarized for all the sample groups.

Sample code	A	b	Axb
S4-1-2	6.975	6.085	42.44
S4-1-1	7.155	5.668	40.55
R-1-1	6.446	6.072	39.14
s3-1-1	6.697	5.376	36.00
S3-1-2	6.985	5.061	35.35
R-1-2	5.655	6.063	34.29

The comparison between the A*b index for all sample groups is illustrated in Figure 6-1

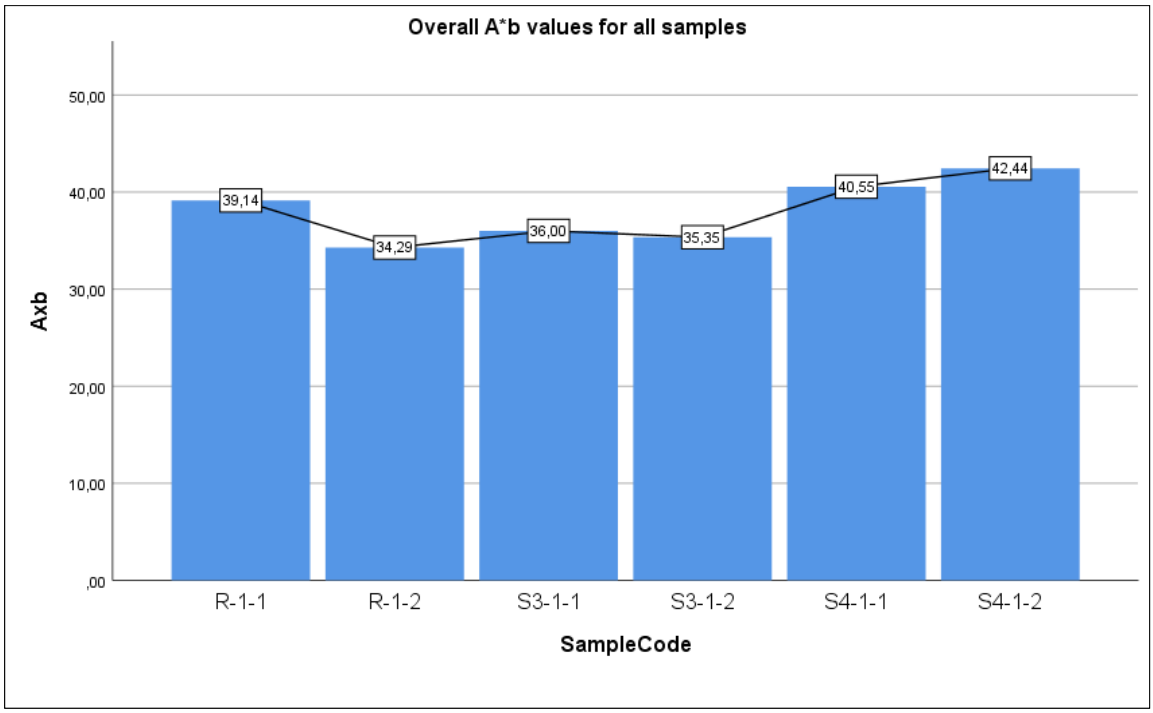

Figure 6-1 A b Drop Weight parameters for all the sample groups.*

The parameters A and b have no physical meaning, but it has been found that the product A x b is a useful index of ore hardness which can be applied to AG and SAG mills for optimization of the process. (Morrell 2009). Higher values of A x b indicate softer ore in contrast to most hardness indicators where higher values indicate harder ores. Based on the A*b drop weight index it is possible to classify the different ore types according to their crushability (Table 6-4).

*Table 6-4 Classification of the sample groups based on their crushability as a function of the A*b parameter from the Drop weight test.*

Sample Group	A*b	Range
S4-1-2	Moderate hard crush	(38-43)
S4-1-1	Moderate hard crush	(38-43)
R-1-1	Moderate hard crush	(38-43)
S3-1-1	Hard crush	(30-38)
S3-1-2	Hard crush	(30-38)
R-1-2	Hard crush	(30-38)

Overall relationship between specific comminution energy and t10 parameter is provided in (Figure 6-2) for sample R-1-2. Nonlinear regression was performed on the test results of each test size fraction to establish the Ecs-t10 relationship by particle size.

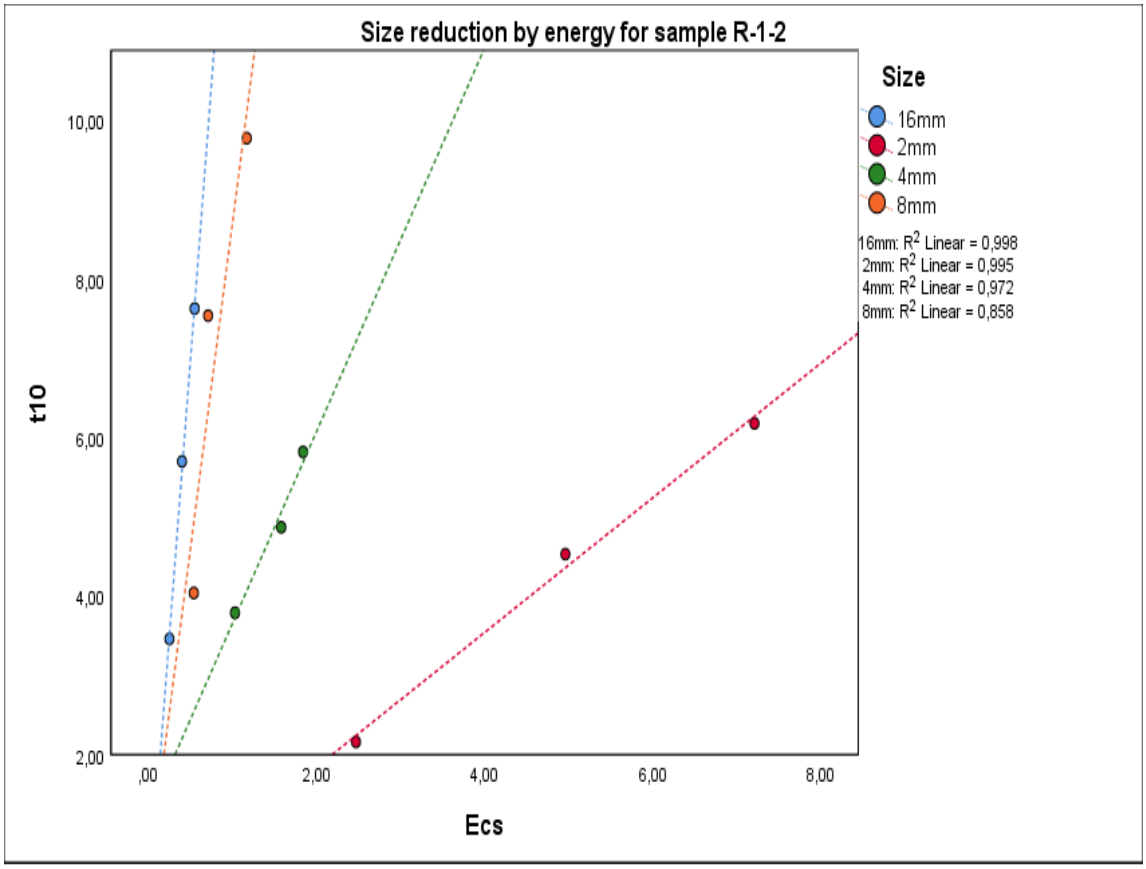

Figure 6-2 Breakage parameter t10% plotted by specific comminution energy for 4 size fractions, sample R-1-2

In principal, it became difficult to break particles by impact as the particle size got finer. It was concluded that the coarsest test size fraction were easy to break, without having to increase the Ecs significantly. On the contrary, the finer particle size reduction could not be easily achieved even though the level of impact energy was highly increased. This can be seen especially in the particle size of 2mm, were the energy was increased from 2.27 KWh/t to 7.21KWh/t but the t10 value barely reached 6%. This condition indicated that the size reduction had reached a limit. Additional comminution energy is required or the comminution mechanism should be modified for further breakage of the ore particles. The Ecs-t10 relationships were plotted for all sample groups, leading to the same conclusion, finer particles were more difficult to break. The Ecs-t10 models are provided in (Figure 6-3).

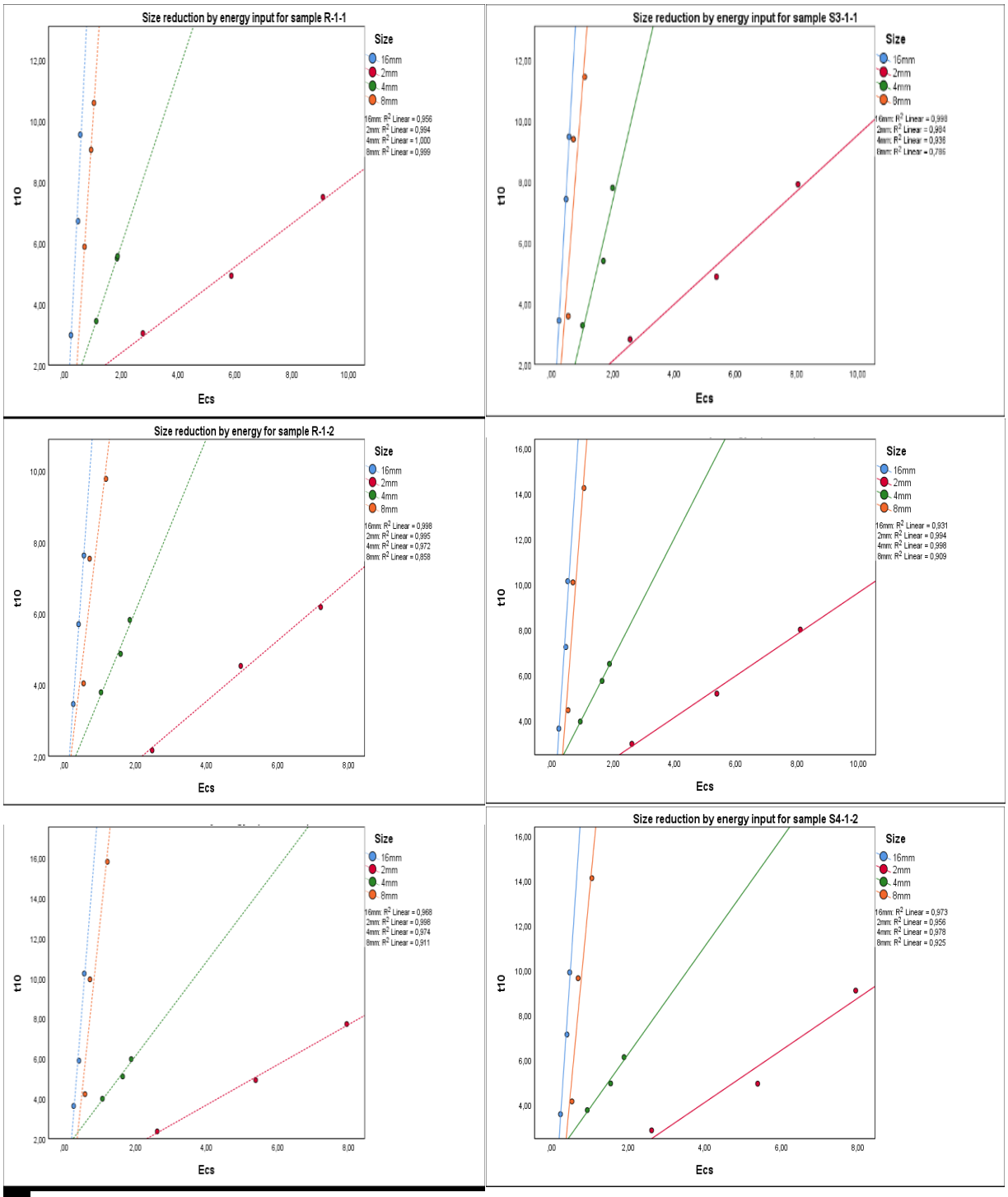

Figure 6-3 Ecs-t10 relationship for all sample groups. The adequate size fractions are color coded according to the legend.

From the findings it is indicated that the Ecs-t10 relationships vary by sample group even for a constant fraction and energy input.(Figure 6-4). These differences are connected to the mineral composition and the microtextures which characterize each rock,as well as the graphite and albite alterations which affect the geometallurgical properties of the ores.

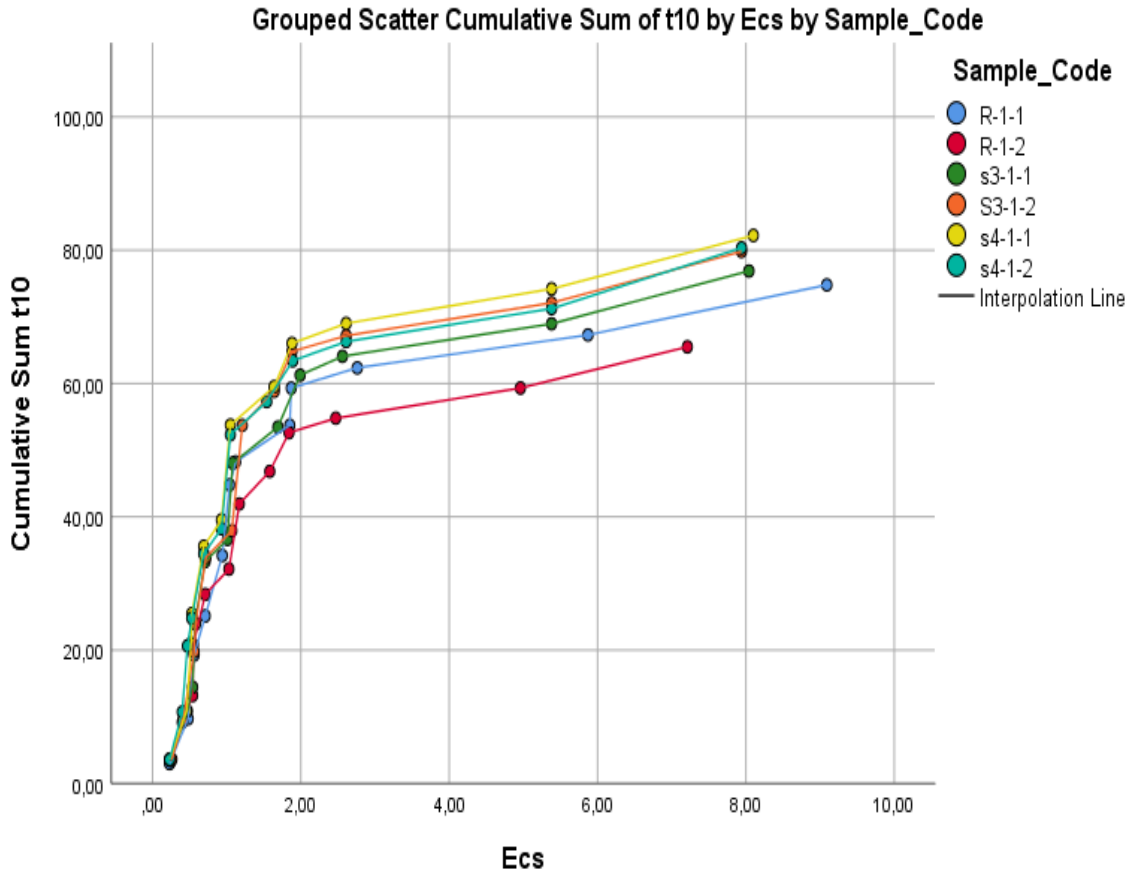

Figure 6-4 Size reduction plotted by specific comminution energy for all sample groups

The relationship between the specific comminution energy and the t10 parameter for the Kittilä ore samples indicated that the impact breakage is particle size dependent. Additionally, the particle size and the A*b breakage index are characterized by a linear relationship. The function which describes the impact breakage would not change significantly for specific comminution energy higher than 2.5 kWh/t.

There is a standard breakage model which was developed at the JKMRC which predicts the behavior of t-curves as a function of the t10. The distribution is used in AG/SAG modelling and is based on the fact that the t-curves for most brittle ores behave in the same way, which make calculations much easier. The Standard appearance function data used in JKMRC AG/SAG modelling is provided in (Table 6-5).

Table 6-5 Standard breakage function developed by JKMRC

t10 (%)	t75	t50	t25	t4	t2
10	2.33	3.06	4.98	23.33	50.53
30	6.89	9.41	15.62	61.58	92.49
50	10.32	14.71	25.88	82.86	96.47

In order to provide more easily understood Drop Weight Test results, an additional parameter has been included to determine the specific energy in KWh/t utilized by a standard SAG mill in a closed circuit. This parameter is called SAG Circuit Specific Energy (SCSE). The relationship between the A*b parameter and the SCSE for the standard circuit is provided in (Figure 6-5).

In AG/SAG milling, the particle size degradation is achieved by impact, abrasion and chipping. Impact will lead to the breakage of an entire particle into smaller pieces, while abrasion and chipping will leave the original particle mostly intact, the products being mostly fine particles.

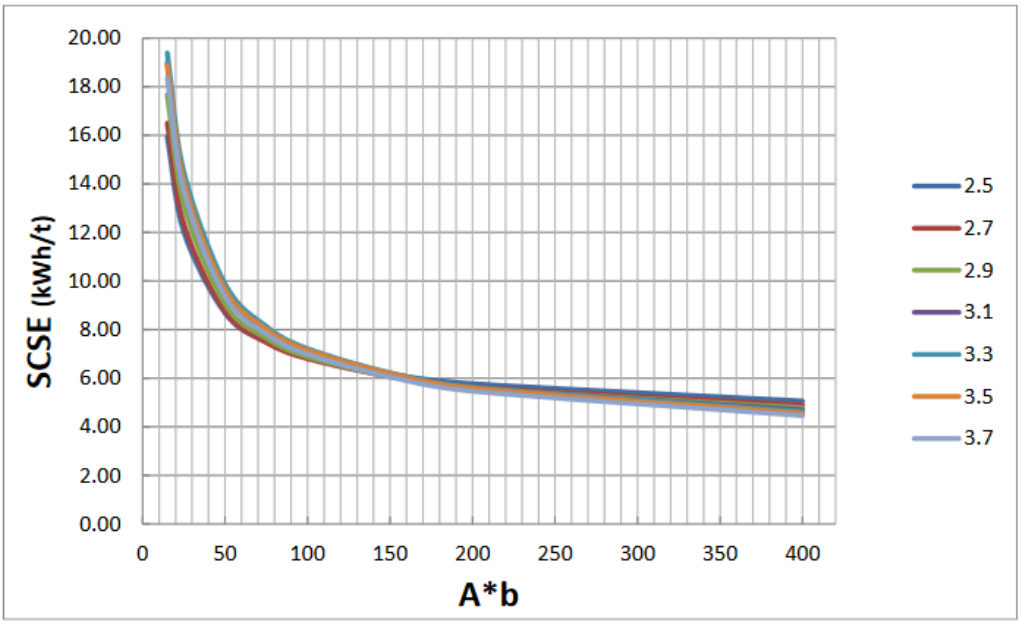

*Figure 6-5 The relationship between A*b and specific energy for the standard circuit (image courtesy JKMRC)*

In AG/SAG mills it is important to consider the specific gravity of the ore since it has a significant effect on the charge density and the power draw. However, it is common in processing plants that the ore types are blended and therefore the specific gravities are mixed. This has to be taken into consideration when trying to forecast the metallurgical behavior of the ore. The second part of the JK Drop Weight test is the abrasion breakage low energy test, which measures the resistance of the ore to abrasion. The SCSE and t_a can be approximated from the A*b breakage index, according to the classification in (Table 6-6).

Table 6-6 Typical parameters for the JK Drop weight test (data courtesy JKMRC)

Property	Very hard	Hard	Moderate hard	Medium	Moderate soft	Soft	Very soft
Axb	<30	30-38	38-43	43-56	56-67	67-127	>127
t_a	<0.24	0.24-0.35	0.35-0.41	0.41-0.54	0.54-0.65	0.65-1.38	>1.38
SCSE	>10.7	10.7-9.7	9.7-9.3	9.3-8.4	8.4-7.9	7.9-6.5	<6.5

A limitation to the Drop Weight test is the fact that it does not consider the effect of the particle shape. The particles behave differently when they are flaky, non-flaky, regular or irregular. Specifically, the flaky particles are expected to align themselves during impact in such a way that they behave like smaller particles, presenting their longest dimensions parallel to the impact face.

The Drop weight test provides the exact same data to the twin pendulum test for single particle breakage. However, there are multiple advantages that transfuse the test as a more efficient and simpler one to use. These advantages are mostly the extended input energy range of the test, the shorter test duration, the extended particle fraction range, the better accuracy of the test and finally the possibility to conduct particle bed breakage studies.

6.2 Point Load Test

When estimating the mean value of the Is(50) the extreme values are not included. The highest and lowest values are excluded from the statistical mean calculation. An illustrative example of the calculations followed to determine the Point Load Strength Index for sample group S4-1-2 is provided in (Table 6-7). In summary, ten point load tests are carried out for each sample group. Only axial cores are used in this study. Additionally, the samples were prepared in such a way that the force from the steel cone platens is applied parallel to the direction of the structural planes of the sample.

Table 6-7. Point Load Strength Index report for sample group S4-1-2

Test no.	Type	W(mm)	D	P(bar)	De 2	Is	Is_{50}	Is_{50} MEDIAN
1	a //	11.5	25.44	3.42	647.19	5.28	5.28	5.28
2	a //	8.9	25.44	3.49	647.19	5.39	5.39	
3	a //	9.96	25.44	4.43	647.19	6.85	6.85	
4	a //	8.92	25.44	2.96	647.19	4.57	4.57	
5	a //	11.7	25.44	4.4	647.19	6.8	6.8	
6	a //	8.68	25.44	3.04	647.19	4.7	4.7	
7	a //	11.77	25.44	3.3	647.19	5.1	5.1	
8	a //	10.34	25.44	5.22	647.19	8.07	8.07	
9	a //	8.34	25.44	3.4	647.19	5.25	5.25	
10	a //	9.66	25.44	3.1	647.19	4.79	4.79	

A detailed report for all the sample groups together is provided in Appendix B. The summary of the results is provided in (Table 6-8), including the mean values of the Point Load strength index and the standard deviations, which characterize the test results.

Table 6-8 The point load strength index for all sample groups and their standard deviation.

Sample Code	$\mathbf{Is_{50}}$ MEDIAN	$\mathbf{Is_{50}}$ (SD)
S4-1-2	5.28	0.77
S4-1-1	5.56	1.04
R-1-1	5.59	1.00
S3-1-1	6.83	1.39
S3-1-2	7.01	1.12
R-1-2	7.53	0.89

From the results, it can be concluded that the sample groups appear to have similar values however the fluctuations in their strength index are a result of the variation in the microstructure and mineral composition of the specimens. The range of the Is_{50} values are illustrated in (Figure 6-6). The horizontal line represents the mean Is_{50} value.

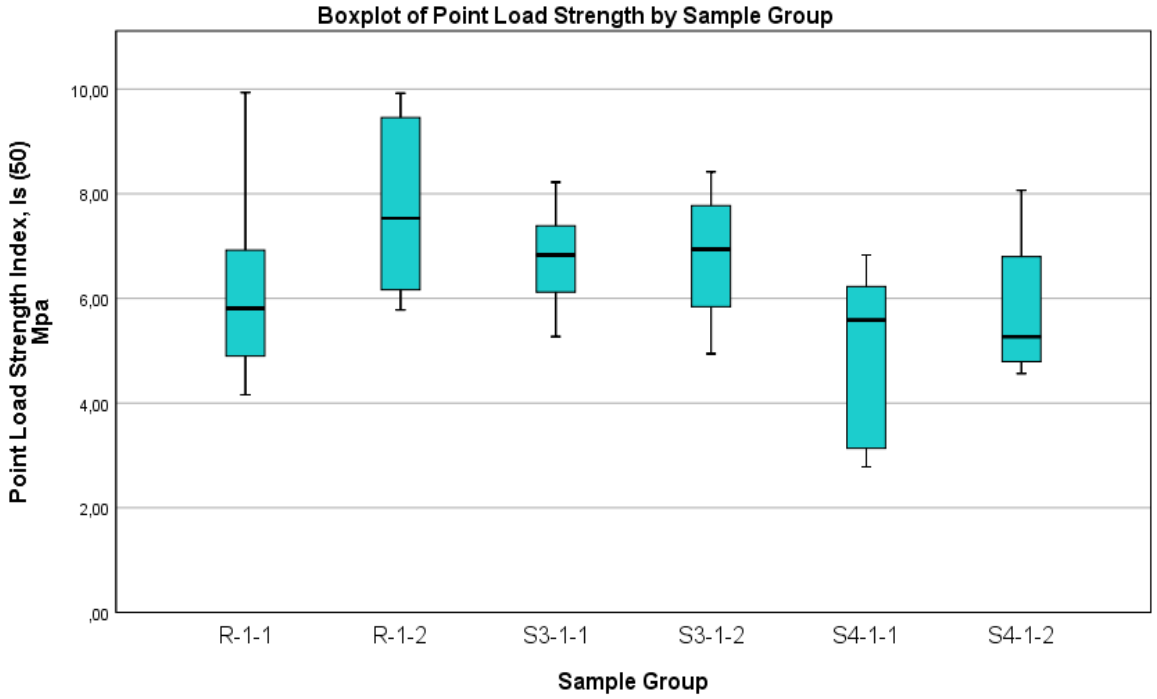

Figure 6-6 The range of Point Load Strength Index values per sample group.

The summarized results from all the sample groups are provided in (Table 6-9), including all the UCS values and the Is_{50} values. Extreme values were not included in the median calculation. The reason for the difference in the UCS values is the mineralogical heterogeneity which characterizes the particular ore group. Minerals like quartz, micas, pyrite and graphite affect the geometallurgical properties of the ore in such a way that the Uniaxial Compressive Strength of the ore types may vary significantly.

Table 6-9 Summary of the results from the Point Load test and estimation of the UCS median and standard deviation per sample group.

Sample Code	Is_{50} MEDIAN	UCS MEDIAN	UCS SD
S4-1-2	5.28	126	37.8
S4-1-1	5.56	134	37.5
R-1-1	5.59	139	31.2
S3-1-1	6.83	164	23.6
S3-1-2	7.01	167	28.2
R-1-2	7.53	181	27.0

Most extreme values and the highest standard deviation were noticed in sample groups S4-1-1 and S4-1-2. (Figure 6-7).

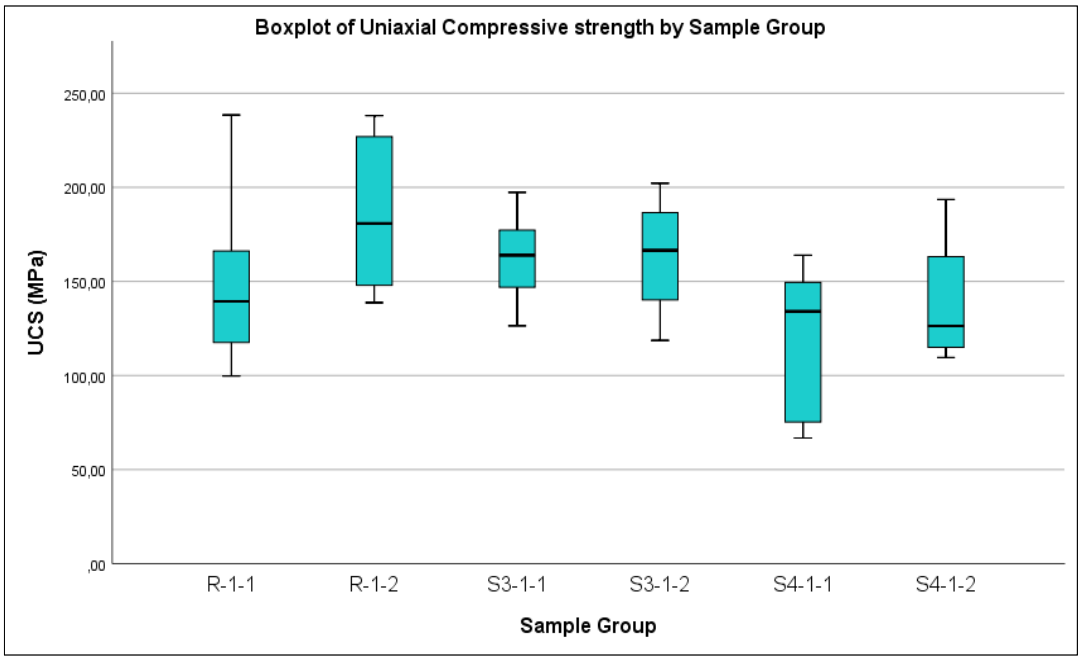

Figure 6-7 The range of the Uniaxial Compressive Strength values for each sample group.

According to the engineering classification of intact rock on basis of strength (Deer and Miller, 1966) all the sample groups are categorized as High Strength rocks (Table 6-10)

Table 6-10 The engineering classification of intact rock on basis of strength (Deer and Miller, 1966)

Class	Uniaxial Compressive Strength(Mpa)	Description
A	>200	Very high strength
B	110-220	High strength
C	55-110	Medium strength
D	27.5-55	Low strength
E	<27.5	Very low strength

6.3 Los Angeles Abrasion Test

Results from six sample groups are in total. The amount of steel balls placed in the drum is adjusted to the original weight of the feed. The overall data from the test is provided in (Table 6-11).

Table 6-11 Los Angeles abrasion test sample specifications and test results.

Sample code	W1(g)0	no.Balls	Wballs(g)	W2(g) 1.6mm	LosAngeles(%)
S3-1-1	4000	9	3870	3139.7	21.51
S4-1-1	3514	8	3440	2795.0	20.46
S3-1-2	4985	11	4730	4076.0	18.23
R-1-2	4923	11	4730	4120.0	16.31
R-1-1	4000	9	3870	3212.0	19.70
S4-1-2	5001	11	4730	3993.0	20.16

The sample groups were classified as moderately hard rocks based on their resistance to abrasion. In summary, sample group R-1-2 appeared to have the highest resistance to abrasion, while S3-1-1, S4-1-1 and S4-1-2 had the lowest resistance to abrasion (Figure 6-8).

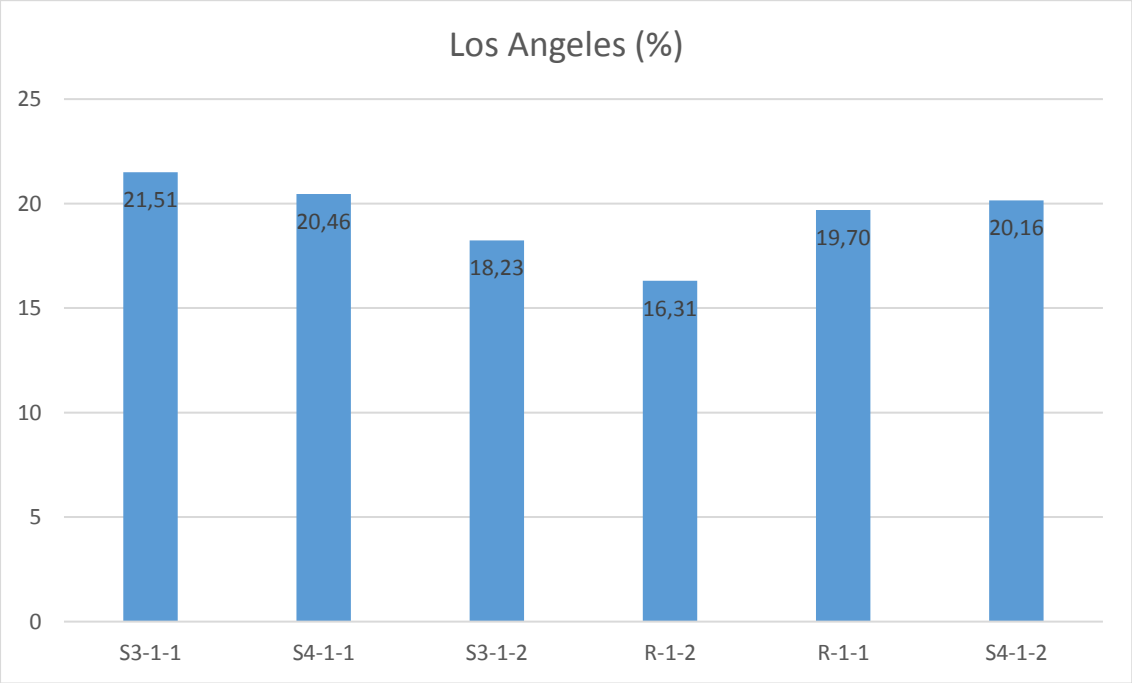

Figure 6-8 The L.A abrasion values for all the sample groups

6.4 Bond Ball Mill Grindability Test

The Bond grindability test is conducted in five grinding stages per each sample group. The first cycle is carried out with an initial setting of 150 revolutions (Bond 1953). Additionally, a closing sieve of 125µm is used to determine the mass of passing and retained material. Based on the mass of the oversized (>125 µm) and undersized (<125 µm) material, the required mass to refill the mill is calculated (Table 6-12). Before placing the refill in the mill together with the oversized from the previous cycle, a screen analysis is carried out for the required refill in

order to determine the amount of undersized and oversized material. Mill losses are taken into consideration. The target is to achieve a 250% recirculation load for three consecutive cycles. This meaning that the oversized material produced per cycle has to be 2.5x times the amount of undersized material for three cycles. (Bond 1953).

An example of the whole process is provided in (Table 6-12), regarding sample group S3-1-2. The same methodology is applied on all six sample groups. The detailed calculations for all sample types are illustrated in Appendix B.

Table 6-12 An example of the calculations required to define the grindability parameters for the Bond Ball Mill test. Sample group S3-1-2.

			A	B	C	D	E	F	G	H	
Grinding stage	Mill revs reqd. revs	Mass +125 µm produced g	Mass - 125 µm produced g	Loss from milling g	Refill mass Reqd g	Total refill used g	Mass -125 µm in refill g	Mass - 125 µm from milling g	Mass -125 µm per rev g	250% recyl g	Revs for next run
Initial feed	-	-	-	-	1346.3						
1	152	1096.8	245.7	3.8	249.5	1346.3	94.1	155.4	1.02	367.2	359
2	359	1011.8	327.3	7.2	334.5	249.5	17.4	317.1	0.88	361.3	409
3	409	984.6	358.9	2.8	361.7	334.5	23.4	338.3	0.83	359.4	435
4	435	923.1	417.2	6	423.2	361.7	25.3	397.9	0.92	355.1	388
5	388	973.4	369.2	3.7	372.9	423.2	29.6	343.3	0.88	358.6	405
6	405	966.7	378.5	1.1	379.6	372.9	26.1	353.5	0.87	358.1	410
Column calculations					A + B	C of last run	D * Y	C - E	F/revs	Z-C*Y	H/G

The information about the feed and product analysis is provided in (Table 6-13). The F80 and P80 represent the 80% of material passing from the closing sieve (125 µm) both in the feed and the product respectively.

Table 6-13 F80 and P80 analysis for sample group S3-1-2

Starting weight		1346.3					
Feed				Final product			
Sieve size microns	Grams stayed	Grams passed	Cum % Pass	Sieve size microns	Grams stayed	Grams passed	Cum % Pass
3500	0	1346.3	100 %	125	0	378.5	100 %
3150	120.7	1225.6	91 %	88	73.2	**305.3**	**81 %**
2500	142.6	**1083**	**80 %**	75	58.2	247.1	65 %
2000	414.8	668.2	50 %	63	71.2	175.9	46 %
1000	271.6	396.6	29 %				0 %
350	203.5	193.1	14 %				0 %
250	36.6	156.5	12 %				
125	62.4	94.1	7 %				
Y	94.1	0	0 %				

The product distribution ranges from 125 microns to 63 microns, while the feed ranges from 3150 microns to 125 microns (Figure 6-9).

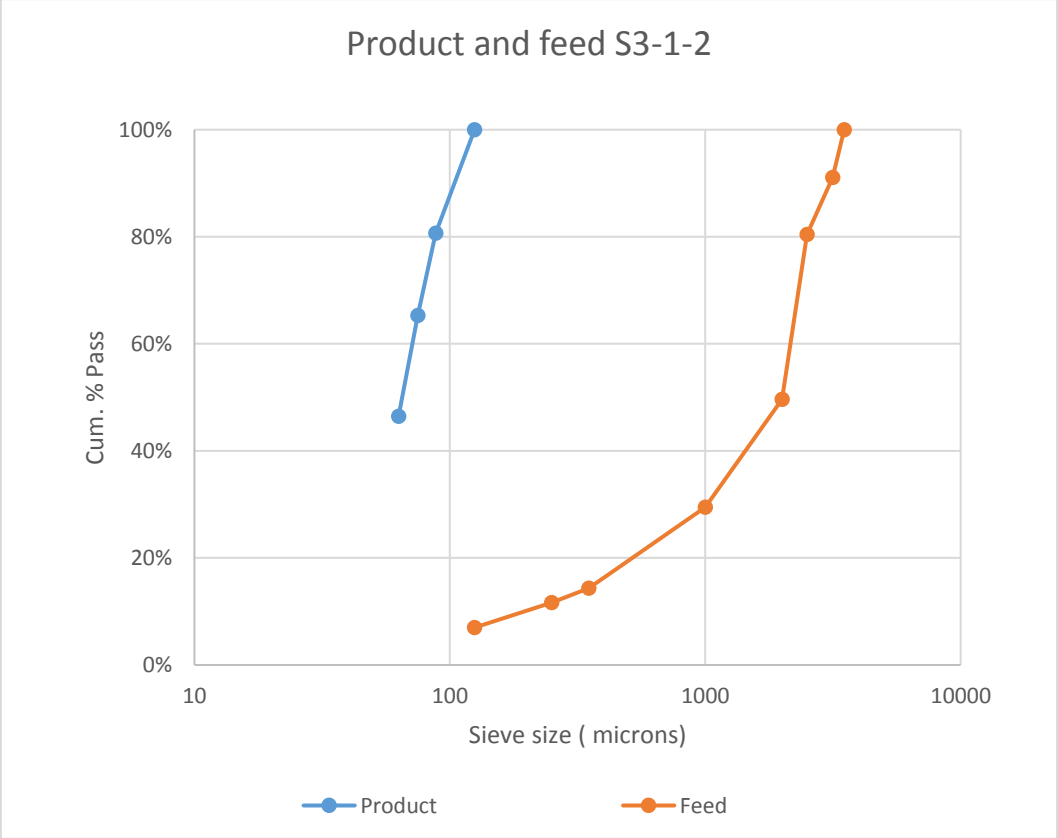

Figure 6-9 Graphic representation of the F80 at 2500 microns and P80 at 87 microns

The Bond Work Index and the Plant energy consumption are calculated based on equations (11) and (12) from Chapter 5.4.2. The same process is followed for all the sample groups, leading to six different BMWi and six different Plant data W values in total (Table 6-14).

Table 6-14 Cumulative results and information derived from the bond ball mill grinding test, including plant data, feed and product analysis.

Sample	Mass of feed	Feed F80	Product P80	Bond Work Index	Plant data W
	(g)	(μm)	(μm)	(kWh/ton)	(kWh/ton)
S3-1-1	1380.6	2597	85	20.15	17.90
S3-1-2	1346.3	2500	87	20.39	17.78
S4-1-1	1314.4	2469	92	18.32	15.41
S4-1-2	1274.5	2500	95	17.14	14.16
R-1-1	1395.3	2531	87	17.75	15.50
R-1-2	1384.8	2352	95	21.55	17.66

From the results it is concluded that the Bond Work Index ranges between 17.14 and 21.55. Energy consumption in kWh/t is relevant to the Bond Work Index, therefore the samples with higher BMWi require more specific comminution energy to reduce the particle size.

Based on the results, the more resistant to grinding the ore is, the lower the corresponding P80 value seems to be in comparison to ores that are easier to grind. The controlling factor that explains this relationship is the Gbp values. As stated in Chapter 5.4.2, Gbp represents the amount of under size material produced per 1 revolution, resulting to the ball mill grindability in net g/rev. Lower Gbp leads to an increased number of revolutions in order to achieve a 250% recirculation load. When compared to tests where other closing sieves were used, the P80 values seem a lot smaller in comparison. (Bond 1961) states that if the P80 value can't be found from particle size analysis results, P80 value of 50μm
should be used when a closing sieve of 75μm is applied. For comparison, when a 150μm closing sieve is used, then the P80 value of 114μm should be used.

It should be noted that sample group R-1-2 seems to be the most resistant to grinding while group S4-1-2 seems to be the least resistant to grinding (Figure 6-10). Another important factor to be mentioned is the fact that material is not homogenous to grinding when ground to different size. Due to the heterogeneity of the mineral composition. Consequently it can be concluded that the Bond Work index is not a material specific constant but that it changes depending on the size the product is ground to. It is therefore acceptable that when the material is ground to a finer size, more comminution energy is consumed in the process.

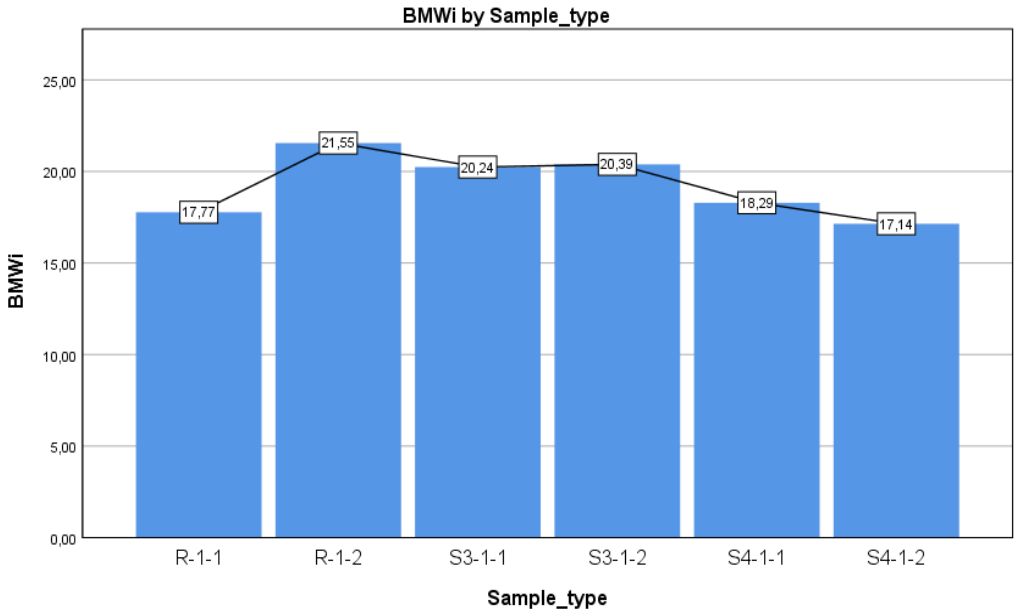

Figure 6-10 Bond Mill Work index for all the ore groups

Based on the bond mill work index it was possible to classify the different ore types (Table 6-15) into three categories, moderately hard, hard and very hard to grind based on the range limits provided by (Lenin 1989).

Table 6-15 Ore type classification based on Bond Grindability (Levin 1989)

Sample Code	BMWi	Range
S4-1-2	Moderate hard grinding	(16-18)
S4-1-1	Hard Grinding	(18-20)
R-1-1	Moderate hard grinding	(16-18)
S3-1-1	Hard Grinding	(18-20)
S3-1-2	Hard Grinding	(18-20)
R-1-2	Very hard grinding	>20

In principal, the mineral content, textures and micro structures control the breakage mechanisms which result to the corresponding grindability values from the Bond Grindability test. It is difficult to distinguish which are the controlling factors in each case, due to the heterogeneity which characterizes the ore types and the significant amount of graphitic and albitic alteration that have occurred during the green-schist metamorphic phase at which these rocks were formed.

The BMWi can be used as a reference to estimate the range of the Uniaxial Compressive Strength (UCS) of the different ore types according to (Table 6-16). All sample groups are classified as hard rocks except sample group R-1-2 which is classified as very hard. These classifications are based on the BMWi values from (Table 6-15).

Table 6-16 Relationship between Ball Work Index and Uniaxial compressive strength (UCS)

Property	Soft	Medium	Hard	Very Hard
UCS(MPa)	50-100	100-150	150-250	>250
BMWi	7-9	9-14	14-20	>20

6.5 Summary of results

The results from all the comminution tests are summarized in (Table 6-17). The Uniaxial compressive strength indicated in the summarized results represents the average value from ten point load tests, in order to have one value per sample group. It is concluded that the differences in the test results are consistent within the sample groups, therefore the tests can be done with good reproducibility. (Table 6-17) provides a basis for principal component analysis and statistical interpretation of the covariance between the tests. Furthermore, these values are correlated with the mineral composition provided from the SEM results in order to identify the relatedness between geometallurgical properties and mineralogy.

Table 6-17 Summarized results from all comminution tests

Sample Code	Los Angeles(%)	BMWi(kWh/t)	UCS from PL(MPa)	Drop Weight (A*b)
S4-1-2	20.16	17.14	126	42.44
S4-1-1	20.46	18.29	134	40.55
R-1-1	19.7	17.77	139	39.14
S3-1-1	21.51	20.24	164	36
S3-1-2	18.23	20.39	167	35.35
R-1-2	16.31	21.55	181	34.29

7 Discussion

It appears that the results from the comminution tests are consistent. This allows for correlations to be carried out in order to determine the relationship between the various test indices and the corresponding mineral composition. Additionally, the relatedness between the indices is examined in Chapter 7.6 in order to provide a basis for empirical estimation of one comminution index from another.The statistical method used to interpret the relationship between the comminution tests and the mineral composition is multicollinearity. In statistics, multicollinearity is a phenomenon in which one predictor variable in a multiple regression model can be linearly predicted from the others with a substantial degree of accuracy. Multicollinearity refers to a situation in which two or more explanatory variables in a multiple regression model are highly linearly related. We have perfect multicollinearity if the correlation between two independent variables is equal to 1 or −1. In practice, it is very rare to face perfect multicollinearity in a data set. More commonly, the issue of multicollinearity arises when there is an approximate linear relationship among two or more independent variables.

The variation in the crushability properties of the six sample groups is related to the different mineralogical and textural characteristics described in Chapter 4. It appears that the sample groups that are rich in quartz, carbonates (ankerite) and sulphides (pyrite and arsenopyrite) are more resistant to crushing and grinding. These sample groups are R-1-1, R-1-2, S3-1-1 and S3-1-2. In contrary, the samples that contain more micas (muscovite) and graphite are softer and therefore easier to crush and grind. These groups are S4-1-1 and S4-1-2.

*7.1 Correlation between Drop Weight A*b index and mineral composition*

The correlation between the Drop Weight test and the mineral composition appears to be significantly positive with sulphides and muscovite content, while the carbonates and graphite have a weaker correlation. (Figure 7-1). Furthermore, there is a strong negative correlation with the quartz content. This implies that the quartz-rich samples were more resistant to particle breakage while the sulphide and muscovite rich samples were easier to crush to smaller particles. The soft crush is a result of the brecciation caused by the sulphides and the structural features that are related to micas.

		Quartz	Sulphides	Ankerite	Muscovite	Graphite
Drop.Weight	Pearson	-.900	.937	.632	.920	.706
	Sig(2 tailed)	.014	.006	.178	.009	.117
	No. groups	6	6	6	6	6

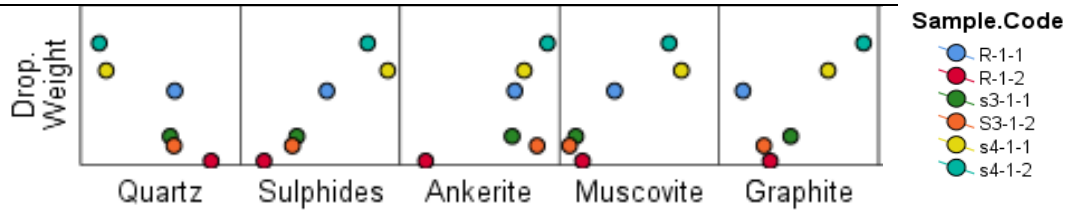

Figure 7-1 The correlation between the drop weight index and the mineral composition of the different sample groups. Correlation is significant at the 0.05 level (2 tailed)

7.2 Correlation of the Point Load test with the mineral content

The Point Load strength index appears to have a positive correlation with quartz and a negative correlation with all the other major minerals (Figure 7-2). This means that the quartz-rich specimens were more resistant to uniaxial compression from the Point Load test. In contrary, soft minerals like graphite and muscovite result to lower point load strength values, while carbonate and sulphide veins brecciate the rock and cause changes in the strain and stress gradients in such a way that uniaxial failure occurs easier.

		Quartz	Sulphides	Ankerite	Muscovite	Graphite
Point.Load	Pearson	.875	-.940	-.701	-.879	-.604
	Sig(2 tailed)	.023	.005	.121	.021	.205
	No. groups	6	6	6	6	6

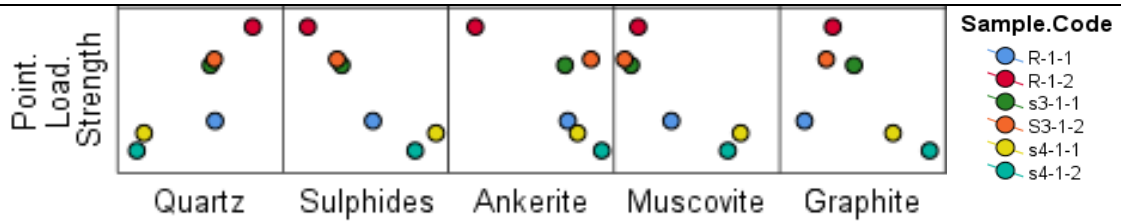

Figure 7-2 Correlation between the Point Load test and the mineral composition of the Kittilä sample groups

7.3 Correlation between the Los Angeles Abrasion test and the mineral content

The correlation between the L.A abrasion test and the corresponding mineral content of the sample groups appeared to be significantly weak as it can be seen from (Figure 7-3). Thus, it is assumed that the resistance of the ore to attrition and abrasion depends more on other factors such as grain size, shape and textural characteristics than it depends on the mineral content.

		Quartz	Sulphides	Ankerite	Muscovite	Graphite
LosAngeles	Pearson	-,619	,605	,690	,401	,422
	Sig(2 tailed)	,190	,203	,129	,430	,405
	No. groups	6	6	6	6	6

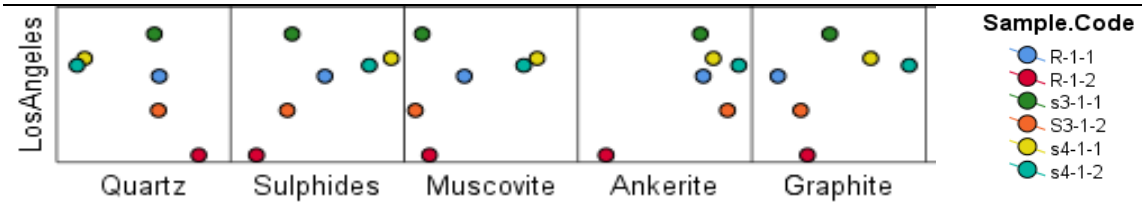

Figure 7-3 The correlation between the mineral composition and L.A values for all sample groups.

7.4 Correlation between the Bond Ball Mill Grindability test and the mineral content

The variation in the grindability properties of the six sample groups is related to the different mineralogical and textural characteristics (Chenje et al. 2004) described in Chapter 4. Sample groups S4-1-2 and R-1-1 appear to have the weakest resistance to grinding. According to the results from the scanning electron microscope (SEM) illustrated in Chapter 4.2.3, these sample groups were characterized by a significant percentage of graphite and muscovite.

Ore type R-1-2 had the highest BMWi value, which means it was the most resistant to grinding. This sample group has the highest quartz content and the lowest muscovite content. The combination of low mica content and high quartz (Table 7-1) makes the specific ore type difficult to grind to smaller particles.

Table 7-1 Average mineral composition (%) for sample group R-1-2, based on SEM results

MINERAL(%)	Quartz	Ankerite	Pyrite	Muscovite	Graphite	Arsenopyrite
R-1-2	27.80	12.50	5.80	4.20	11.00	1.02

It is important to consider the lack of homogeneity among the ore types. They are all highly heterogeneous when it comes to the mineral content and the textures, since they have been formed in a highly metamorphic environment. The difference in the textures and the mineralogical heterogeneity is described in the sample characterization in Chapter 4.1.

The correlation between the BMWi values and the corresponding mineralogy can be seen in (Figure 7-4). It appears the correlation is not very strong between the BMWi values and the mineral composition, showing a positive correlation of 0.789 with quartz and a negative correlation with the sulphides, ankerite, muscovite and graphite. From the negative correlations the sulphides seem to have the strongest correlation of -0.867. However, the amount of sulphides is not very high so its effect is rather limited. Thus, we can conclude that the major contributors to the difference in the grindability properties are mostly the textural characteristics and the grain size.

		Quartz	Sulphides	Ankerite	Muscovite	Graphite
Bond.Mill	Pearson	.789	-.867	-.689	-.804	-.503
	Sig(2 tailed)	.062	.025	.130	.054	.309
	No. groups	6	6	6	6	6

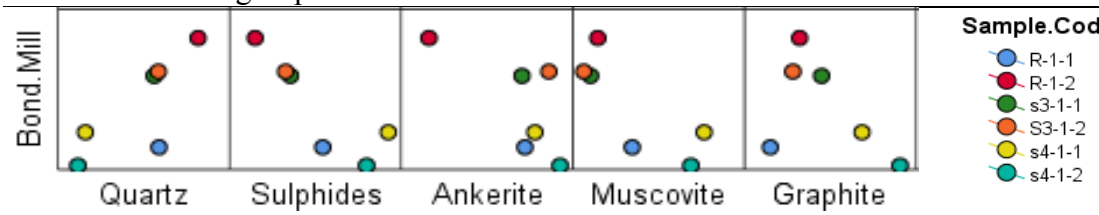

Figure 7-4 Correlation between the BMWi values and the corresponding mineral composition

7.5 Comparison of the Bond Mill test results with similar studies

Similar grindability studies have been carried out regarding the Bond Mill Work Index (BMWi) for the Kittilä gold ore deposit. In this chapter, a comparison has been facilitated between the BMWi from this thesis and the BMWi from the study of (Kirpala 2013) for the Geological Survey of Finland (GTK). The F80 and P80 values are included in the comparison, as well as the closing sieve Pi and the net grams per cycle Gbp (Table 7-2)

Table 7-2 Bond Ball Mill grindability test results comparison with other studies

Sample code	F_{80}(µm)	P_{80}(µm)	Pi(µm)	Gbp(g/cycle)	BMWi(kWh/t)
S4-1-2	2500	95	125	1.18	17.14
S4-1-1	2469	92	125	1.06	18.29
R-1-1	2531	87	125	1.05	17.77
S3-1-1	2597	85	125	0.88	20.24
S3-1-2	2500	87	125	0.89	20.39
R-1-2	2469	95	125	0.90	21.55
GTK study	2555	78	100	0.92	19.5

From the results it can be concluded that the BMWi values calculated in this thesis positively relate to the values determined by the test work of (Kirpala 2013). In principal the results are similar. The average BMWi from this study is 19.23kWh/t, which is significantly close to the value of 19.5kWh/t from the (GTK) samples. Sample group S3-1-1 seems to have the highest correlation with the sample group from the GTK study, as the Work Index of 20.24kWh/t is the closest to 19.5kWh/t. Furthermore, the net grindability per cycle (Gbp) accounts to 0.92 g/cycle which is significantly close to the average net grindability 0.98g/cycle derived from the sample groups used in this study.

It can be concluded from the comparison that the BMWi is cross validated between the two studies. This finding increases the confidence level of the classification made in Chapter 6.4.

7.6 Correlations between the comminution tests

Correlations were carried out between all the comminution tests to determine the consistency of the results. An overall correlation matrix is provided in (Table 7-3) in order to illustrate the relationship between the tests. In summary, the comminution tests correlate consistently.

The most significant correlations between the comminution tests include the correlation between the Point Load Strength test, Drop Weight test and Bond Mill test (Figure 7-5). Most of the correlations can be explained with the mineral content, textures and microstructures which characterize the samples.

In contrast, sample R-1-2 had the highest values from the Bond Ball Mill tests and the lowest in the Drop Weight test. Thus, sample group R-1-2 can be characterized as the hardest from all the sample groups and most resilient to breakage mechanisms like impact and attrition.

Table 7-3 Correlations between all the comminution tests, including Pearson and two tailed significant correlation

		LosAngeles	Bond. Mill	Point. Load	Drop. Weight
LosAngeles	Pearson Correlation	1	-.584	-.617	.560
	Sig. (2-tailed)		.223	.192	.248
	N	6	6	6	6
Bond.Mill	Pearson Correlation	-.584	1	.985**	-.961**
	Sig. (2-tailed)	.223		.000	.002
	N	6	6	6	6
Point.Load	Pearson Correlation	-.617	.985**	1	-.985**
	Sig. (2-tailed)	.192	.000		.000
	N	6	6	6	6
Drop.Weight	Pearson Correlation	.560	-.961**	-.985**	1
	Sig. (2-tailed)	.248	.002	.000	
	N	6	6	6	6

Correlation is significant at the 0.01 level (2-tailed

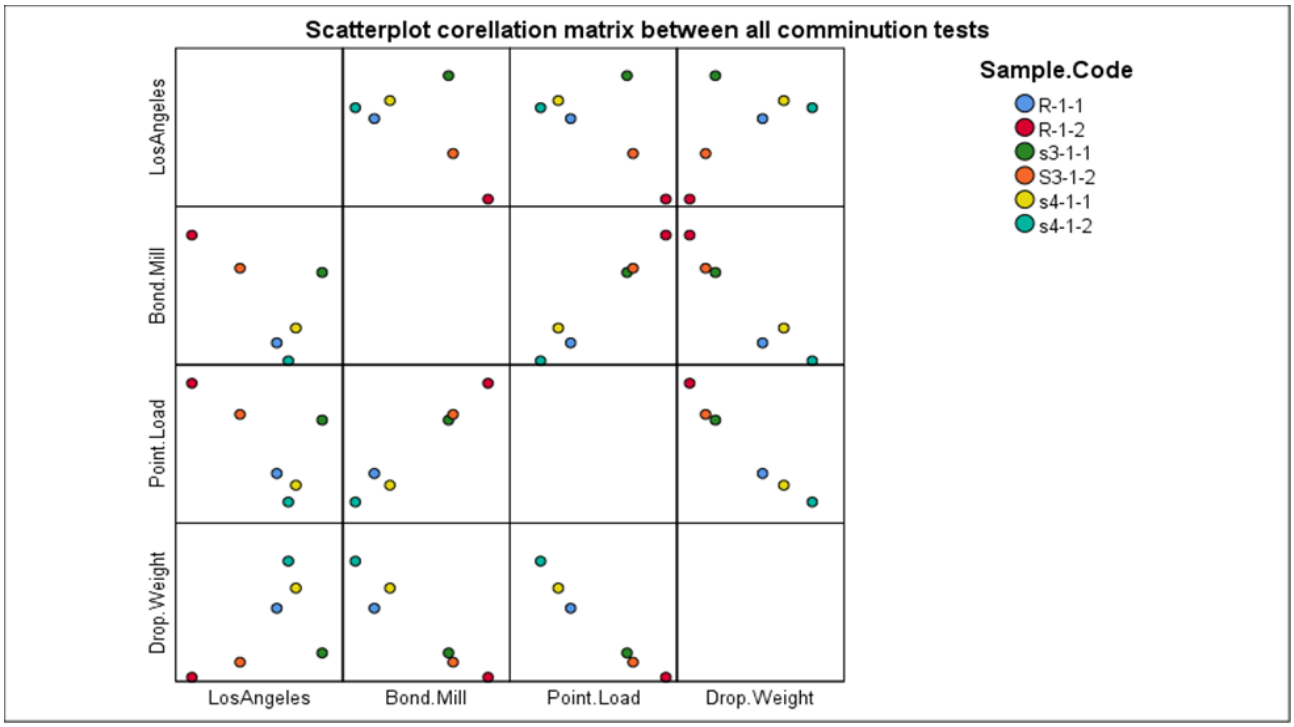

Figure 7-5 Correlation matrix between all the comminution test values

Another important factor influencing the ability to reduce particle size during grinding and crushing is the amount of graphite in the samples. Being a carbon-based mineral, graphite was

not traceable from the Scanning Electron Microscope. In addition, it was characterized as ‘’unclassified material’’, therefore only a poor estimate has been made about the exact amount of graphite in the samples. Thus, conclusions regarding graphite are limited in this study. In summary, graphite is a rather soft mineral which makes the ore easier to crush or grind. Thus, it can be concluded that graphite affects the breakage mechanisms of the ore in such a way that it becomes easier to crush and grind.

7.6.1 The correlation between the Bond Ball Mill test and the Point Load test

The correlation between the point load and bond ball mill test is significantly positive. (Figure 7-6) This means that the samples that were easy to grind in the bond mill were also less resistant to point load failure. This linear relatedness allows for estimation of one comminution index from another. In future studies this correlation can possibly be used to determine the grindability of the ore directly from the point load test

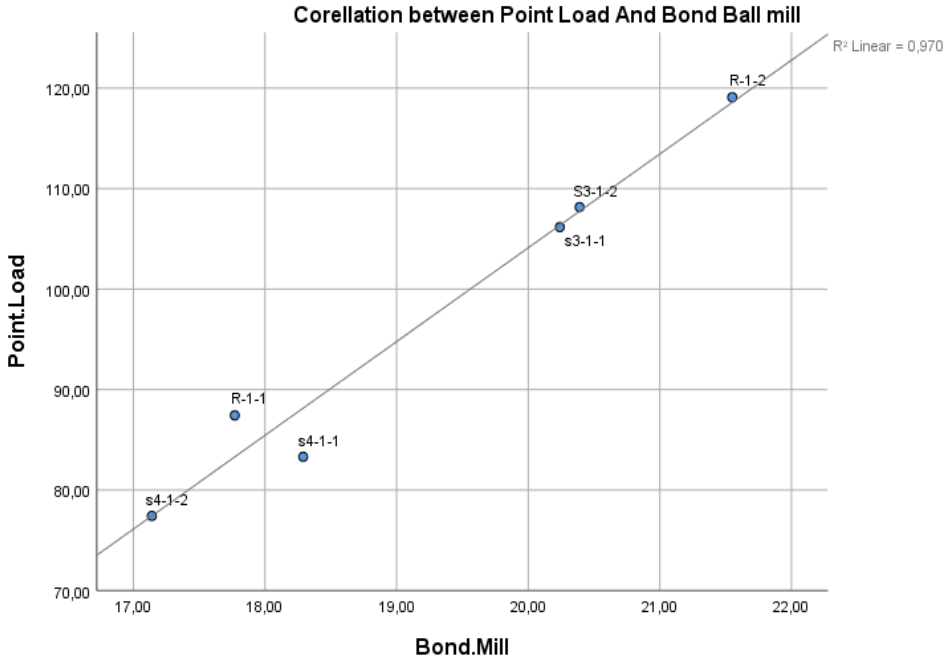

Figure 7-6 Correlation between the Bond Ball mill and Point Load values

7.6.2 The correlation between the Drop Weight Test and the Point Load test

The Point Load test appeared to have a strong negative correlation with the Drop Weight test, (Figure 7-7) reaching -0.985 on the 2 tailed correlation. The negative correlation is reasonable since the lower the Drop Weight Index the harder the rock is. Once again, this relatedness can be used to approximate one comminition index from another. The point load test, being the most simple and rapid, can possibly be used to estimate the drop weight parameters of the specimens being tested..

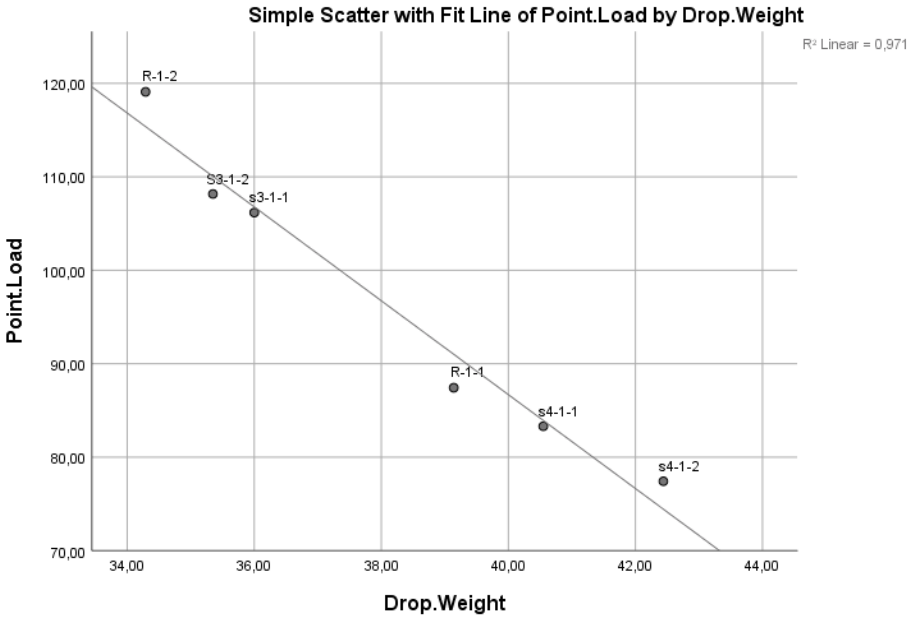

Figure 7-7 Correlation between the Drop Weight and the Point Load values

7.6.3 The correlation between the Drop Weight Test and the Bond Ball Mill test

The Drop Weight Test and the Bond Ball Mill test appear to have a strong correlation. (Figure 7-8) They correlate negatively with -0.961 on the 2 tailed correlation. This means that the samples which were easy to grind with the bond mill were also easy to crush with the drop weight impact test. This correlation allows to possibly estimate the grindability of the ore from the drop weight test, without having to conduct the time consuming and demanding bond mill.

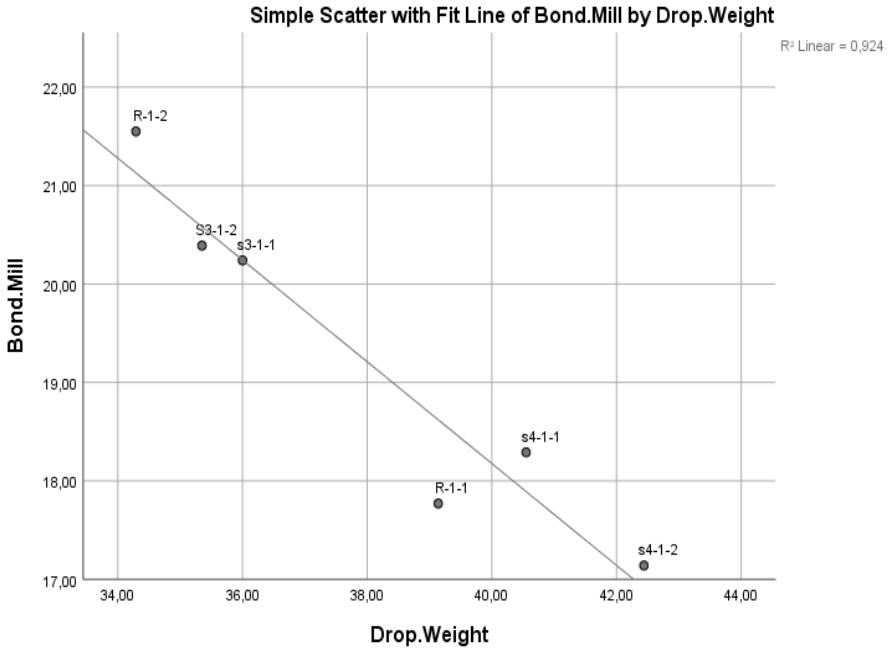

Figure 7-8 Correlation between the Drop Weight and the Bond Mill values

7.7 Principal component analysis (PCA)

Principal component analysis (PCA) is a statistical procedure that is used to transform a set of observations of correlated variables into a set of values of linearly uncorrelated variables called principal components. PCA is widely applied to minimize the noise or the dimensionality in a data set, while retaining the most variance, by finding patters within it (Ten et al. 1996). It is used as a tool in exploratory data analysis for making predictive models.

In this study, PCA is used in order to visualize relatedness between sample populations and distinguish clusters of sample groups, which correlate the most. PCA for this study is conducted in Matlab programming software. The dataset contains the results from the comminution tests. Based on the values from the Point Load, Drop Weight, Los Angeles and Bond test, two principal components are determined. The first principal component corresponds to the greatest variance of the data. Four main clusters are detected which contain sample groups that covary the most (Figure 7-9).

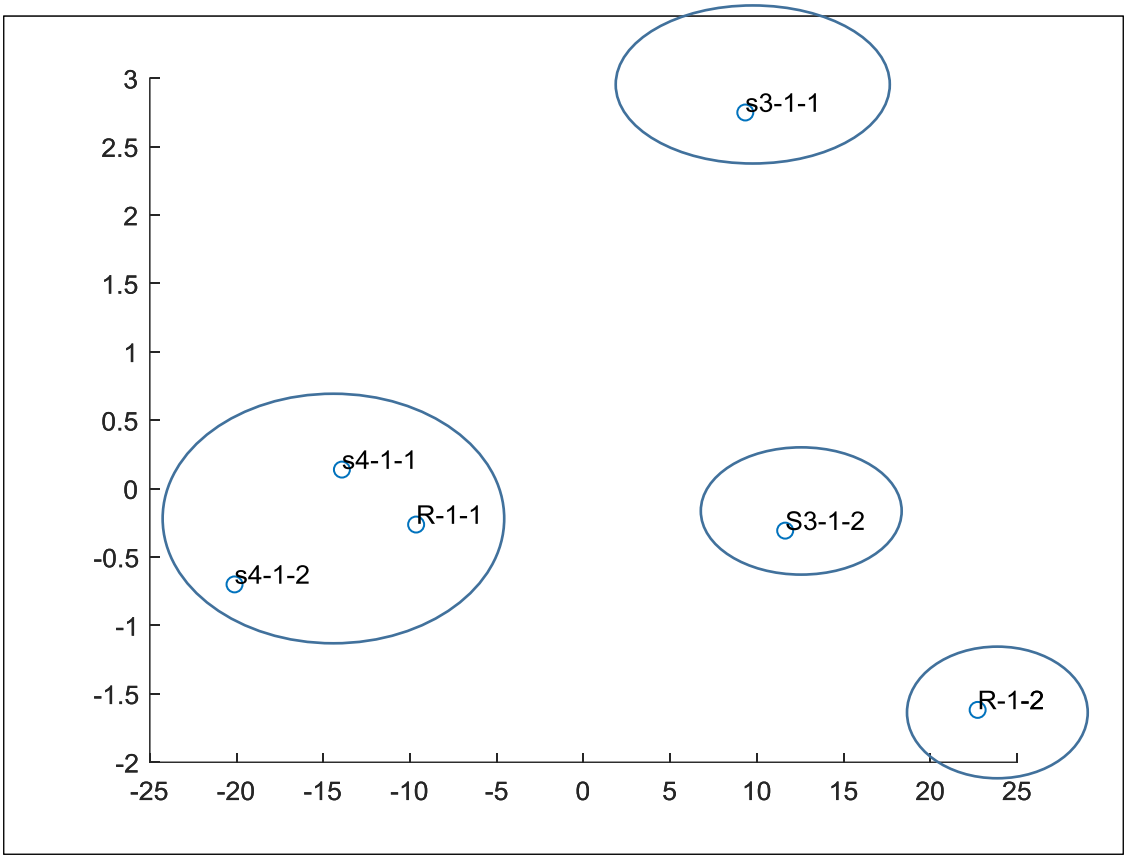

Figure 7-9 Principal component analysis for the six sample groups from the Kittilä Au-deposit.

8 Conclusions

In this study, comminution tests have been carried out for six ore types from the Kittilä gold deposit in order to determine their geometallurgical properties related to grinding and crushing. Rock mechanical tests, particle breakage and bench-scale grindability tests have been conducted. Additionally, the correlations between the tests have been determined along with the principal component analysis for the various sample groups. For the individual test categories, the following is concluded:

- Regarding particle breakage tests, the parameters A*b from the Drop Weight test results in Chapter 6.1 range from 34.29 to 42.44. Based on the A*b values, the sample groups are classified in the range from moderate hard crush to hard crush. Based on the t10-Ecs breakage distribution, it is concluded that the finer the particles become, the more specific comminution energy is required to further reduce the particle size.

- From the rock mechanical tests, the Point Load Strength Index (Is50) ranges between 5.28 and 7.53. This range corresponds to a Uniaxial Compressive Strength between 126-181 MPa. Based on the classification in Chapter 6.2 the sample groups are categorized as high strength rocks.

- The bench scale grindability tests are well established and provide most of the reference data for this study. Based on the results from Chapter 6.4, the Bond Work Index ranges from 17.14 to 21.55, while the Plant data W ranges from 14.14-17.9 kWh/t. In terms of grindability, the ore types are classified between moderate hard grinding and very hard grinding.

- Resistance to abrasion and attrition breakage mechanisms has been determined from the Los Angeles abrasion test. The loss of material from the abrasion test ranged between 16.31-21.51% for the Kittilä ore samples.

Several correlations were identified between the comminution tests that enable the possibility to estimate one comminution index from another. The most significant correlations include the Point Load test – Drop Weight test with an R^2 of 0.971, the Point Load test-Bond mill test with an R^2 of 0.970 and the Bond Mill test-Drop Weight test with an R^2 of 0.924. It can be concluded that the Point Load test correlates best with the other comminution tests and since it is the most simple and rapid method among the methods used in this study, it is considered a valuable predictor for breakage mechanisms and comminution properties of the ore samples.

Furthermore, strong relationships are determined between the comminution tests and the corresponding mineral content of the ore types. Sulphides, quartz, carbonates, muscovite and graphite highly influence the comminution tests according to the correlations conducted in Chapter 7. In principal, it is concluded that Sulphides, quartz and carbonates increase the resistance of the ore types to grinding and crushing, while muscovite and graphite content affect the breakage mechanisms in such a way that the ore becomes easier to crush and grind.

Due to the heterogeneity of the ore types and the vast limitations of the comminution tests, controlling factors such as chemical alterations and microstructures have not been incorporated into the geometallurgical characterization of the Kittilä ore.

Based on the results from the Bond Mill grindability test and the Drop Weight impact test, a classification has been made in (Table 8-1) regarding the resistance of the ore groups to crushing and grinding. It is concluded that the grinding and crushing indices are consistent per sample group. Consequently, there is a positive correlation between crushability and grindability. Ore type S4-1-2 indicated the lowest values from the comminution tests, while ore type R-1-2 is considered the most resistant to grinding and crushing.

Table 8-1 Classification of the sample groups based on crushability and grindability.

Sample Code	Drop Weight Index	Range	BMWi	Range
S4-1-2	Moderate hard crush	(43-56)	Moderate hard grinding	(16-18)
S4-1-1	Moderate hard crush	(38-43)	Hard Grinding	(18-20)
R-1-1	Moderate hard crush	(38-43)	Moderate hard grinding	(16-18)
S3-1-1	Hard crush	(30-38)	Hard grinding	(18-20)
S3-1-2	Hard crush	(30-38)	Hard grinding	(18-20)
R-1-2	Hard crush	(30-38)	Very hard grinding	>20

9 Recommendations and path forward

The work developed in this study provides a basis for geometallurgical characterization of the Kittilä gold deposit. Comminution testing is a key factor relevant to predicting the breakage mechanisms of the ore. The knowledge from the various tests can be exploited in future mill design as a function of mine to mill information and equipment performance.

With the appropriate geometallurgical characterization, mine planning and economic modelling of the resource can be enhanced as the project life cycle advances. The geotechnical properties of the ore, including grindability and crushability, can be implemented in the block model of the deposit and serve as key factors for geometallurgical mapping.

For the next part of this research, it is recommended that drill hole data is extracted regarding the locations from which the samples were derived. With sufficient drill hole data and knowledge about the geometallurgical characteristics, it will be possible to enable geometallurgical mapping with respect to the block model of the deposit. By this, the deposit can be divided into different wireframes and domains that will correspond to specific crushability and grindability values.

Furthermore, data interpretation is one of the critical steps for any modelling process. The correct development of measurements protocols is an indispensable need before simulating the crushing and grinding units of the processing plant. There are various types of data that can assist to understand geological behavior. It is recommended that logging data is acquired in order to comprehend the overall lithology and alterations that characterize the different ore types. Additionally, mineralogy approximated from assays and small-scale geophysical tests are important parameters to estimate comminution indices correctly.

For future work, 3D models can be developed to describe spatial variability across the deposit, an important feature to estimate spatial distribution of hardness and resistance to breakage.

Finally, the ultimate purpose of this research is to implement the knowledge from the geometallurgical testing in the development of remote-laser spectral techniques which will provide real time information about the ore's properties, simply and rapidly. The device setup is already undergoing and is based on Laser induced breakdown spectroscopy. Currently, investigation is ongoing whether geometallurgical characteristics can be determined with a simple laser scan. The device is a prototype and therefore the corresponding error in the results is still significant. However, with further work this could be an innovative method to provide real time mine to mill information, while it can be crucial for drilling and blasting optimization.

10 References

Agnico Eagle. "Kittilä Mineral Processing Plant Flowsheet." Retrieved from https://www.agnicoeagle.com/English/operations-and-development-projects/operations/Kittilä/maps-and-surveys/default.aspx#flowsheet. (2018).

Agnico Eagle. "Kittilä Mine-Regional Geology Map." Retrieved from https://s21.q4cdn.com/374334112/files/doc_downloads/Kittilä_maps/Kittilä-Mine-Regional-Geology-Map.pdf. (2018).

Anticoi, H. et al. "Breakage Function for HPGR: Mineral and Mechanical Characterization of Tantalum and Tungsten Ores." *Minerals* 8.4 (2018): 170.

Austin, L. and Brame, K. "A comparison of the Bond method for sizing wet tumbling ball mills with a size—mass balance simulation model." *Powder Technology* 34.2 (1983): 261-274.

Austin, L., Klimpel, R. and Luckie, P. "Process engineering of size reduction: ball milling." *American Institute of Mining, Metallurgical, and Petroleum Engineers.*" (1984).

Bieniawski, Z. "The point-load test in geotechnical practice." *Engineering Geology* 9.1 (1975): 1-11.

Bond, F. "Work indexes tabulated." *Mining Engr* 315 (1953): 316.

Broch, E. and Franklin, J. "The point-load strength test." *International Journal of Rock Mechanics and Mining Sciences & Geomechanics Abstracts*. Vol. 9. No. 6. Pergamon, (1972)

Brook, N. "Size correction for point load testing." *Int. J. Rock Mech. Min. Sci. & Geomech. Abstr* 17.6 (1980): 231-235.

Cargill, J. and Shakoor, A. "Evaluation of empirical methods for measuring the uniaxial compressive strength of rock." *International Journal of Rock Mechanics and Mining Sciences & Geomechanics Abstracts*. Vol. 27. No. 6. Pergamon, (1990).

Chenje, T., Simbi, D. and Navara, E. "Relationship between microstructure, hardness, impact toughness and wear performance of selected grinding media for mineral ore milling operations." *Materials & design* 25.1 (2004): 11-18.

Deutch, C.V. "Geostatistical modelling of geometallurgical variables -problems and solution." *Proceedings of GEOMET 2013*: Australasian Institute of Mining and Metallurgy, Melbourne. (2013): 7–1

Doucet, D. et al. "Mineral Resource and Mineral Reserve Estimate and the Suuri Extension Project, Kittilä Mine"*, Finland Technical Report* (2010).

Eilu, P. et al. "Characteristics of gold mineralization in the greenstone belts of northern Finland." *Geological Survey of Finland, Special Paper* 44 (2007): 57-106.

Franklin, J. "Suggested method for determining point load strength." *International Journal of Rock Mechanics and Mining Sciences & Geomechanics Abstracts*. Vol. 22. No. 2. Pergamon, (1985)

Ghosh, D. and Srivastava, M. "Point-load strength: an index for classification of rock material." *Bulletin of the International Association of Engineering Geology-Bulletin de l'Association Internationale de Géologie de l'Ingénieur* 44.1 (1991): 27-33.

Haffez, G. "Correlation between Bond work index and mechanical properties of some Saudi ores." *J. Eng. Sci.* 40.1 (2012): 271-280.

Hanski, E. and Huhma, H. "Central Lapland greenstone belt." *Developments in Precambrian Geology*. Vol. 14. Elsevier, (2005). 139-193.

Härkönen, Ilkka, and Veikko Keinänen. "Exploration of structurally controlled gold deposits in the central Lapland greenstone belt." *Special Paper-Geological Survey of Finland* 10 (1989): 79-82.

Hassani, F. Scoble, M. and Whittaker, B. "Application of the point load index test to strength determination of rock and proposals for a new size-correction chart." *The 21st US Symposium on Rock Mechanics (USRMS)*. American Rock Mechanics Association, (1980).

Hölttä, P. et al. "Paleoproterozoic metamorphism and deformation in Central Lapland, Finland." *Geological Survey of Finland, Special Paper* 44 (2007): 9-58.

JKMRC, CO. "Procedure for BBMWI Test." (2006).

Kirpala, A. "Jauhautuvuuden laboratoriomääritys Bond-ja Mergan-menetelmällä." (2013).

Kojonen, K. and Johanson, B. "Determination of refractory gold distribution by microanalysis, diagnostic leaching and image analysis." *Mineralogy and Petrology* 67.1-2 (1999): 1-19.

Kojovic, T. Michaux, S. and Walters, S. "Development of new comminution testing methodologies for geometallurgical mapping of ore hardness and throughput." *XXV International Mineral Processing Congress 2010, IMPC 2010*. Vol. 2. Australasian Institute of Mining and Metallurgy, (2010).

Krogh, S. "Crushing characteristics." *Powder Technology* 27.2 (1980): 171-181.

Lamberg, P. "Particles-the bridge between geology and metallurgy." *Konferens i mineralteknik 2011: 08/02/2011-09/02/2011*. Luleå tekniska universitet, (2011).

Levin, J. "Observations on the Bond standard grindability test, and a proposal for a standard grindability test for fine materials." *Journal of the Southern African Institute of Mining and Metallurgy* 89.1 (1989): 13-21.

Lynch, A., and Rowland, C. "The history of grinding." *SME* (2005)

Lynch, Alban. "Comminution handbook to prove highly useful for students and industry practitioners alike." *AusIMM Bulletin* Jun 2015 (2015): 80.

Magdalinović, N. "A procedure for rapid determination of the Bond work index" *International Journal of Mineral Processing*27.1-2 (1989): 125-132.

Man, Y. "Why is the Bond Ball Mill Grindability Test done the way it is done" *European journal of mineral processing and environmental protection* 2.1 (2002): 34-39.

McKen, A. and Williams, S.. "'An overview of the small-scale tests available to characterize ore grindability for design purposes, SGS Minerals." *Technology Bull* 2006 (2005): 1-8.

Morrell, S. "An alternative energy–size relationship to that proposed by Bond for the design and optimization of grinding circuits." *International journal of mineral processing* 74.1-4 (2004): 133-141.

Morrell, S. "Predicting the overall specific energy requirement of crushing, high pressure grinding roll and tumbling mill circuits." *Minerals Engineering* 22.6 (2009): 544-549.

Mwanga, A., Rosenkranz J. and Lamberg, P. "Testing of Ore Comminution Behavior in the Geometallurgical Context—A Review." *Minerals* 5.2 (2015): 276-297.

Patison, N. "Structural controls on gold mineralisation in the Central Lapland Greenstone Belt." *Gold in the Central Lapland Greenstone Belt, Finland* (2007): 107-22.

Powell, M. and Morrison, R. "The future of comminution modelling." *International Journal of Mineral Processing* 84.1-4 (2007): 228-239.

Rowland, C. "Selection of rod mills, ball mills, pebble mills and regrind mills." *Design and installation of comminution circuits* (1982): 393-438.

Rusnak, J. and Mark, C. "Using the point load test to determine the uniaxial compressive strength of coal measure rock." *Proceedings of the 19th international conference on ground control in mining. Morgantown, WV: West Virginia University*. (2000).

Russell, A., Wood, D. and Kikumoto. M. "Crushing of particles in idealised granular assemblies." *Journal of the Mechanics and Physics of Solids* 57.8 (2009):

Swain, R. and Rao, R. "Alternative approaches for determination of Bond work index on soft and friable partially laterised Khondalite rocks of Bauxite mine waste materials." *Journal of Minerals and Materials Characterization and Engineering* 8.09 (2009): 729.

Ten Berge, J. and Kiers, H. "Optimality criteria for principal component analysis and generalizations." *British Journal of Mathematical and Statistical Psychology* 49.2 (1996): 335-345.

Thomas, A. and Filippov, L. "Fractures, fractals and breakage energy of mineral particles." *International Journal of Mineral Processing* 57.4 (1999): 285-301.

Ugur, I., Demirdag, S. and Yavuz, H. "Effect of rock properties on the Los Angeles abrasion and impact test characteristics of the aggregates." *Materials characterization* 61.1 (2010): 90-96.

Vaughan, M. and Guggenheim, S. "Elasticity of muscovite and its relationship to crystal structure." *Journal of Geophysical Research: Solid Earth* 91.B5 (1986): 4657-4664.

Walters, S., and Kojovic, T. "Geometallurgical mapping and mine modelling (GEMIII)-the way of the future." *SAG* (2006). Vol. 4. 2006.

Wills, B. and Napier-Munn, T. "Wills' mineral processing technology." *An Introduction to the Practical Aspects of Ore Treatment and Mineral Recovery* (2006): 267-352.

Appendix A- Drop Weight Test report

Sample code	Size selection(mm)	Energy levels (Ecs)	Starting weight	Weight passing 10% sieve	t10%
R-1-2	16	0.25	57.2	1.98	3.46
		0.40	78.6	4.48	5.70
		0.55	114.9	8.77	7.63
	8	0.54	26.5	1.07	4.04
		0.71	44.8	3.38	7.54
		1.17	53.6	5.24	9.78
	4	1.03	13.9	0.527	3.79
		1.58	20.05	0.976	4.87
		1.84	34.1	1.983	5.82
	2	2.47	5.8	0.125	2.16
		4.96	6.4	0.29	4.53
		7.21	8.7	0.538	6.18
S3-1-2	16	0.26	55.7	2.02	3.63
		0.41	76.8	4.52	5.89
		0.56	112.7	11.54	10.24
	8	0.58	24.9	1.05	4.22
		0.72	43.8	4.36	9.95
		1.21	51.7	8.18	15.82
	4	1.07	13.4	0.535	3.99
		1.64	19.3	0.985	5.10
		1.88	33.4	1.995	5.97
	2	2.61	5.5	0.13	2.36
		5.38	5.9	0.29	4.92
		7.94	7.9	0.61	7.72
S3-1-1	16	0.24	60.4	2.08	3.44
		0.47	67.6	5.02	7.43
		0.57	111	10.52	9.48
	8	0.54	26.5	0.95	3.58
		0.71	44.4	4.18	9.40
		1.08	58	6.64	11.45
	4	1.01	14.18	0.47	3.28
		1.69	18.8	1.02	5.40
		1.99	31.6	2.47	7.80
	2	2.56	5.6	0.16	2.82
		5.38	5.9	0.29	4.88
		8.04	7.8	0.62	7.92
S4-1-2	16	0.23	65.7	2.36	3.59
		0.40	69.3	4.95	7.14

		0.47	120.7	11.96	9.91
	8	0.53	26.9	1.12	4.16
		0.69	45.7	4.41	9.65
		1.05	59.9	8.45	14.11
	4	0.93	15.4	0.58	3.77
		1.54	20.58	1.02	4.96
		1.89	33.14	2.03	6.13
	2	2.61	5.5	0.16	2.87
		5.38	5.9	0.29	4.95
		7.94	7.9	0.72	9.10
S4-1-1	16	0.23	63.6	2.32	3.65
		0.46	69.3	5.02	7.24
		0.52	120.7	12.24	10.14
	8	0.53	26.9	1.20	4.46
		0.69	45.7	4.61	10.09
		1.05	59.9	8.53	14.24
	4	0.93	15.4	0.61	3.96
		1.64	19.3	1.11	5.75
		1.88	33.4	2.17	6.50
	2	2.61	5.5	0.16	2.98
		5.38	5.9	0.31	5.19
		8.10	7.75	0.62	8.01
R-1-1	16	0.23	62.1	1.85	2.98
		0.48	66.7	4.48	6.72
		0.56	112.4	10.74	9.56
	8	0.71	15.3	0.90	5.88
		0.94	44.7	4.05	9.06
		1.04	60.3	6.39	10.60
	4	1.12	12.8	0.44	3.44
		1.85	17.1	0.94	5.50
		1.87	33.6	1.87	5.57
	2	2.76	5.2	0.16	3.04
		5.87	5.4	0.27	4.93
		9.09	6.9	0.52	7.51

Appendix B- Point Load Test Report

Type	W(mm)	D	P(bar)	De 2	Is	Is_{50}	Is_{50} MEDIAN	Is_{50}SD	UCS
a //	11.5	25.44	3.415	647.2	5.28	5.28			126.6
a //	8.9	25.44	3.49	647.2	5.39	5.39			129.4
a //	9.96	25.44	4.431	647.2	6.85	6.85			164.3
a //	8.92	25.44	2.955	647.2	4.57	4.57			109.6
a //	11.7	25.44	4.4	647.2	6.80	6.80	5.3	0.9	163.2
a //	8.68	25.44	3.04	647.2	4.70	4.70			112.7
a //	11.77	25.44	3.3	647.2	5.10	5.10			122.4
a //	10.34	25.44	5.22	647.2	8.07	8.07			193.6
a //	8.34	25.44	3.4	647.2	5.25	5.25			126.1
a //	9.66	25.44	3.1	647.2	4.79	4.79			115.0
			0.5						0.0
a //	9.4	25.44	4.03	647.2	6.23	6.23			149.4
a//	9.8	25.44	4.42	647.2	6.83	6.83			163.9
a //	8.74	25.44	3.6	647.2	5.56	5.56			133.5
a //	8.41	25.44	2.03	647.2	3.14	3.14			75.3
a //	9.21	25.44	3.4	647.2	5.25	5.25	5.6	1.2	126.1
a //	9.45	25.44	3.649	647.2	5.64	5.64			135.3
a //	9.65	25.44	3.63	647.2	5.61	5.61			134.6
a //	8.81	25.44	1.9	647.2	2.94	2.94			70.5
a //	7.8	25.44	1.8	647.2	2.78	2.78			66.7

a //	9.73	25.44	4.42	647.2	6.83	6.83			163.9
			0.5						0.0
a //	11.45	25.44	6.43	647.2	9.94	9.94			238.4
a //	10.33	25.44	4.48	647.2	6.92	6.92			166.1
a //	11.71	25.44	4.7	647.2	7.26	7.26			174.3
a //	11.8	25.44	3.9	647.2	6.03	6.03			144.6
a //	15.1	25.44	3.3	647.2	5.10	5.10	5.6	1.1	122.4
a //	8.26	25.44	2.69	647.2	4.16	4.16			99.8
a //	10.2	25.44	4.15	647.2	6.41	6.41			153.9
a //	9.4	25.44	2.78	647.2	4.30	4.30			103.1
a //	8.5	25.44	3.17	647.2	4.90	4.90			117.6
a //	10.73	25.44	3.62	647.2	5.59	5.59			134.2
			0.5						0.0
a //	10.87	25.44	5.49	647.2	8.48	8.48			203.6
a //	8.8	25.44	3.97	647.2	6.13	6.13			147.2
a //	9.55	25.44	4.86	647.2	7.51	7.51			180.2
a //	8.87	25.44	3.99	647.2	6.17	6.17			148.0
a //	9.8	25.44	4.57	647.2	7.06	7.06	7.5	1.5	169.5
a //	9.62	25.44	3.74	647.2	5.78	5.78			138.7
a //	9.64	25.44	6.42	647.2	9.92	9.92			238.1
a //	8.94	25.44	4.89	647.2	7.56	7.56			181.3
a //	9.88	25.44	6.25	647.2	9.66	9.66			231.8

a //	9.73	25.44	6.12	647.2	9.46	9.46			226.9
			0.5						0.0
a //	10.88	25.44	4.95	647.2	7.65	7.65			183.6
a //	9.77	25.44	4.45	647.2	6.88	6.88			165.0
a//	9.37	25.44	4.24	647.2	6.55	6.55			157.2
a //	10.32	25.44	4.53	647.2	7.00	7.00			168.0
a //	10.95	25.44	5.03	647.2	7.77	7.77	7.0	1.2	186.5
a //	9.68	25.44	5.45	647.2	8.42	8.42			202.1
a //	9.22	25.44	3.78	647.2	5.84	5.84			140.2
a //	10.03	25.44	5.31	647.2	8.20	8.20			196.9
a //	9.86	25.44	3.55	647.2	5.49	5.49			131.6
a //	8.98	25.44	3.2	647.2	4.94	4.94			118.7
			0.5						0.0
a //	10.11	25.44	3.96	647.2	6.12	6.12			146.8
a //	11.08	25.44	5.32	647.2	8.22	8.22			197.3
a //	11.24	25.44	3.41	647.2	5.27	5.27			126.5
a //	10.77	25.44	5.03	647.2	7.77	7.77			186.5
a //	9.65	25.44	4.47	647.2	6.91	6.91	6.8	1.0	165.8
a //	9.97	25.44	3.97	647.2	6.13	6.13			147.2
a //	11.05	25.44	4.78	647.2	7.39	7.39			177.3
a //	9.87	25.44	4.37	647.2	6.75	6.75			162.1
a //	10.45	25.44	4.69	647.2	7.25	7.25			173.9

a //	9.68	25.44	3.48	647.2	5.38	5.38	129.0

Appendix C- Bond Ball Mill Test report

S3-1-1	Input	SQR	Unit	**S3-1-2**	Input	SQR	Unit	**S4-1-1**	Input	SQR	Unit
p1	125		µm	p1	125		µm	p1	125		µm
Gbp	0.88			Gbp	0.89			Gbp	1.06		
P80	85	9.22	µm	P80	87	9.33	µm	P80	92	9.59	µm
F80	2500	50	µm	F80	2500	50	µm	F80	2500	50	µm
Wi		Plant data W		Wi		Plant data W		Wi		Plant data W	
20.2392161		17.90	kW·h /ton	20.386831		17.78	kW·h /ton	18.29		15.41	kW·h / ton
S4-1-2	Input	SQR	Unit	**R-1-1**	Input	SQR	Unit	**R-1-2**	Input	SQR	Unit
p1	125		µm	p1	125		µm	p1	125		µm
Gbp	1.18			Gbp	1.05			Gbp	0.90		
P80	95	9.75	µm	P80	87	9.33	µm	P80	95	9.75	µm
F80	2500	50	µm	F80	2500	50	µm	F80	2352	48.50	µm
Wi		Plant data W		Wi		Plant data W		Wi		Plant data W	
17.14		14.16	kW·h / ton	17.77		15.50	kW·h / ton	21.55		17.66	kW·h / ton

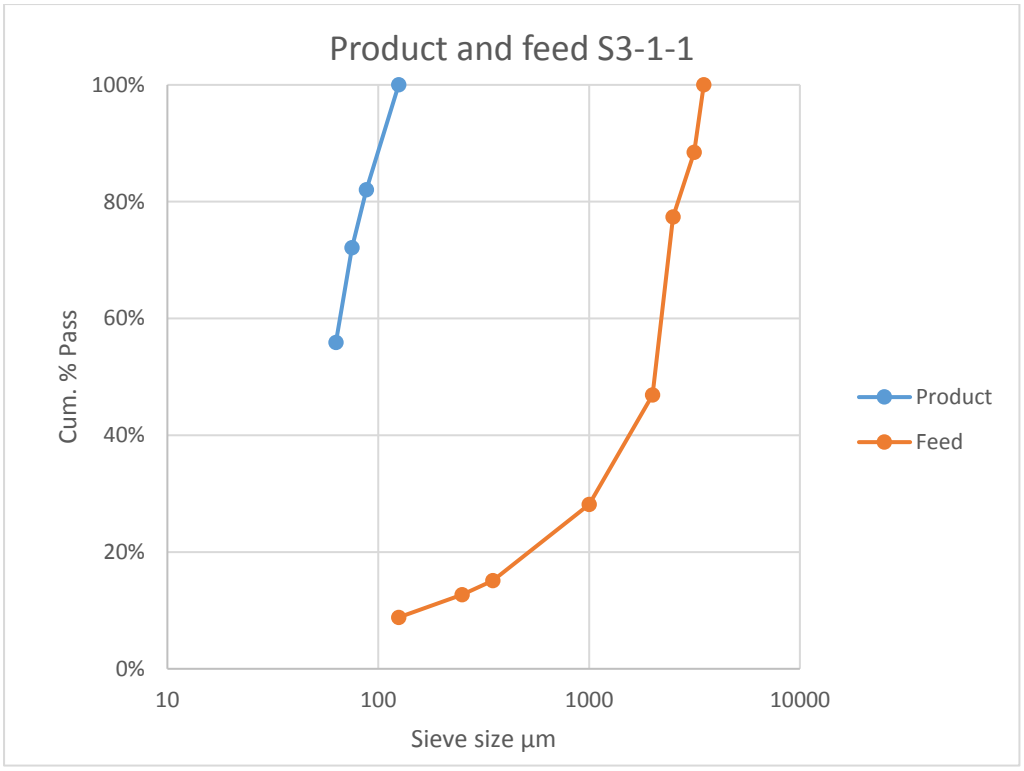
Product and feed S3-1-1
100%
80%
60%
40%
20%
0%
Cum. % Pass
10
100
1000
10000
Sieve size µm
Product
Feed

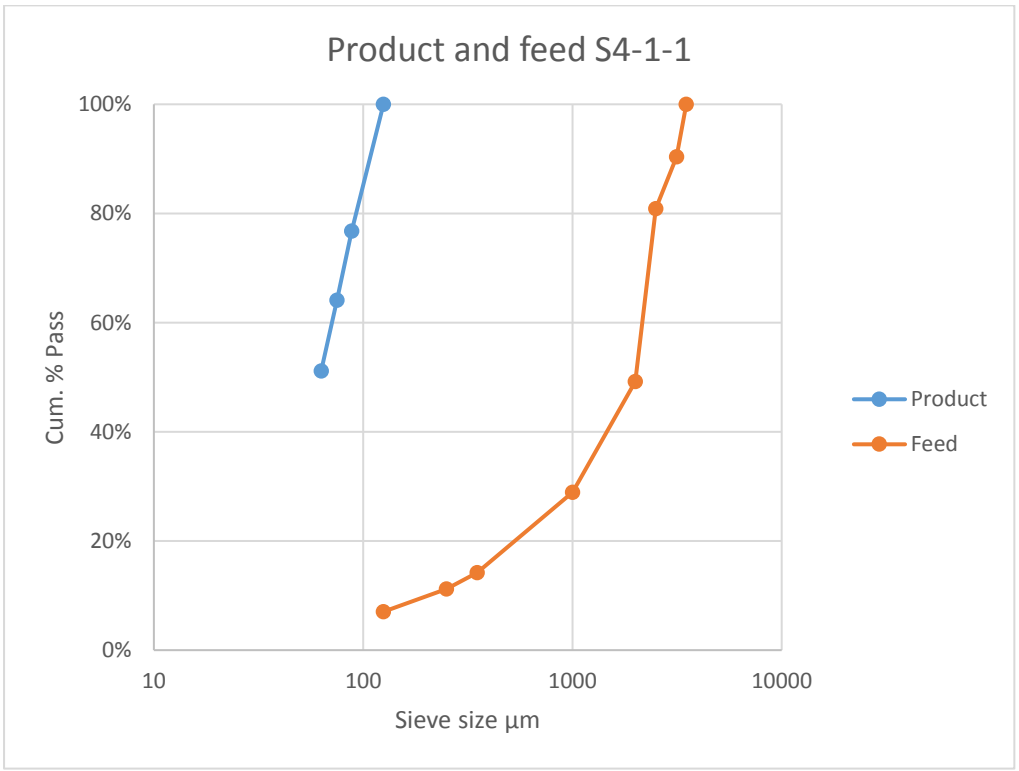
Product and feed S4-1-1
100%
80%
60%
40%
20%
0%
Cum. % Pass
10
100
1000
10000
Sieve size µm
Product
Feed

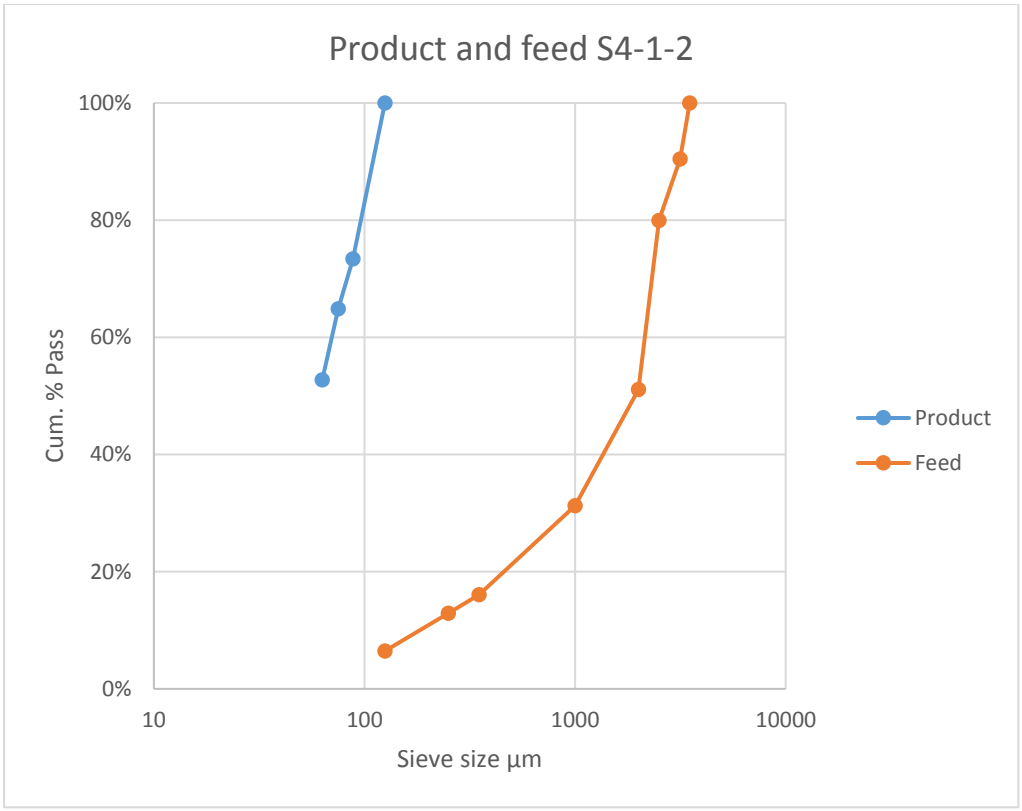
Product and feed S4-1-2
100%
80%
60%
40%
20%
0%
Cum. % Pass
10
100
1000
10000
Sieve size µm
Product
Feed

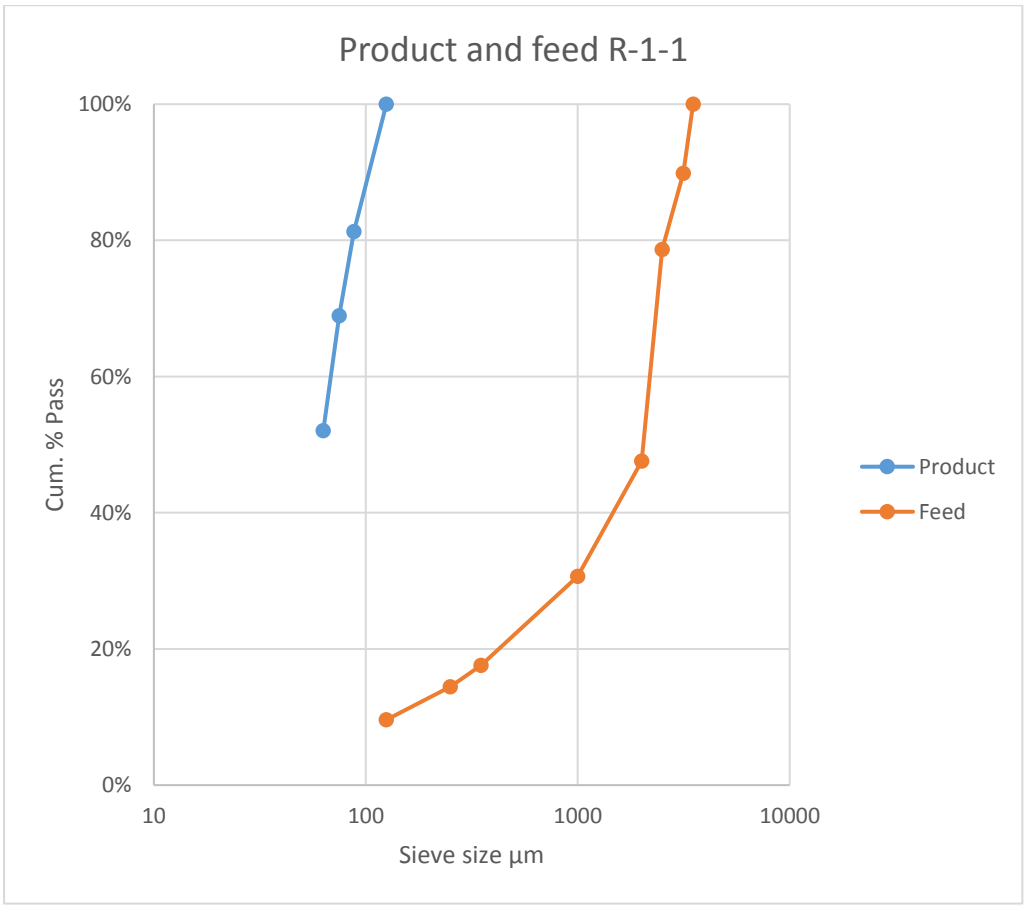
Product and feed R-1-1
100%
80%
60%
40%
20%
0%
Cum. % Pass
10
100
1000
10000
Sieve size µm
Product
Feed

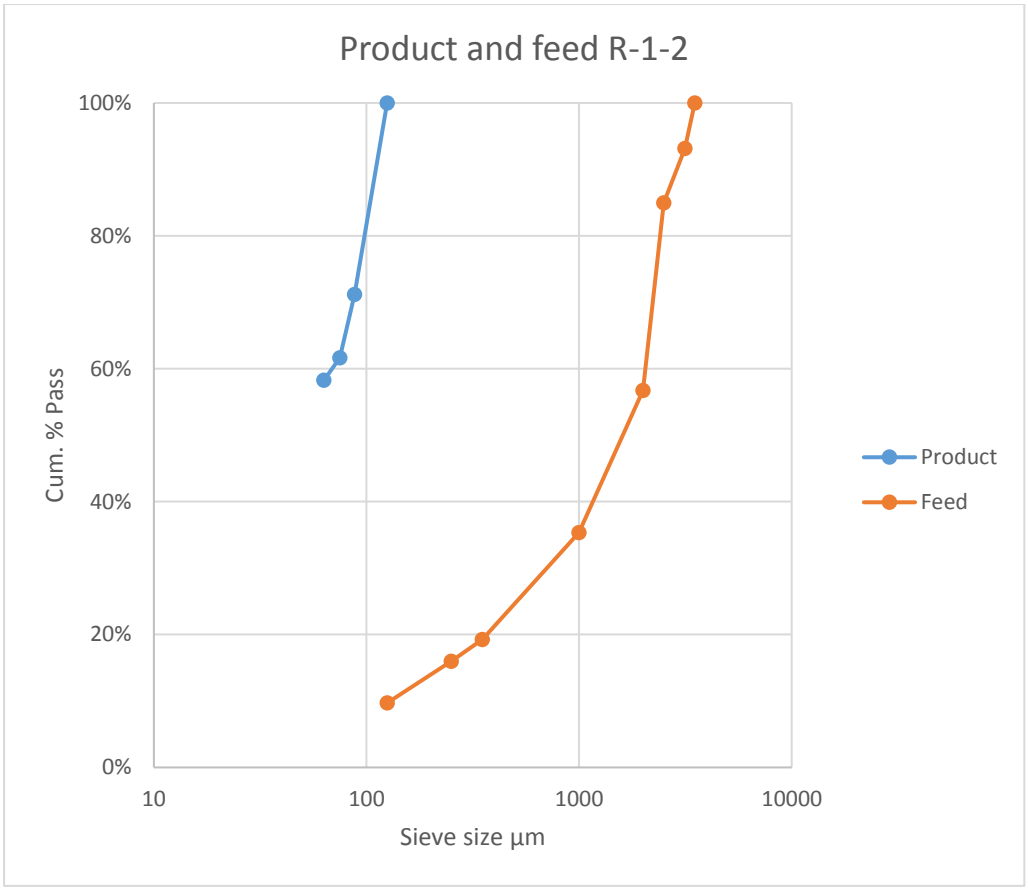
Product and feed R-1-2
100%
80%
60%
40%
20%
0%
Cum. % Pass
10
100
1000
10000
Sieve size µm
Product
Feed

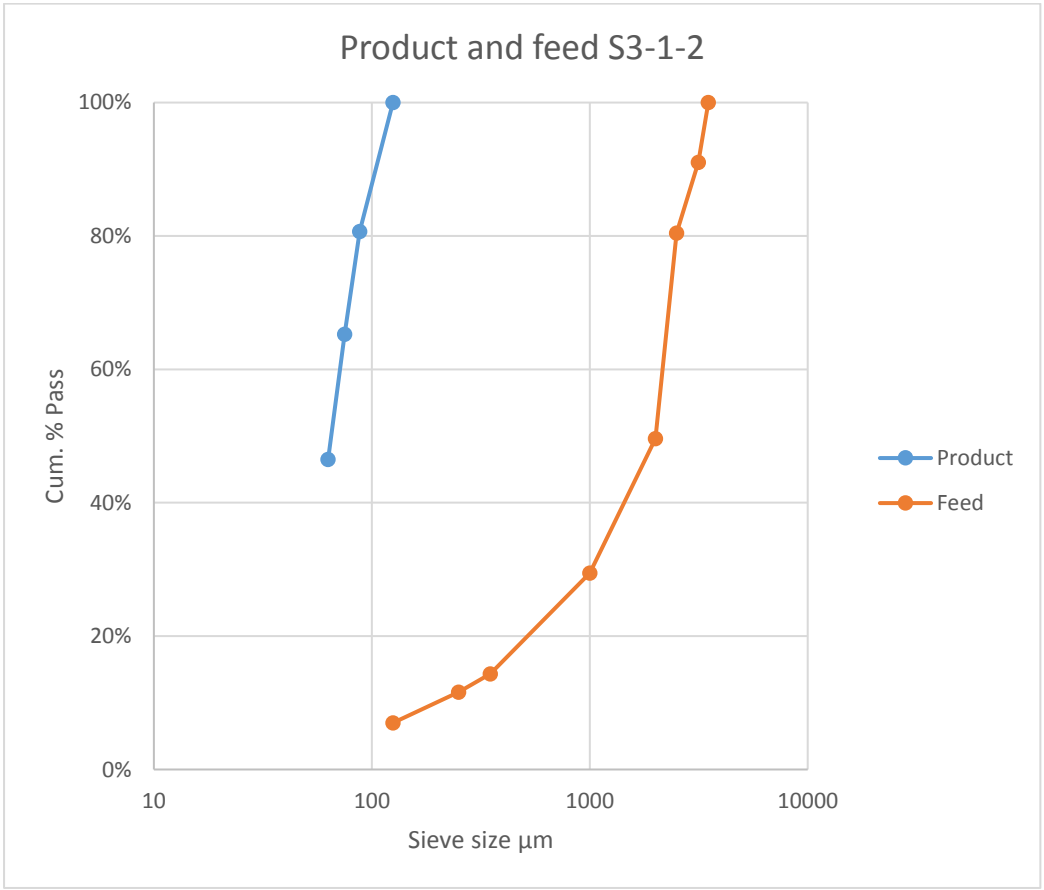
Product and feed S3-1-2
100%
80%
60%
40%
20%
0%
Cum. % Pass
10
100
1000
10000
Sieve size µm
Product
Feed

Appendix D- Density Measurements Report

Sample Code	W(dry) [gr]	W(wet) [gr]	p (solid)	p (average)
S3-1-2	502.79	326.24	2.84330522	
S3-1-2	774.38	500.24	2.82024145	
S3-1-2	477.37	302	2.71771801	2.755819372
S3-1-2	671.71	418.5	2.64853388	
S3-1-2	591	376.38	2.74929829	
S3-1-1	782.35	522	3.00018529	
S3-1-1	1316.7	859.1	2.8728	
S3-1-1	485.61	314.51	2.83362375	2.856061358
S3-1-1	456.35	294.8	2.82030232	
S3-1-1	705.53	449.7	2.75339543	
S4-1-2	361.16	233	2.81353109	
S4-1-2	306.17	189.67	2.62386376	
S4-1-2	450.7	300	2.98592488	2.891411356
S4-1-2	430	291.16	3.09213483	
S4-1-2	520.29	343.7	2.94160222	
S4-1-1	312.36	194.36	2.64288325	
S4-1-1	541.8	337.39	2.64631437	
S4-1-1	496.56	308.84	2.64098393	2.775184146
S4-1-1	637.1	431.24	3.08987001	
S4-1-1	656.93	427.27	2.85586916	
R-1-1	594.35	396.1	2.99318557	
R-1-1	367.41	242.54	2.93763229	
R-1-1	173.08	116.7	3.06497112	3.021717797
R-1-1	402.11	279.48	3.27380432	
R-1-1	316.97	205.5	2.83899568	
R-1-2	492.44	317.8	2.81523188	
R-1-2	400	266.34	2.98787969	
R-1-2	979.5	654.5	3.009024	2.942218124
R-1-2	1027.1	675.2	2.91405695	
R-1-2	472.28	314.31	2.98489809	

Appendix E – Principal component analysis

```
[coeff,score,latent] = pca(A);

figure
scatter(score(:,1), score(:,2))

clear all
load A
andrewsplot(X(A,:), 'group',Cylinders(A), 'standardize','on')

names = ["s4-1-2", "s4-1-1", "R-1-1","s3-1-1", "S3-1-2", "R-1-2"];
```

DATA SET A:

LosAngeles	Bond.Mill	Point.Load	Drop.Weight
20.1600	17.1400	77.4200	42.4400
20.4600	18.2900	83.3100	40.5500
19.7000	17.7700	87.4300	39.1400
21.5100	20.2400	106.1700	36.0000
18.2300	20.3900	108.1600	35.3500
16.3100	21.5500	119.0900	34.2900